

Dissertation zur Erlangung des Doktorgrades
der Fakultät für Chemie und Pharmazie
der Ludwig-Maximilians-Universität München

**Toward unraveling biogenesis of Dicer-
independent priRNAs and siRNAs in
*Schizosaccharomyces pombe***

Mirela Marasovic
aus
Zagreb, Kroatien

2015

Erklärung

Diese Dissertation wurde im Sinne von § 7 der Promotionsordnung vom 28. November 2011 von Herrn Prof. Dr. Mario Halic betreut.

Eidesstattliche Versicherung

Diese Dissertation wurde eigenständig und ohne unerlaubte Hilfe erarbeitet.

München, den 28.04.2015.

.....
Mirela Marasovic

Dissertation eingereicht am 28.04.2015.

1. Gutachterin / 1. Gutachter: Prof. Dr. Mario Halic

2. Gutachterin / 2. Gutachter: Prof. Dr. Klaus Förstemann

Mündliche Prüfung am 15.06.2015.

SUMMARY

RNA interference (RNAi) is a highly conserved process of gene silencing in which Argonaute family proteins are guided by small RNA molecules to complementary targets. In the fission yeast *Schizosaccharomyces pombe*, RNAi is required for heterochromatin formation at centromeres. Although it seems counterintuitive, pericentromeric heterochromatin in fission yeast is transcribed. The transcripts are processed by RNAi machinery, which is in turn guided back to the pericentromeric repeats by sequence complementarity of the Argonaute-bound small interfering RNA (siRNA) and the nascent transcript. This generates a positive-feedback loop of siRNA amplification that recruits factors required for the assembly of heterochromatin. Previously, it was suggested that a fission yeast class of Dicer-independent small RNAs called primal small RNAs (priRNAs) initiates the positive-feedback loop of siRNA generation and heterochromatin assembly. However, the biogenesis of priRNAs as well as of Dicer-independent small RNAs from other organisms was not well understood.

The results presented here identify Triman, a novel 3'-5' exonuclease that is involved in the final step of biogenesis of both priRNAs and siRNAs in fission yeast. It was observed that Argonaute binds longer priRNA and siRNA precursors from the total RNA fraction. This is followed by the recruitment of Triman to trim 3' ends of Argonaute-bound small RNAs to the mature size. The final trimming of priRNAs and siRNAs is required for *de novo* heterochromatin formation at centromeres and the mating-type locus as well as for the maintenance of facultative heterochromatin islands. Furthermore, it was shown that in cells lacking Rrp6, a nuclease subunit of the exosome, RNAi targets various genes across the yeast genome. This demonstrated that the exosome protects the genome against aberrant RNAi. Spurious RNAi targeting in *rrp6Δ* cells at majority of loci occurs via accumulation of antisense transcripts that are processed into priRNAs in a Triman-dependent manner. These results suggest that Argonaute association with cellular degradation products which are processed into priRNAs might serve as a surveillance mechanism to guard the genome against invading genomic elements (Marasovic et al. 2013).

CONTENTS

SUMMARY	i
1 INTRODUCTION	1
1.1 Classes of small RNAs	1
1.1.1 miRNAs	2
1.1.2 piRNA	2
1.1.3 siRNAs	3
1.2 Eukaryotic chromatin comes in two flavors	4
1.3 Heterochromatin formation in <i>S. pombe</i>	5
1.3.1 Heterochromatin formation at pericentromeric region	7
1.3.1.1 The 'nascent transcript' model for RNAi-dependent heterochromatin formation	9
1.3.1.2 The nucleation of positive-feedback loop of siRNA generation and heterochromatin formation at the pericentromeric repeats	13
1.3.2 Heterochromatin formation at the silent mating-type locus	17
1.3.3 Heterochromatin at subtelomeres	18
1.3.4 Islands of heterochromatin at euchromatic region	19
1.5 Aim of the thesis	21
2 RESULTS	23
2.1 SPBC29A10.09c and Rrp6 are involved in biogenesis of priRNAs and siRNAs	23
2.2 Caf1 does not have an effect on the levels of Argonaute-associated small RNAs	27
2.3 In <i>SPBC29A10.09cΔ</i> cells both priRNAs and siRNAs are longer	28
2.4 SPBC29A10.09c is a Mg ²⁺ -dependent 3'-5' exonuclease named Triman	30
2.4.1 Purification of FLAG-Triman and FLAG-TrimanD28A	30
2.4.2 Reconstitution of Triman activity <i>in vitro</i>	31

2.5	Argonaute acts as a ruler for the final length of small RNA.....	35
2.6	Triman processes longer priRNA precursors purified from <i>dcr1Δtri1Δ</i> cells ...	38
2.7	Triman overexpression generates more small RNAs <i>in vivo</i>	39
2.8	Argonaute and Triman cooperate to generate small RNAs	42
2.9	Trimming is important for the stability of Ago1:sRNA complex.....	43
2.10	Trimming is important for the Argonaute-slicer activity.....	44
2.11	Triman is a general factor involved in biogenesis of siRNAs and priRNAs	45
2.12	Triman is not required for maintenance of centromeric heterochromatin	47
2.13	Triman is important for establishment of pericentromeric heterochromatin	50
2.14	Triman is important for formation of heterochromatin islands.....	53
2.15	In <i>rrp6Δ</i> cells RNAi is nucleated at various clusters in a Triman/priRNA dependent manner	55
3	DISCUSSION.....	64
3.1	Triman is required for the biogenesis of priRNAs and mature siRNAs	64
3.2	Triman is a CAF1 family 3'-5' exonuclease.....	65
3.3	The final processing of 3' end is a conserved process in small RNA biogenesis	65
3.4	Argonaute and Triman cooperate to generate priRNAs and siRNAs	66
3.5	Trimming is important for the stability of the complex between Ago1 and small RNA and for the proper Argonaute-slicing activity.....	67
3.6	priRNA and siRNA trimming is required for <i>de novo</i> heterochromatin assembly.....	68
3.7	Triman is important for H3K9me at heterochromatin islands	69
3.8	In <i>rrp6Δ</i> cells RNAi is nucleated at euchromatic loci in priRNA/Triman- dependent manner	70
3.9	The model of Triman-dependent priRNA biogenesis and RNAi nucleation	74
4	MATERIALS AND METHODS.....	76
4.1	Materials.....	76
4.1.1	Consumables and Chemicals.....	76
4.1.2	Oligonucleotides	76

4.1.3	Plasmids	78
4.1.4	Strains.....	79
4.1.5	Antibodies	80
4.1.6	Buffers, solutions and media.....	80
4.2	Methods.....	81
4.2.1	Working with <i>S. pombe</i> cells	81
4.2.1.1	Strain construction	81
4.2.1.2	Silencing assays	82
4.2.2	Nucleic acid analysis.....	82
4.2.2.1	Purification of total RNA	82
4.2.2.2	Quantitative PCR (qPCR)	83
4.2.2.3	<i>In vitro</i> RNA synthesis.....	83
4.2.2.4	Radioactive labeling of small RNAs.....	83
4.2.2.5	Splinted ligation	84
4.2.2.6	Periodate oxidation/ β -elimination of RNA	84
4.2.2.7	High throughput sequencing	85
4.2.2.8	Triman activity assays.....	87
4.2.2.9	Argonaute slicer assay.....	87
4.2.3	Protein analysis	88
4.2.3.1	Protein affinity purification.....	88
4.2.3.2	Western blotting	89
4.2.3.3	<i>In-vitro</i> co-immunoprecipitation assay	89
4.2.3.4	Chromatin immunoprecipitation (ChIP) assay.....	90
5	APPENDIX	91
6	REFERENCES	95
7	CURRICULUM VITAE	106
8	ACKNOWLEDGEMENTS	108

1 INTRODUCTION

The observation by Fire and Mello that in *Caenorhabditis elegans* double-stranded RNA (dsRNA) triggers specific mechanism of gene silencing, RNA interference (RNAi) (Fire et al. 1998), has dramatically changed the understanding of gene regulation. To date, RNAi has turned out to be a widely utilized mechanism of gene silencing on the both transcriptional and posttranscriptional level, as well as of maintenance of genome stability and defense against foreign genetic elements (reviewed in Ghildiyal & Zamore 2009; Hannon 2002).

In all small RNA silencing pathways, small RNAs (sRNAs) of 20-30 nucleotides in length interact with Argonaute (Ago) family of proteins, the central players of small RNA silencing pathways. Small RNAs guide Argonaute RNA-induced silencing complex (RISC) or RNA-induced transcriptional silencing (RITS) complex to target RNAs by sequence complementarity (reviewed in Ghildiyal & Zamore 2009).

In *Schizosaccharomyces pombe*, plants, *Tetrahymena* and *Drosophila*, RNAi is required for heterochromatin formation or DNA methylation (Volpe et al. 2002; Mochizuki; Brennecke et al. 2008; Gu et al. 2012). In fission yeast heterochromatin is found at the pericentromeric, subtelomeric and mating-type (*mat*) regions (Volpe et al. 2002; Noma et al. 2004; Cam et al. 2005). First seemingly counterintuitive, heterochromatic region was found to be transcriptionally active (Djupedal et al. 2005). Moreover, resulting pericentromeric transcripts are targeted by RNAi machinery that in turn triggers heterochromatin formation in a self-reinforcing feed forward mechanism.

1.1 Classes of small RNAs

Small RNAs can be generally divided into three main classes according to the molecules that trigger their production, mechanism of biogenesis and protein partners: small interfering RNAs (siRNAs), microRNAs (miRNAs) and Piwi-interacting small RNAs (piRNAs) (reviewed in Ghildiyal & Zamore 2009).

1.1.1 miRNAs

miRNAs are 20-24 nt-long sRNAs present in various organisms: flies, worms, plants, mammals, where they regulate diverse cellular pathways at the post-transcriptional level (reviewed in Ghildiyal & Zamore 2009). They are encoded in the genome and originate as primary miRNAs (pri-miRNAs) that generally fold back on themselves to form hairpins. The biogenesis involves subsequent action of two RNase III endonucleases. First, primary miRNA is processed in the nucleus by the Drosha and its double-stranded RNA-binding domain (dsRBD) protein (DGCR8 in mammals, Pasha in *Drosophila*). The resulting 60-70 nt-long precursor-miRNAs (pre-miRNAs) are exported into the cytoplasm. There, pre-miRNAs are processed by Dicer, which acts with its dsRBD partner protein Loqs (*Drosophila*) or TRBP (mammals), to form mature miRNAs. Mature miRNAs are loaded onto Argonaute RISC complex and regulate gene expression by inhibiting translation or inducing degradation of mRNA.

1.1.2 piRNA

Piwi-interacting RNAs (piRNAs) are 21-30 nt-long sRNAs that can be found mainly in the germline of various animals, from *Drosophila*, mouse to humans (reviewed in Ghildiyal & Zamore 2009). They have a general function in repression of mobile genetic elements by post-transcriptional silencing. Recently, piRNAs have been also found to have a nuclear role in transposon silencing by promoting methylation of histone H3 on lysine 9 (H3K9me) in *Drosophila* (Wang & Elgin 2011; Sienski et al. 2012) and DNA methylation in mice (Aravin et al. 2008; Carmell et al. 2007).

Biogenesis of piRNAs is first elucidated in *Drosophila*, where a mode of amplification known as the ping-pong cycle is discovered (Brennecke et al. 2007; Gunawardane et al. 2007). piRNAs originate from single-stranded precursors in a Dicer-independent manner and their biogenesis involves primary processing and a secondary amplification pathway (the ping-pong amplification). piRNAs in *Drosophila* bind to three Piwi-family members: Piwi, Aubergine (Aub), and Ago3. Primary piRNAs originate from transcription of piRNA clusters which lie in heterochromatin region of the genome, or are maternally deposited. These long single-stranded

precursors are loaded onto Piwi family proteins, which are involved in the ping-pong mode of amplification. Piwi and Aub have bias to antisense piRNAs which begin with 5' uridine (5'U), while Ago3 binds sense piRNAs which have bias to adenine at position ten. Piwi/Aub loaded with antisense primary piRNAs targets complementary sense mRNA transcript of transposons and cleaves it between the phosphates 10 and 11 through its slicer activity. In this way, a new 5' end of the future sense piRNA is generated. Newly generated sense piRNA is then loaded onto Ago3, the complex is guided to a complementary antisense transposon transcript, and the Ago3-directed cleavage generates 5' end of a new antisense piRNA. The cycle continues as new antisense piRNA is able to create additional sense piRNAs. The ping-pong model originally proposed that the tenth adenine bias of Ago3-bound piRNAs is a consequence of base pairing of the 5' uridine of Aub/Piwi-bound guide piRNA to its target. However, it was reported that the fly protein Aub, as well as its silkworm and mouse homologs Siwi and Mili, show intrinsic property for the tenth adenine of their targets, regardless of the identity of the nucleotide at the 5' end of the guide RNA (Wang et al. 2014).

The ping-pong amplification mechanism of piRNAs is analogous to RNA-dependent RNA polymerase (RDRP) amplification of secondary siRNAs in worms, plants and *S. pombe*. However, many aspects of the piRNA pathway remain unknown, for example how 3' end of piRNAs is generated. It was found that the 3' end is shaped by the trimming activity of 3'-5' exonuclease, but the identity of the protein is unknown (Kawaoka et al. 2011).

1.1.3 siRNAs

siRNAs in general originate from long double-stranded RNAs, which are then processed by Dicer into 21-nt long siRNAs. siRNAs are then loaded onto Argonaute protein which is guided by siRNA to perfectly base-paired target RNA to induce its destruction. siRNAs can be classified according to their origin into exogenous-siRNAs (exo-siRNAs) and endogenous-siRNAs (endo-siRNAs) (reviewed in Ghildiyal & Zamore 2009).

Exo-siRNA pathway in *Drosophila*, plants and *C. elegans* serves as a defense mechanism against viruses and foreign sequences. In *Drosophila*, long double-stranded trigger of siRNA-response derive from intermediates of viral infection. Because plants and *C. elegans* possess genes coding

for RNA-dependent RNA polymerases, the response can also be triggered by single-stranded RNA molecules. Endo-siRNAs are found in plants, *C. elegans*, flies and mammals (reviewed in Ghildiyal & Zamore 2009). The pathway guards the somatic genome against transposons. In plants and *C. elegans*, endo-siRNAs are produced by RDRP-activity, while in mammals and *Drosophila* they originate from transposon sequences, repetitive sequences, convergent transcripts, structured loci that form hairpins (reviewed in Ghildiyal & Zamore 2009).

Besides its role in direct destruction of complementary sequences, siRNA-pathways in fungi, plants and *C. elegans* can repress target genes by directing chromatin modifications. The principles of siRNA-guided heterochromatin modification were first deciphered in *S. pombe* (discussed in further chapters). In plants, siRNAs direct *de novo* DNA methylation and H3K9me (reviewed in Matzke et al, 2014). Exo-siRNAs in somatic cells of *C. elegans* lead to a production of secondary siRNA. These in turn have a role in the nucleus, where they induce H3K9me (Gu et al. 2012; Guang et al. 2008; Burkhart et al. 2011). In the germ line of *C. elegans*, inheritance of exo-siRNA triggered H3K9me involves piRNAs (21U-RNAs) and Piwi family protein PRG1 (Batista et al. 2008).

1.2 Eukaryotic chromatin comes in two flavors

In order to ensure proper cell division, genomic DNA in eukaryotes is organized in a structure with histone and non-histone proteins called chromatin. The classical division of chromatin into heterochromatin and euchromatin is based on differential chromosomal staining in interphase cells, although to date it has become clear that chromatin adopts more states (reviewed in (van Steensel 2011)). Generally, euchromatin includes regions that are loosely packaged, gene-rich and associated with transcription, while heterochromatin is condensed during interphase, composed mainly of repetitive sequences and was previously considered transcriptionally inert. Chromatin condensation is mainly achieved through modifications of amino-terminal histone tails, which represent specific histone code. In euchromatic region characteristic modification mark is histone H3 and H4 acetylation and di-methylation of histone H3 lysine 4, while in heterochromatic region histones are hypoacetylated and main heterochromatin mark is histone H3 methylated on lysine 9 (H3K9me). H3K9me represents the binding site for for the HP1 family of

chromodomain proteins (Lachner et al. 2001). Heterochromatin can be further divided into facultative and constitutive. Facultative heterochromatin usually forms over genes that are silent upon development, while constitutive heterochromatin is formed over centromeres, subtelomeres and regulatory regions. Constitutive heterochromatin is important for maintenance of genome stability by ensuring proper centromere function, nuclear organisation and repression of repetitive sequences.

Studies in many organisms ranging from yeast to mammals, uncovered that RNAi mechanisms play an important role in epigenetic inheritance. Heterochromatin structure and the associated proteins are conserved from *S. pombe* to metazoans, and the studies in fission yeast provided basic mechanistic principles.

1.3 Heterochromatin formation in *S. pombe*

Proper heterochromatin formation is essential for maintenance of genome stability and proper centromere function. Vast portions of the eukaryotic genomes contain repetitive sequences and transposons embedded into pericentromeric heterochromatin domains. Thus, major function of heterochromatin is to inhibit their transcription. It was shown that heterochromatin and RNAi machinery are necessary to establish Cenp-A chromatin at centromeres (Folco et al. 2008), a site upon which kinetochore assembles. Moreover, pericentromeric heterochromatin is required for recruitment of cohesin which mediates cohesion between sister chromatids (Bernard et al. 2001). Therefore, heterochromatin is required for ensuring proper cell division.

In fission yeast *Schizosaccharomyces pombe*, heterochromatin is preferentially localized at pericentromeric region, the silent mating-type (*mat*) locus, and the subtelomeres (Cam et al. 2005). In addition to major constitutive heterochromatin domains, heterochromatin is also found at around 30 additional locations in euchromatic region of the genome (Zofall et al. 2012; Hiriart et al. 2012). The main characteristic of heterochromatin is di- and trimethylated H3K9 nucleosomes that are bound by HP1 family of proteins. HP1 proteins are highly conserved and fundamental for heterochromatin packaging in almost all eukaryotes: yeast, nematode, insects, chicken, frog and mammals (Eissenberg & Elgin 2000). They are characterized by an N-terminal

chromodomain, which binds H3K9me nucleosomes and a C-terminal ‘chromo shadow’ domain. In fission yeast two HP1 homologs, Swi6 and Chp2, and two chromodomain containing proteins, Chp1 and Clr4, bind to H3K9me nucleosomes and are required for heterochromatin silencing (Partridge et al. 2002; Halverson et al. 2000; Thon & Verhein-Hansen 2000).

Heterochromatin formation involves establishment, spreading and maintenance

The process of heterochromatin formation in fission yeast can be divided in three main steps: establishment, spreading and maintenance of heterochromatin (Buscaino et al. 2013). Establishment of heterochromatin is an RNAi-based mechanism at all three major heterochromatic regions (centromeric, subtelomeric and *mat* locus). In addition to RNAi-dependent mechanism, at mating-type locus and subtelomeres, DNA-based mechanisms also function in parallel to recruit heterochromatin factors (discussed in the following chapters).

RNAi-dependent establishment of heterochromatin occurs at specific nucleation sites which are defined by the production of siRNAs. These sites are found at *otr* region of centromeres and are designated as *dg* and *dh* repeats (Figure 1.3.1.1). Elements homologous to *dg* and *dh* repeats are also present at silent mating-type region (*cenH* element) and subtelomeres. It was shown that *dg* and *dh* repeats and their homologous sequences are transcribed by RNA polymerase II (RNAPII). The transcripts are processed by RNAi machinery into siRNAs, which leads to establishment of heterochromatin. After the establishment at nucleation loci, heterochromatin mark H3K9me spreads to the surrounding regions which are not targeted by RNAi and forms large heterochromatic domains. It was demonstrated that histone deacetylase (HDAC) Sir2, Clr3 and Swi6 are required to initiate the formation of heterochromatin at nucleation (siRNA producing) loci, but then are also necessary for the spreading of heterochromatin from the nucleation loci to the surrounding chromatin to create large heterochromatic domains (Buscaino et al. 2013). These processes are discussed in detail in the following chapters.

The established state of heterochromatin is stably maintained through mitotic and meiotic division. During the DNA replication, parental histones are randomly distributed into daughter DNA, preexisting H3K9me mark is recognized and newly deposited histones are modified (Ragunathan et al. 2014). The process of maintenance of heterochromatin mark does not require

nucleation DNA sequences (siRNA producing loci). Instead, it is dependent on the coordinate action of H3K9 methylation by Clr4, demethylation of H3K9 mark by Epe1 and random distribution of parental histones (Ragunathan et al. 2014; Audergon et al. 2015).

1.3.1 Heterochromatin formation at pericentromeric region

At pericentromeric region, heterochromatin is nucleated in an RNAi-dependent manner. Fission yeast has been shown to be an excellent model organism for the study of RNAi for several reasons; unlike higher eukaryotes, it contains single gene copy of Argonaute (*ago1*⁺), Dicer (*dcr1*⁺), and RNA-dependent RNA polymerase (*rdp1*⁺), but it still shares great similarity of the heterochromatin structure with metazoans. Studies on the RNAi-dependent heterochromatin formation have been mainly focused on the pericentromeric region.

Centromeres in *S. pombe* are between 35-110 kb and have two distinct domains (Volpe et al. 2002; Folco et al. 2008) (Figure 1.3.1.1). Central kinetochore domain is composed of central core (*cnt/cc*) that is flanked by innermost repeats (*imr*). This domain is flanked by outermost region (*otr*), which contains copies of *dg* and *dh* repeats from which siRNAs originate and direct heterochromatin formation. At the central kinetochore domain a histone H3 is replaced by a Cenp-A and it is a site where kinetochore assembles. It was shown that heterochromatin and RNAi machinery are necessary to establish Cenp-A chromatin at centromeres (Folco et al. 2008).

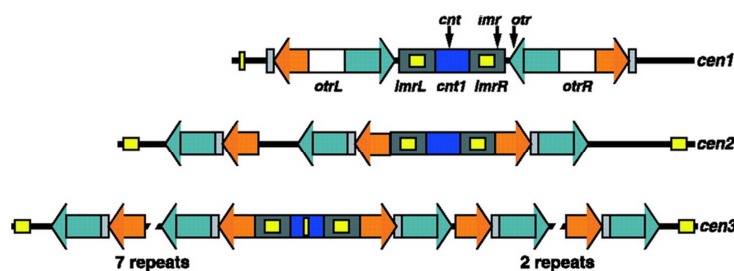


Figure 1.3.1.1. Schematic representation of three *S. pombe* centromeric regions. (Adapted from (Volpe et al. 2002)). Centromeres have two distinct domains: central kinetochore domain and outermost repeats domain. Central kinetochore domain is composed of unique central core (*cnt*) of 4–7 kb flanked with innermost repeats (*imr*) which contain transfer RNA (tRNA) genes (yellow boxes). Outermost region (*otr*) is composed of tandem alternating copies of *dg* (green) and *dh* (orange) repeats.

Although early observations described heterochromatin as a transcriptionally inert structure, later on a contra intuitive result was found - small levels of transcription occur at pericentromeric region (Djupedal et al. 2005). Moreover, the pericentromeric transcription correlates with siRNA generation (Figure 1.3.1.2) and is absolutely required for proper heterochromatin formation (Reinhart & Bartel 2002; Volpe et al. 2002).

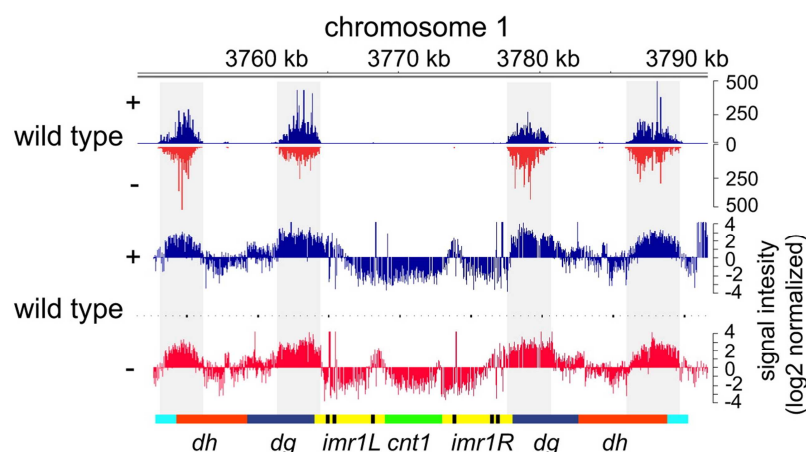


Figure 1.3.1.2. small RNAs generation correlates with the transcription from centromeric repeats. (Adapted from (Halic & Moazed 2010)). Upper panel: small RNA reads from wild-type cells were plotted over centromeric region on chromosome 1. Small RNAs originating from sense (+) strand are depicted in blue. Small RNAs originating from antisense (-) strand are depicted in red. Scale bars on the right denote small RNA read numbers normalized per one million reads. Lower panel: transcription over centromeric region on chromosome 1. Sense (+) transcripts are depicted in blue, antisense (-) transcripts are depicted in red.

Early studies for factors required for heterochromatin formation in *S. pombe* utilized a simple method where a reporter gene (*ade6⁺*) was inserted in the pericentromeric region. These studies have shown that transgenes integrated in centromere are silenced, demonstrating that heterochromatin is able to spread to the surrounding genes (Allshire et al. 1994). Thus, a simple screening method by plating the cells which contain reporter genes on corresponding selective plates enabled quick testing for the factors required for the silencing. Deletion of RNAi factors *ago1⁺*, *dcr1⁺* or *rdp1⁺* resulted in accumulation of pericentromeric transcripts originating from heterochromatin region and decrease in the levels of histone H3 lysine 9 methylation (Volpe et al. 2002; Provost et al. 2002), a main mark for heterochromatin. This demonstrated that RNAi is required for centromeric silencing and suggested that transcripts originating from

heterochromatin region are processed by RNAi, which drives heterochromatin formation. Furthermore, finding that small RNAs are matching pericentromeric region (Reinhart & Bartel 2002) confirmed the connection between RNAi and heterochromatin formation in *S. pombe*.

1.3.1.1 The 'nascent transcript' model for RNAi-dependent heterochromatin formation

It was demonstrated that *otr* region of *S. pombe* is transcribed in both sense and antisense direction by RNA polymerase II (RNAPII) (Kato et al. 2005) (Figure 1.3.1.1.1). The transcripts are processed by Dicer, ribonuclease III-like nuclease, into 21-25 nt-long double-stranded siRNAs, which as a result of Dicer-processing contain phosphate groups on 5' ends and 2-nt overhangs on 3' ends (Bernstein et al. 2001; Knight & Bass 2001; Provost et al. 2002). These double-stranded siRNAs are then loaded onto Argonaute siRNA chaperone (ARC) complex that, in addition to Argonaute, contains Arb1 and Arb2 proteins. It was shown that ARC binds dsRNA Dicer-products and mediates their loading onto Ago1-containing RNA-induced transcription silencing (RITS) complex (Buker et al. 2007; Holloch & Moazed 2015).

Besides Ago1, RITS complex contains Tas3, a conserved glycine and tryptophan (GW) motif-containing protein, and Chp1, a chromodomain containing protein (Verdel et al. 2004). In the RITS complex, the strand with less thermodynamic stability of the 5' end of siRNA duplex is selected as a guide, while the other, the passenger strand, is sliced by Argonaute's endonucleolytic slicer activity and subsequently removed. This creates mature RITS complex that is targeted to pericentromeric transcripts by sequence complementarity of small RNA with the nascent transcript (Verdel et al. 2004).

At the pericentromeric region, RITS is involved in recruitment of complexes necessary for siRNA amplification and heterochromatin formation. One complex recruited by RITS is RNA-dependent RNA polymerase complex (RDRC). RDRC is composed of Rdp1, RNA helicase Hrr1, and the non-canonical poly(A) polymerase Cid12 (Motamedi et al. 2004; Sugiyama et al. 2005) (discussed in the chapter 1.3.1.3). RDRC exhibits RNA-dependent RNA-polymerase activity on the nascent transcript. Thus, it generates double-stranded RNA precursors which act as a substrate for Dicer to generate siRNAs.

The other multisubunit complex that is recruited is Clr4-Rik1-Cul4 (CLRC) complex (Hong et al.; Zhang et al. 2008). The central component of CLRC complex is Clr4, highly conserved protein which methylates surrounding nucleosomes on the histone H3 lysine-9, which is the main heterochromatic mark. H3K9me is a main recruiting mark for chromodomain containing proteins: Swi6 and Chp2 (HP1 family proteins), Chp1 and Clr4. All of these proteins have variable heterochromatin roles.

Clr4 binds the H3K9me nucleosomes with its N-terminal chromodomain, which makes Clr4 a protein with a dual 'write and read' function (Zhang et al. 2008). This binding is important for stable association of CLRC to heterochromatic loci that is crucial for the further spreading of heterochromatin from initial nucleation sites to surrounding chromatin, as well as heterochromatin maintenance (Ragunathan et al. 2014). Clr4 is a highly conserved protein from yeast to human; it shares similarity to mammalian Suv39h (Rea et al. 2000; Motamedi et al. 2004; Nakayama et al. 2001). Other protein members of CLRC complex: Cul4, Pip1, Rik1, Raf1 (delocalization of Swi6 (Dos1)/Clr8) and Raf2 (Dos2/Clr7), are components of an E3 ubiquitin ligase, whose activity is essential for heterochromatin assembly. Cul4 is a member of cullin family of proteins, which serve as a scaffold for the assembly of ubiquitin ligases. Rik1 contains WD repeats and shares similarity to several nucleic acid binding proteins. Raf1 also has several WD repeats; however Raf2 shares no obvious similarity with other proteins. Rik1 associates with both RDRC and the RITS complex, and is targeted to transcribed centromeric repeats in an RNAi-dependent way (Zhang, 2008). Stc1, a small protein that is peripherally associated with CLRC complex, provides a link between CLRC and RITS by interacting with Ago1 (Bayne et al. 2010). It was shown that Stc1 is critical for recruitment of CLRC complex in a process of establishment of H3K9me via RNAi.

Fission yeast HP1 homologs, Swi6 and Chp2, bind H3K9me marks and provide platform for factors necessary for heterochromatic gene silencing (Motamedi et al. 2008; Nakayama et al. 2001). When bound to H3K9me nucleosomes, Swi6 promotes additional recruitment of RDRC complex in an interaction that is mediated by silencing factor Ers1 (Motamedi et al. 2008; Sugiyama et al. 2007; Moazed 2011). Additionally, Swi6 interacts with a large number of proteins, including chromatin-remodeling complexes and DNA-binding and DNA replication proteins (Motamedi et al. 2008). Swi6 associates with HDAC Clr6. Clr6 can be found in two

distinct complexes and is required for deacetylation of histones, particularly lysines on histone H3 and H4 (Wirén et al. 2005; Nicolas et al. 2007). Moreover, it was found that Swi6 also recruits histone chaperone complex HIRA/Asf1, which acts synergistically with Clr6 in the deacetylation of chromatin and nucleosomal occupancy and positioning at heterochromatin (Yamane et al. 2011).

Swi6 and mainly Chp2 are required for the recruitment of Snf2-histone deacetylase repressor complex (SHREC) (Sugiyama et al. 2007). SHREC complex contains quartet of Clr1, Clr2, Clr3, and Mit1 (the Snf2 family chromatin-remodeling protein). SHREC is required for deacetylation of H3K14 (via the activity of histone deacetylase Clr3), nucleosome positioning at heterochromatin, and promotes transcriptional gene silencing by limiting RNA polymerase II (Pol II) access to heterochromatin (Motamedi et al. 2008; Sugiyama et al. 2007). Another deacetylase found to be important in heterochromatin silencing is Sir2, which preferentially deacetylate histone H3K9 (Wirén et al. 2005).

H3K9me mark is also binding point for the Chp1, a component of RITS complex. This binding further localizes RITS to chromatin and promotes the interaction of RITS with RDRC and Dcr1 (Motamedi et al. 2004; Colmenares et al. 2007).

Besides RNAi-based processing, pericentromeric transcripts are also degraded via RNAi-independent pathways which involve Trf4-Air2-Mtr4 polyadenylation (TRAMP) complex and exosome (Bühler et al. 2007; Reyes-Turcu et al. 2011).

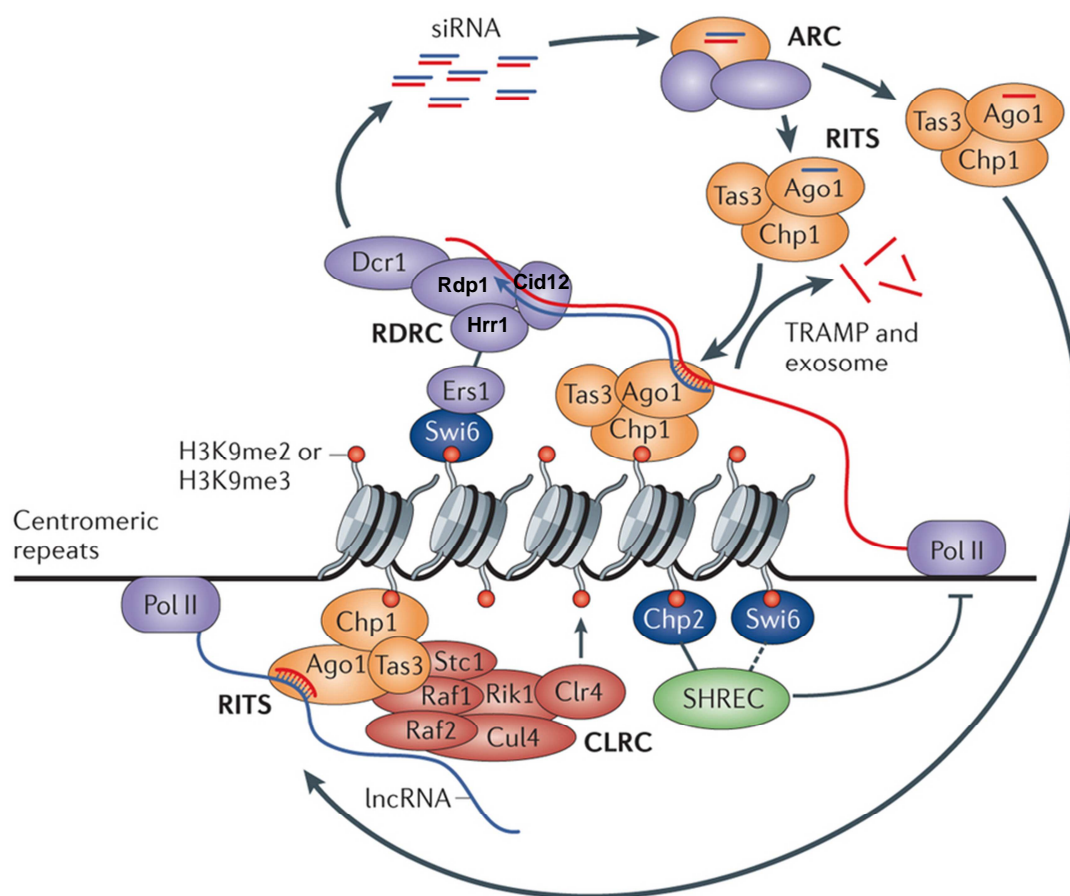


Figure 1.3.1.1.1. Positive feedback loop of siRNA generation and heterochromatin formation at fission yeast pericentromeric region. (Adapted from (Holoch & Moazed 2015)). Centromere sequences are transcribed by RNA Polymerase II (Pol II) and targeted by RNA-induced transcriptional silencing (RITS) complex via siRNA loaded Ago1. RITS recruits two complexes: RNA-dependent RNA polymerase complex (RDRC, composed of Rdp1, Hrr1 and Cid12) and Clr4-Rik1-Cul4 (CLRC) complex. RDRC amplifies the signal by synthesizing new long double-stranded precursors using pericentromeric transcript as template. Double-stranded precursors are processed by Dicer into ds siRNAs, which are further loaded onto RITS via Ago1-containing chaperon complex, ARC. The cycle is repeated by RITS targeting of centromeric transcript via sequence complementarity between Ago1-loaded small RNA and the pericentromeric transcript. Second complex recruited by RITS is CLRC complex. The recruitment occurs via Rik1 and Stc1 proteins. CLRC methylates nucleosomes on histone H3 lysine 9 (H3K9me). This leads to recruitment of fission yeast homologs of HP1 proteins, Swi6 and Chp2, and heterochromatin formation. RITS complex is further stabilized on chromatin by binding of Chp1. Swi6 further promotes localization of RDRC via Ers1. Swi6 and mainly Chp2 recruit Snf2-histone deacetylase repressor complex (SHREC), which restrict RNA polymerase II (Pol II) access. Trf4-Air2-Mtr4 polyadenylation (TRAMP) complex and exosome act in parallel to RNAi-mechanism to degrade pericentromeric transcripts.

1.3.1.2 The nucleation of positive-feedback loop of siRNA generation and heterochromatin formation at the pericentromeric repeats

The interdependence of RNAi and heterochromatin formation has been extensively studied. One of the fundamental questions asked was how this positive feedback loop is initiated in the first place. The first model proposed that pericentromeric transcripts, which are transcribed in both forward and reverse direction, could base-pair to form dsRNAs (Figure 1.3.1.2.1). These dsRNAs could then serve as substrates for Dicer to initiate RNAi machinery (Halic & Moazed 2010). In the second model, RDRC specifically recognizes pericentromeric transcript and generates long dsRNA precursors for Dicer, which then generates the trigger siRNAs. The third, alternative model suggested that low levels of H3K9 methylation, which are found in RNAi mutants (Noma et al. 2004; Sadaie et al. 2004), could recruit RNAi factors RITS and RDRC to trigger siRNA generation and H3K9me loop.

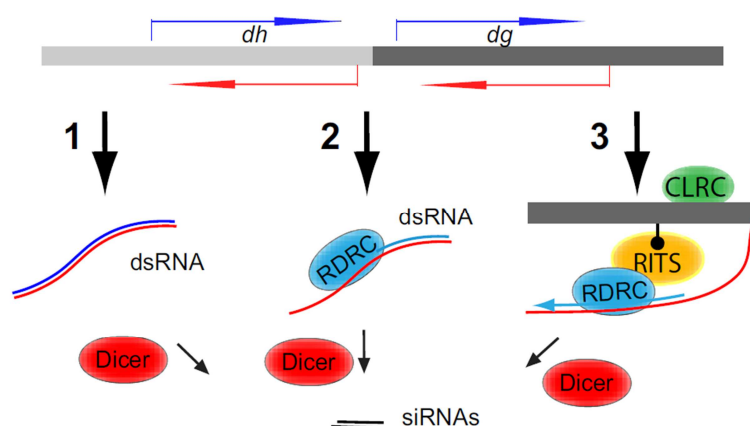


Figure 1.3.1.2.1. Models explaining nucleation of siRNA generation and heterochromatin formation. (Adapted from (Halic & Moazed 2010)). (1) Pericentromeric transcripts are bidirectionally transcribed and base-pair to generate dsRNAs, which are processed by Dicer. (2) RDRC recognizes pericentromeric transcripts and generates dsRNA precursors for Dicer. (3) Low-levels of H3K9me recruit RITS and RDRC to generate siRNAs.

Splinted ligation assays and deep-sequencing of FLAG-Argonaute associated small RNAs have enabled detection of small RNAs in mutants of RNAi factors and heterochromatin (Halic & Moazed 2010). In cells lacking heterochromatin, siRNAs are dramatically reduced, but small levels of siRNAs are still generated at the pericentromeric *dg* and *dh* repeats (Figure 1.3.1.2.2). This argued against the third model saying that heterochromatin is necessary to induce siRNA generation at these sites, and demonstrated that siRNA generation precedes heterochromatin formation. The levels of siRNAs generated from *dg* repeats in the absence of heterochromatin are higher than the ones generated from *dh* repeats, and their generation was dependent on Rdp1, Dicer and Ago-slicer activity (Halic & Moazed 2010). This indicates that siRNA generation at *dg* repeats could be a nucleation site for siRNA generation in a heterochromatin independent manner.

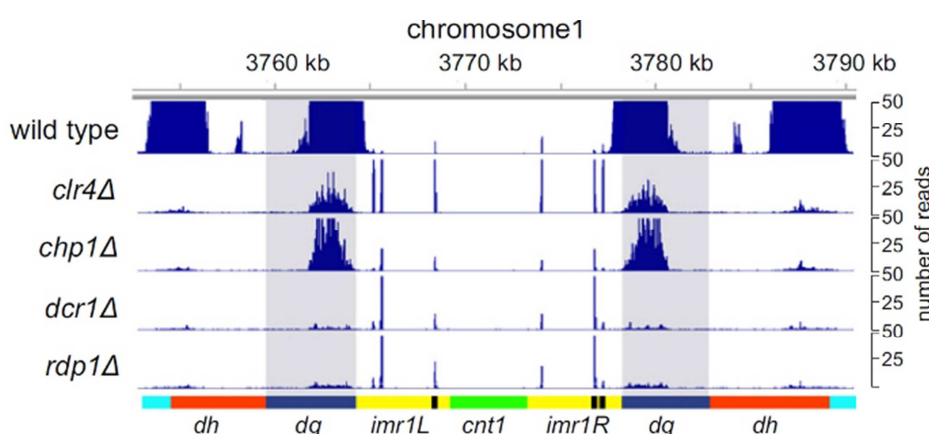


Figure 1.3.1.2.2. Pericentromeric *dg* siRNAs are generated independently of Clr4 and Chp1, indicating siRNA generation precedes heterochromatin formation. (Adapted from (Halic & Moazed 2010)). small RNA reads from indicated strains were plotted over centromeric region on chromosome 1. Scale bars on the right denote small RNA read numbers normalized per one million reads.

Next, the distinction between the first and the second model of siRNA induced heterochromatin formation was elucidated from the levels of Argonaute-associated small RNAs from *rdp1Δ* and *dcr1Δ* cells. The first model postulated that the trigger siRNAs are generated by Dicer-processing of double-stranded RNA precursors and that RDRC activity acts upstream to amplify the siRNA pool. In that scenario, the levels of small RNAs would be higher in cells lacking *rdp1⁺* in comparison to the levels in *dcr1Δ* cells. However, deep sequencing of Ago1-associated small RNAs revealed that siRNA levels in *dcr1Δ* and *rdp1Δ* cells were similar (Figure 1.3.1.2.3)

favoring the second model (Halic & Moazed 2010). Moreover, Dicer- and Rdp1-independent small RNAs were also generated in Ago-slicer independent manner.

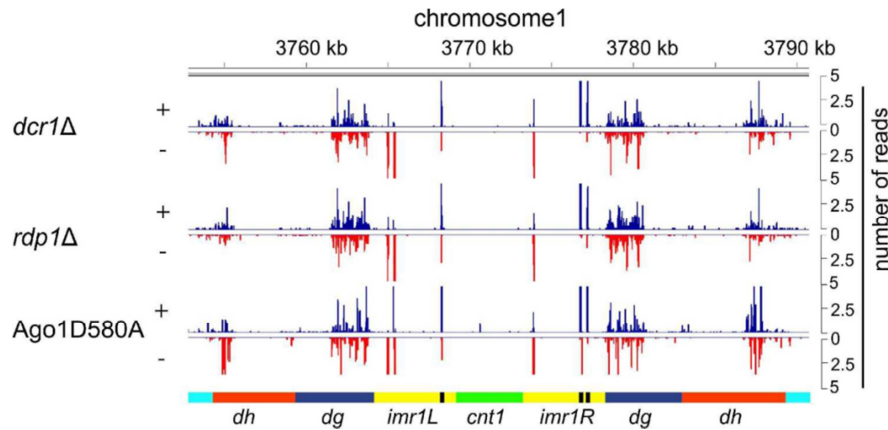


Figure 1.3.1.2.3. priRNAs are generated independently of Dcr1, Rdp1, and Argonaute's slicer activity. (Adapted from (Halic & Moazed 2010)). Small RNA reads from indicated strains are plotted over centromeric region on chromosome 1. Small RNAs originating from sense (+) strand are depicted in blue. Small RNAs originating from antisense (-) strand are depicted in red. Scale bars on the right denote small RNA read numbers normalized per one million reads.

These small RNAs were called primal small RNAs (priRNAs), and it was suggested they represent triggers that guide Argonaute to centromeric transcripts to initiate silencing and heterochromatin formation (Halic & Moazed 2010). priRNAs are degradation products of various cellular transcripts (rRNA, tRNA, and mRNA), which are able to randomly associate with Argonaute according to their cellular abundance. Argonaute loaded priRNA would initiate silencing specifically at centromeric repeats because they are, unlike other genomic regions, bidirectionally transcribed (Figure 1.3.1.2.3, Figure 1.3.1.2.4). In that way antisense priRNA from centromeric region is able to find its sense complement, and could initiate siRNA generation. Once heterochromatin independent siRNAs accumulate from *dg* repeats, RNAi machinery will target centromeric transcripts and initiate positive-feedback loop of siRNA amplification and induce heterochromatin formation (described in Figure 1.3.1.1.1). This work also speculated that Argonaute associated priRNAs might play a role in RNAi-surveillance against repetitive elements and retrotransposons; these regions produce both sense and antisense transcripts which may generate threshold levels of antisense priRNAs. priRNAs could then guide Argonaute to these loci and induce silencing.

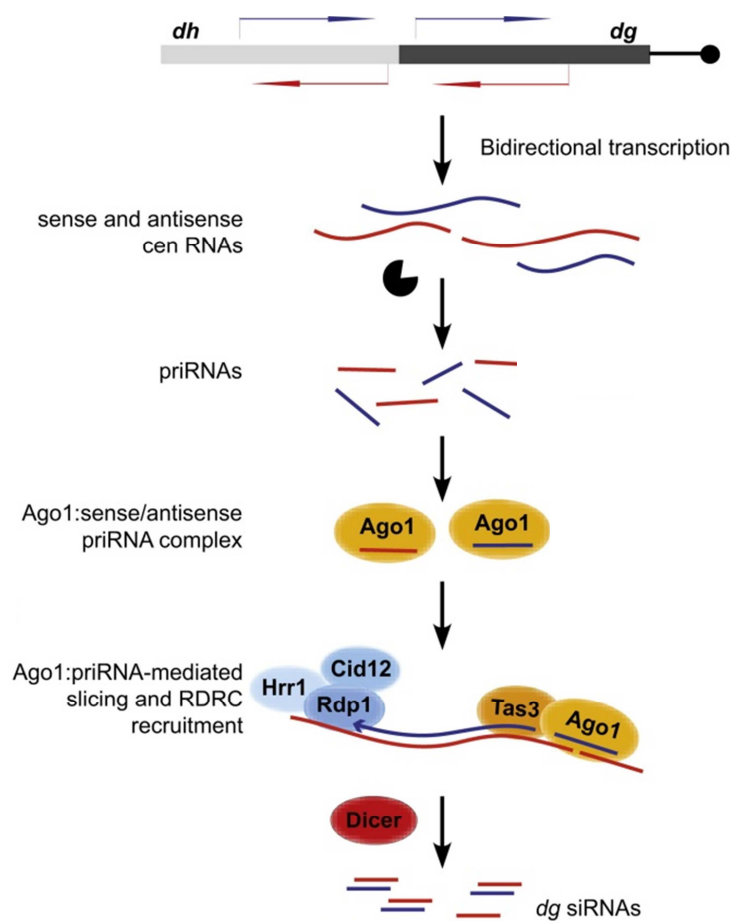


Figure 1.3.1.2.4. A model describing initiation of siRNA amplification and heterochromatin formation. (Adapted from (Halic & Moazed 2010)). priRNAs are degradation products originating from many genomic regions and associate with Ago1. Because centromeric region is bidirectionally transcribed, antisense priRNA from centromeric region loaded onto Ago1 is able to find its sense complement. For that reason, heterochromatin-independent siRNA amplification is initiated specifically on pericentromeric region. Once siRNAs accumulate, they initiate positive feedback loop of siRNA amplification and heterochromatin formation (Described in Figure 1.3.1.1.1).

A recently published study reported a difference in the levels of small RNAs in *dcr1Δ* and *rdp1Δ* cells obtained by deep-sequencing of Ago1-associated sRNAs (Yu et al. 2014). In this study, the levels of Ago1-associated sRNAs in *rdp1Δ* cells were higher than the ones in *dcr1Δ* cells, which suggest an existence of Dicer-dependent and Rdp1-independent small RNAs. This report favors the aforementioned first model of heterochromatin formation (Figure 1.3.1.2.1) and these small

RNAs were called primary siRNAs. It was proposed that convergent transcription and Dicer availability define RNAi initiation sites (Yu et al. 2014). Therefore, in fission yeast two distinct classes of Dicer-dependent and Dicer-independent small RNAs can induce siRNA amplification and heterochromatin formation.

1.3.2 Heterochromatin formation at the silent mating-type locus

Fission yeast mating-type region contains *mat2* and *mat3* silent donor loci with *K*-region, which comprises *cenH* element, in between (Figure 1.3.2.1). It was shown that 20-kb *mat* region is subjected to heterochromatin-mediated silencing (Hall et al. 2002). Similarly to pericentromeric region, at *mat* loci RNAi-mechanism is required for establishment of heterochromatin. In addition to RNAi, DNA-based mechanism operates in parallel to establish heterochromatin albeit at low efficiency. However, once heterochromatin is established, RNAi becomes dispensable for the maintenance of existing heterochromatin state (Hall et al. 2002).

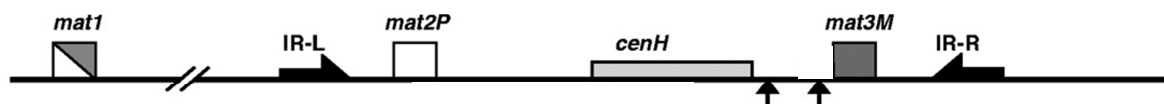


Figure 1.3.2.1. Schematic representation of the fission yeast mating-type region. (adapted from (Jia et al. 2004)). Heterochromatin forms over the entire 20-kb region and is restricted by the IR-R and IR-L boundary elements. Shaded box represents *cenH* element which is an siRNA producing locus and nucleation site of RNAi-dependent heterochromatin formation. *mat2* and *mat3* loci are deciphered in white and grey box. Black arrows represent binding site for Atf/Pcr1, which are operating in a parallel way to RNAi to maintain heterochromatin at *mat* region. Atf/Pcr1 mechanism is also able to nucleate heterochromatin in an RNAi-independent manner, however at very low efficiency.

RNAi-directed heterochromatin establishment occurs at 4.3-kb element of *K*-region, *cenH*, which contains clusters of short repeats homologous to pericentromeric *dg* and *dh* repeats. In an analogous way to pericentromeric repeats, *cenH* element is an siRNA-producing locus, which acts via RNAi-machinery to recruit CLRC complex to methylate nucleosomes on H3K9. This leads to subsequent binding of Swi6 that is required for the spreading of heterochromatin from nucleation site to the rest of the silent locus (Hall et al. 2002).

In the region between *cenH* and *mat3* loci, two heptamer sequences corresponding to the binding site of the transcription factor Atf1/Pcr1 have been found (Jia et al. 2004) (Figure 1.3.2.1, black arrows). Atf1 protein shows homology to the activating transcription factor (ATF), and Pcr1 to the cyclic AMP response element (CRE)-binding protein (CREB). ATF/CREB family proteins are highly conserved and are activated by stress mitogen-activated protein kinase (MAPK) pathway. Atf1/Pcr1 regulates gene expression during sexual differentiation and environmental stress. It was observed that, once bound to their binding sequences at *mat* region, Atf1/Pcr1 recruits histone deacetylase Clr6 and Swi6 (Kim et al. 2004) and are able to nucleate heterochromatin formation in an RNAi-independent way, but with low efficiency and at slow rate (Jia et al. 2004). However, Atf1/Pcr1 mechanism is completely capable of stable maintenance of pre-existing heterochromatin state in the absence of RNAi-machinery (Hall et al. 2002; Jia et al. 2004). It was demonstrated that in the Atf1/Pcr1 mechanism of heterochromatic silencing, upstream conserved MAPK pathway, comprising fission yeast Wis1 and Sty/Spc1 kinases, is required for the heterochromatic silencing (Kim et al. 2004).

1.3.3 Heterochromatin at subtelomeres

At fission yeast subtelomeres, two redundant pathways act to establish heterochromatin (Kanoh et al. 2005). The RNAi-dependent mechanism acts in an analogous manner as in the pericentromeric region and mating-type region: siRNAs are produced from a distal region of the subtelomere (Cam et al. 2005) that is homologous with pericentromeric *dg* and *dh* repeats, as well as with the *cenH* element present at the mating-type locus. These nucleation elements are part of the open reading frame that encodes a telomere-linked helicase (*tlh*). siRNA producing loci act via the RNAi machinery to recruit Swi6 and establish heterochromatin.

The redundant mechanism of heterochromatin establishment at subtelomeric region involves Taz1, a telomere binding protein of the TRF family. Taz1 is a component of the shelterin complex and is recruited to the telomere-associated sequence (TAS). It was demonstrated that Taz1 establishes Swi6 heterochromatin independently of the RNAi-pathway at the subtelomeres (Kanoh et al. 2005).

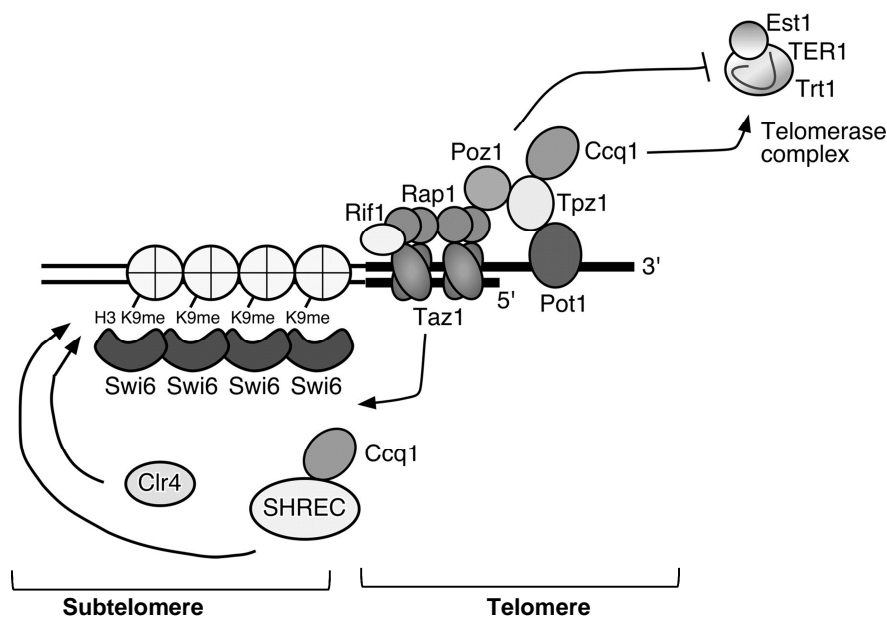


Figure 1.3.3.1. Model representing heterochromatin factors at fission yeast subtelomeres. (Adapted from (Khair et al. 2010)). RNAi-mediated nucleation of heterochromatin formation occurs at subtelomere elements which share homology to pericentromeric *dg* and *dh* repeats. RNAi-factors recruit Clr4 and subsequent heterochromatin formation. RNAi-independent nucleation involves Taz1, a protein that is part of the shelterin complex and binds to telomeric repeats. Taz1 promotes Clr4-dependent H3K9 methylation of surrounding nucleosomes and promotes accumulation of Swi6. Proteins Taz1, Rap1, Poz1, Tpz1, Pot1, and Ccq1 are part of the shelterin complex.

1.3.4 Islands of heterochromatin at euchromatic region

Several groups have observed that H3K9 methylation, in addition to major constitutive heterochromatin domains involving pericentromeric, subtelomeric and mating-type region in *S. pombe*, can be detected at around 30 additional locations across the genome (Zofall et al. 2012; Hiriart et al. 2012; Tashiro et al. 2013). These additional H3K9me containing loci, denoted as heterochromatin islands, are found at both convergent and non-convergent loci (Zofall et al. 2012) and comprise ncRNAs and meiotic mRNAs that are suppressed in vegetative growth phase. It was suggested that heterochromatin islands represent analogy to facultative heterochromatin in higher eukaryotes (Zofall et al. 2012). However, it was reported that deletion of heterochromatic factors at meiotic genes does not have an influence on the expression levels of

corresponding meiotic genes and it also does not restrict Pol II access, indicating that this heterochromatin does not have a functional role (Egan et al. 2014)

Formation of H3K9me at islands comprising meiotic transcripts involves Mmi1-dependent degradation mechanism, specifically proteins Mmi1 and Red1. It was shown that in vegetative cell phase, transcripts involved in sexual differentiation are transcribed, but are rapidly degraded. This degradation of meiotic transcripts during vegetative phase involves Mmi1 RNA elimination pathway (Holm & Thon 2012). Mmi1 is an RNA-binding protein that recognizes determinant of selective removal (DSR) sequences. DSR-containing sequences are found in meiotic transcripts, including the master regulators of meiotic event, Ste11 and Mei4. It was shown that Mmi1 recruits proteins Red1, Pab2 and Rrp6, which are involved in targeting the transcripts for degradation (Sugiyama & Sugiyama 2011). It was demonstrated that Red1 forms a nuclear RNA silencing (NURS) complex containing helicase Mtl1, zinc finger proteins Red5 and Ars2, RNA recognition motif (RRM)-containing protein Rmn1 and Iss10 (Egan et al. 2014; Lee et al. 2013). The complex provides a link between Mmi1 and the exosome-mediated RNA degradation.

Chromatin immunoprecipitation experiments detected that heterochromatin factors are localized at heterochromatin islands - CLRC subunits Raf2, Swi6, components of RITS and SHREC complex (Zofall et al. 2012). At majority of islands heterochromatin present in vegetative cell phase is established in an RNAi-independent manner (for example at *mcp7*, *ssm4*, *mei4*). However, heterochromatin was not established in *ago1Δ* cells at a subset of meiotic islands (for example at *mcp5*, *ncRNA eno101*) (Zofall et al. 2012). Also, components of RITS complex have been detected at some islands (*mei4*, *ssm4*) and in RNAi mutants a slight increase in their transcript levels was observed (Hiriart et al. 2012; Zofall et al. 2012; Tashiro et al. 2013).

In the period when fission yeast cells enter meiosis, which is induced by nitrogen deprivation, more than 200 genes involved in sexual differentiation are induced (Mata et al. 2002). Mmi1 is sequestered into meiosis specific structure, Mei2 dot (Watanabe & Yamamoto 1994), resulting in stabilization of DSR-containing transcripts. It was demonstrated that upon nitrogen starvation, which induces meiosis, H3K9me is reduced at the islands *mei4* and *ssm4*, which is also accompanied with the loss of the localization of RITS at these islands (Hiriart et al. 2012).

1.5 Aim of the thesis

Previously, a class of Dicer-independent Argonaute-associated small RNAs called priRNAs has been identified in fission yeast (Halic & Moazed 2010). priRNAs are degradation products originating from various genomic regions and it was suggested that they drive amplification of siRNAs. This process subsequently leads to heterochromatin formation. priRNAs are produced independently of Dicer, Rdp1 and Argonaute-slicer activity, which raises the question of their biogenesis. Because Argonaute-slicer activity is dispensable for their generation, 5' end of priRNA is likely generated by endo- or exonuclease activity (Figure 1.5.1).

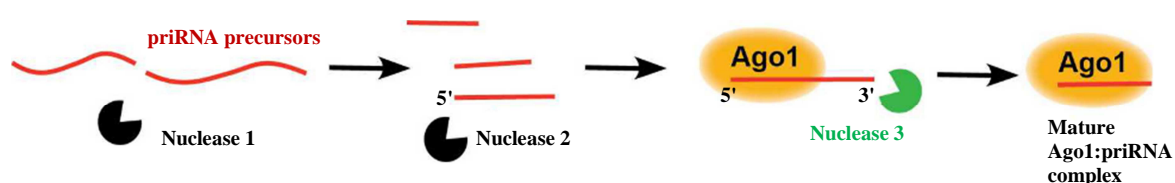


Figure 1.5.1. Schematic representation of predicted steps in biogenesis of priRNAs in *S. pombe*. priRNAs are generated independently of Dicer, Rdp1 and Argonaute-slicer activity (Halic & Moazed 2010). Thus, 5' end of priRNAs is possibly generated by one or more endo/ exonucleases. Then, priRNA precursor is loaded onto Argonaute and 3' end is defined by a nuclease activity. priRNAs are deciphered in red; hypothetical nucleases 1 and 2 which generate 5' end are deciphered in black; hypothetical nuclease generating 3' end is deciphered in green.

Furthermore, it was suggested that the 3' ends of siRNAs are shaped by the trimming activity of an unknown nuclease. This notion came from deep-sequencing data of small RNAs associated with slicer-defective Ago1-D580A (Halic & Moazed 2010). In Ago1-D580A, the passenger strand cannot be released and thus bound siRNAs remain double-stranded. The centromeric Ago1-D580A-bound ds-siRNAs show a broader length distribution (from 21-27-nt) when compared to siRNAs bound to wild-type Argonaute, which are mainly 21-23-nt long. This indicated that Argonaute is able to bind longer ds-RNA precursors, which are then trimmed to the mature size after the release of the passenger strand. This is also consistent with the finding that

Dicer in *S. pombe* lacks a PAZ domain and thus generates products of varying sizes (Colmenares et al. 2007).

The main focus of this work was the identification of factors involved in biogenesis of priRNAs (Figure 1.5.1) and siRNAs. To do that, combination of splinted ligation assays as a screening method and sequencing of Argonaute-associated small RNAs was employed. To validate the results and elucidate the mechanism of small RNA generation, biochemical characterization by a combination of *in vitro* assays was performed. Next, *in vivo* assays were employed to show the effects on cell phenotype. Also, the requirements for establishment and maintenance of heterochromatin at pericentromeric region, heterochromatin islands and in a perturbed system were explored. Parts of this thesis have been published (Marasovic et al. 2013).

2 RESULTS

2.1 SPBC29A10.09c and Rrp6 are involved in biogenesis of priRNAs and siRNAs

In order to gain insight in factors involved in the biogenesis of Dicer-independent priRNAs, several strains with genomic deletion of potential candidate genes were created previously in the laboratory by PCR-based gene targeting method in *dcr1Δ* strain. Endogenously tagged FLAG-Argonaute was purified from the created strains and Argonaute-associated small RNAs were phenol-chloroform extracted and ethanol-precipitated. The levels of Argonaute-associated centromeric *dg* repeats were then assessed by the splinted ligation assay using five different centromeric small RNAs mapping to *dg* transcript (Maroney et al. 2008; Halic & Moazed 2010). Splinted ligation is around 50-times more sensitive than Northern blotting, so it was possible to detect very low levels of small RNAs that are present in *dcr1Δ* background (Halic & Moazed 2010). The deletion of two nucleases resulted in the significant change in the levels of *dg* repeats: Rrp6 and SPBC29A10.09c (Figure 2.1.1). While in *dcr1Δrrp6Δ* cells a 10-fold increase in the *dg* priRNA levels was observed (Figure 2.1.1 D), in *dcr1ΔSPBC29A10.09cΔ* cells *dg* priRNAs were not detectable at all (Figure 2.1.1 A, Figure 2.1.1 B). Gene *SPBC29A10.09c* was also deleted in wild-type (wt) cells where a 2-fold reduction in the levels of Ago1-associated *dg* and *dh* siRNAs was observed by splinted ligation (Figure 2.1.1 C).

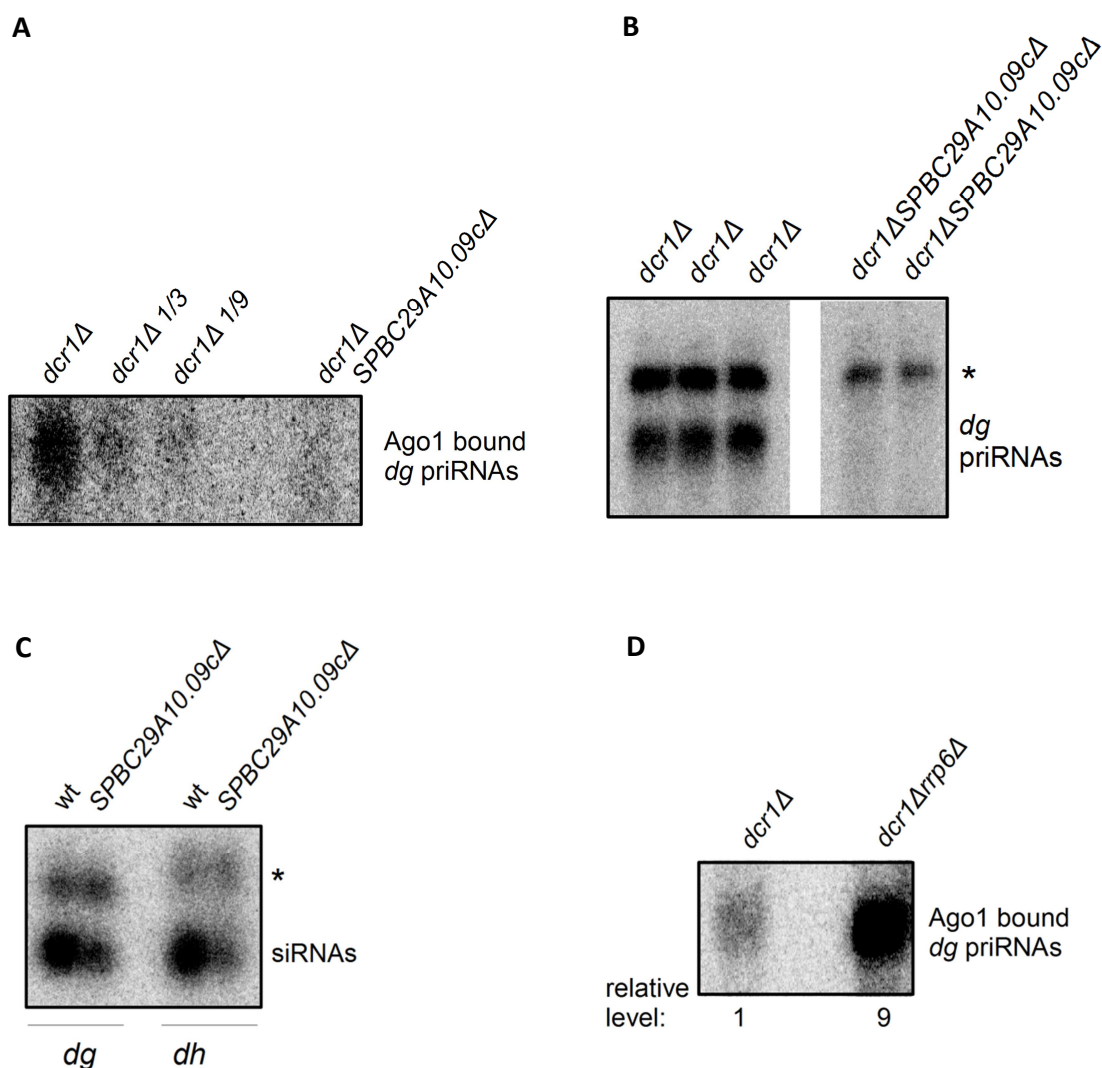


Figure 2.1.1. SPBC29A10.09c and Rrp6 are involved in the biogenesis of priRNAs and siRNAs. (A) Splinted ligation detection of Argonaute-associated *dg* priRNAs in indicated mutant cells. Five different centromeric small RNAs mapping to *dg* transcripts were tested. One-third and one-ninth of Argonaute-associated small RNAs from *dcr1Δ* cells were assayed. (B) Splinted ligation detection of Argonaute-associated *dg* priRNAs in *dcr1Δ* and *dcr1ΔSPBC29A10.09cΔ* cells. Argonaute-associated small RNAs from indicated mutant cells were purified in triplicate and duplicate. *marks nonspecific band. (C) Splinted ligation detection of Ago1-associated *dg* and *dh* priRNAs in wild-type (wt) and *SPBC29A10.09cΔ* cells. Five different centromeric small RNAs mapping to *dg* and *dh* transcripts were tested. *marks nonspecific band. (D) Splinted ligation detection of Argonaute-associated *dg* priRNAs in *dcr1Δ* and *dcr1Δrrp6Δ* cells.

Because SPBC29A10.09c is a previously uncharacterized protein and splinted ligation assay indicated that it has a significant effect on the levels on both priRNAs and siRNAs, the study was focused on the further characterization of this protein. To find out whether SPBC29A10.09c has an effect on the levels of other, noncentromeric priRNAs and siRNAs, endogenously tagged FLAG-Ago1 was purified from wild-type, *SPBC29A10.09cΔ*, *dcr1Δ* and *dcr1ΔSPBC29A10.09cΔ* cells using anti-FLAG-M2 agarose beads. Argonaute-associated small RNAs were phenol-chloroform extracted, ethanol-precipitated and dephosphorylated using CIP (NEB). After resuspending precipitated small RNAs in RNase-free water, they were ³²P labeled on 5' end and separated on polyacrylamide-urea gel (Figure 2.1.2). In *dcr1ΔSPBC29A10.09cΔ* cells Ago1-associated priRNAs were around 10-fold reduced when compared to *dcr1Δ* cells. The effect of *SPBC29A10.09c* deletion on the levels of siRNAs was more modest as reduction of around 2-fold was observed in *SPBC29A10.09cΔ* cells when compared to wt cells (Figure 2.1.2).

Also, the levels of FLAG-Ago1 from immunoprecipitated fraction (IP) and total cell lysate (Input) were detected by western blot and quantified (Figure 2.1.1, lower panel). It was observed that Argonaute was reduced in both Input and IP in *dcr1Δ* and *dcr1ΔSPBC29A10.09cΔ* cells. This is consistent with the findings in various organisms that empty Argonaute is not very stable when RNAi machinery and siRNA production are compromised and is targeted for degradation (Frohn et al. 2012; Gibbings et al. 2012).

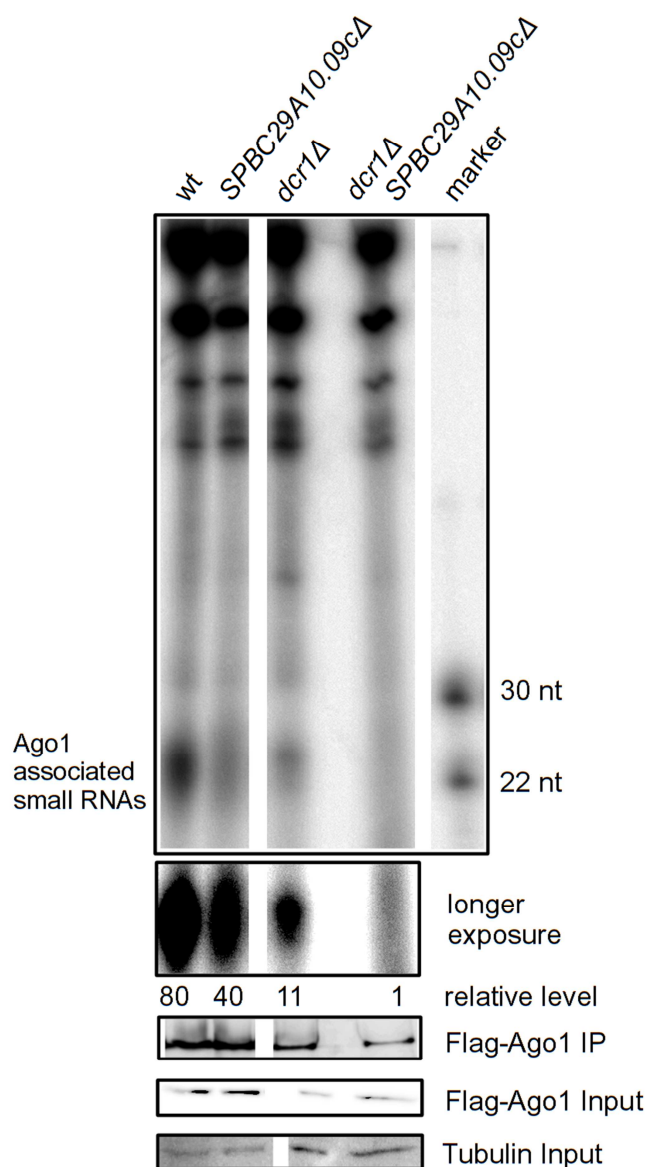


Figure 2.1.2. Gel showing Argonaute-associated RNAs purified from wild-type, *SPBC29A10.09cΔ*, *dcr1Δ* and *dcr1ΔSPBC29A10.09cΔ* cells. RNAs were 5' ^{32}P labeled, separated on polyacrylamide-urea gel and the bands were visualized by phosphor imaging. The assay was performed in five independent replicates which were used for quantification. Lower panels show western blot detection of FLAG-Argonaute in immunoprecipitated fraction (IP) and total cell lysate (Input) in indicated cells. Tubulin was used as a loading control.

2.2 Caf1 does not have an effect on the levels of Argonaute-associated small RNAs

SPBC29A10.09c is a CAF1 family exonuclease. Does canonical Caf1 has a similar effect on the levels of Argonaute-associated small RNAs as SPBC29A10.09c? To answer this question, endogenously tagged FLAG-Ago1 was purified from *caf1* Δ cells and wild-type and Argonaute-associated small RNAs were phenol-chloroform extracted. Ethanol-precipitated small RNAs were resuspended in formamide and analyzed on polyacrylamide-urea gel. The bands were detected by staining with SybrGold. It was observed that the levels of Argonaute-associated small RNAs did not significantly change in *caf1* Δ cells.

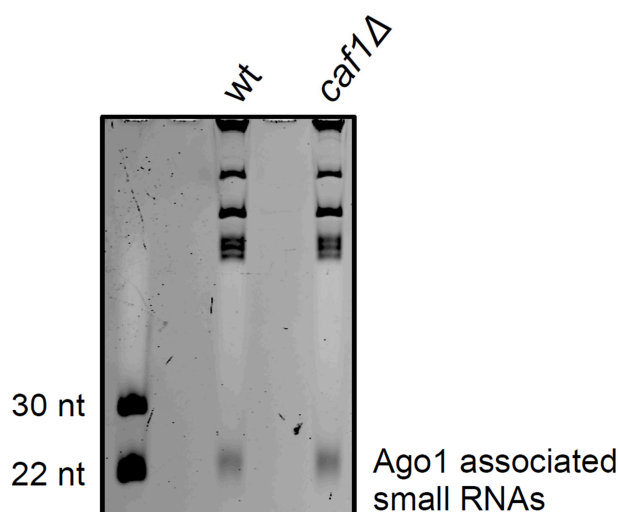


Figure 2.2.1. SybrGold stained denaturing urea-polyacrylamide gel showing Argonaute-associated RNAs purified from wild type and *caf1* Δ cells.

2.3 In *SPBC29A10.09c*Δ cells both priRNAs and siRNAs are longer

Further analysis of the impact of *SPBC29A10.09c* on the length and distribution of Argonaute-associated small RNAs was done by deep sequencing of Argonaute-associated small RNAs using Illumina G2 analyzer. FLAG-Argonaute was purified from wild-type, *SPBC29A10.09c*Δ, *dcr1*Δ and *dcr1*Δ*SPBC29A10.09c*Δ cells and Ago1-associated small RNAs were phenol-chloroform extracted and ethanol-precipitated. Small RNAs were separated on polyacrylamide-urea gels and bands in the size range from 20-27 nt were excised, eluted and used for preparation of small RNA libraries (described in the chapter 4.2.2.7).

In the sequencing libraries of all strains, small RNAs had strong preference for 5' uracil which validated their association with the Argonaute (Figure 2.3.1 A). The predominant length of Ago1-associated priRNAs in *dcr1*Δ cells and siRNAs in wild-type cells was 22-23 nt (Figure 2.3.1 B, Figure 2.3.1 C). However, it was observed that in *SPBC29A10.09c*Δ cells, both the length distribution of priRNAs and siRNAs were severely altered: priRNAs were 23-27 nt long (Figure 2.3.1 B), while siRNAs were 20-27 nt long (Figure 2.3.1 C). The finding that priRNAs and siRNAs are longer in *SPBC29A10.09c*Δ cells indicated that the length of small RNAs is modified by *SPBC29A10.09c*.

Moreover, the length distribution of centromeric siRNAs that are purified from the total RNA fraction from wild-type cells was compared to the length distribution of centromeric Argonaute-associated siRNAs from *SPBC29A10.09c*Δ cells (Figure 2.3.1 D). It was observed that these length distributions strongly correlate. This suggested that in the course of small RNA biogenesis, Argonaute first binds longer small RNAs from the total fraction, which are then subjected to trimming activity, performed by the newly identified protein.

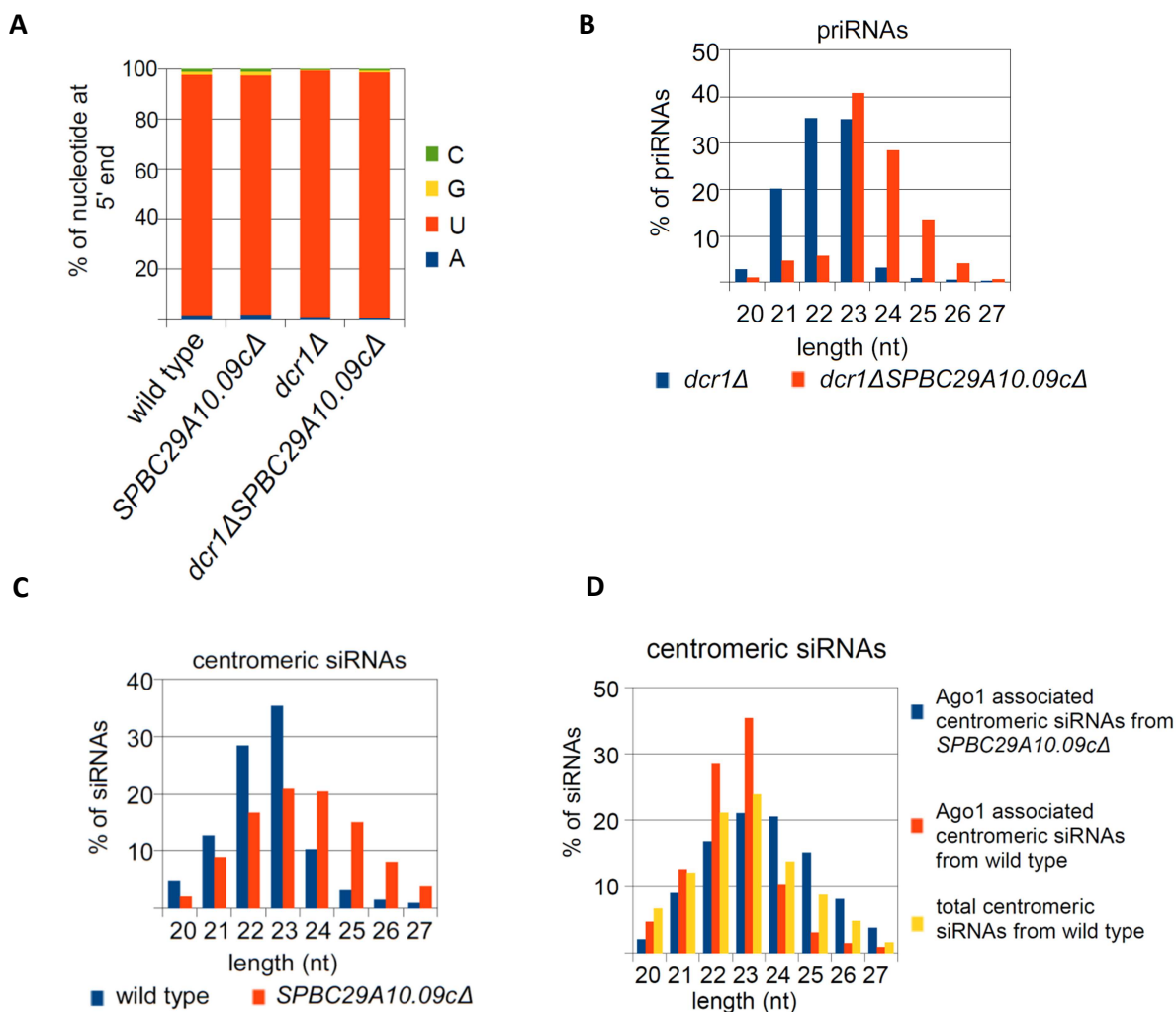


Figure 2.3.1. High-throughput sequencing of Argonaute-associated small RNAs from indicated cells.

(A) 5' nucleotide preference of Argonaute-associated small RNAs from indicated cells. 5' uracil preference validates that small RNAs are associated with the Argonaute. (B), (C) Length distribution of Argonaute-associated small RNAs from indicated cells. Both priRNAs and siRNAs are longer in *SPBC29A10.09cΔ* cells. (D) Length distribution of centromeric siRNAs associated with the Argonaute in *SPBC29A10.09cΔ* cells (blue) or in wild-type cells (red), and centromeric siRNAs from the total fraction in wild-type cells (yellow).

2.4 SPBC29A10.09c is a Mg^{2+} -dependent 3'-5' exonuclease named Triman

The gene *SPBC29A10.09c* codes for a 40.01 kDa protein that has a catalytic domain which belongs to the CAF1 family of 3'-5' exonucleases. Above described findings suggested that it is involved in the generation and final trimming of Argonaute-associated small RNAs in *S. pombe* and therefore we named this previously uncharacterized gene *triman* (*tri1*).

2.4.1 Purification of FLAG-Triman and FLAG-TrimanD28A

To gain further insight in the mechanism of Triman-mediated generation of priRNAs and siRNAs, it was necessary to express and purify the protein and reconstitute the activity *in vitro*. Also, to confirm that the observed activity is specific to Triman nuclease activity, an activity mutant was generated. D28A point mutation in the active site of Triman was designed based on the homology to the catalytic domain of canonical Caf1. PREP1 plasmids bearing FLAG-Triman and FLAG-TrimanD28A activity mutant were created by PCR-based method, and the proteins were overexpressed and purified from *S. pombe* cells using anti-FLAG-M2 agarose beads. Purified proteins were analyzed on SDS polyacrylamide gel and the bands were visualized by staining with SimplyBlue (Figure 2.4.1.1).

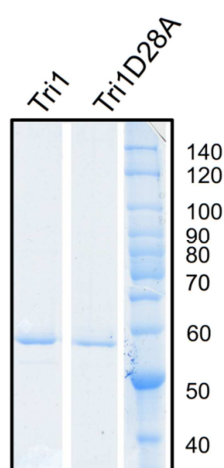


Figure 2.4.1.1. SDS polyacrylamide gel showing purification of FLAG-Triman and FLAG-TrimanD28A activity mutant that were overexpressed in *S. pombe* cells.

2.4.2 Reconstitution of Triman activity *in vitro*

Because CAF1 family nucleases are primarily deadenylases, Triman activity was examined on non-polyadenylated and polyadenylated RNA templates. 100 ng of purified Triman was incubated with a 100 fmol of 5' ^{32}P labeled dgRNA100 or dgRNA100+30A in a 10 μl reaction containing MgCl_2 buffer (25 mM Hepes 7.5, 2 mM MgCl_2 , 2 mM DTT, 0.02 % NP40) or EDTA buffer (25 mM Hepes 7.5, 2 mM EDTA, 2 mM DTT, 0.02 % NP40) for 10 min on 32 °C. Reactions were mixed with formamide, analyzed on 18 % polyacrylamide-urea gel and RNAs were visualized by phosphor imaging (Figure 2.4.2.1 A). In reactions containing MgCl_2 buffer, Triman was capable of degrading both poly(A) RNA template and non-poly(A) RNA template. However, this nuclease activity was abolished in the reactions that contained EDTA. This demonstrated that Triman is a Mg^{2+} -dependent exonuclease.

In order to confirm that the observed degradation is specific to the nuclease activity, 100 fmol of 130-nt-long RNA Ura4RNA100+30A was incubated with 100 ng of purified Triman or TrimanD28A activity mutant for 10 min and 60 min on 32 °C in reactions that contained MgCl_2 buffer (Figure 2.4.2.1 B). It was observed that D28A point mutation in the active site abolished the nuclease activity. Numerous intermediate degradation products indicated that Triman is a 3'-5' exonuclease which removes only few nucleotides before probable dissociation from the RNA template.

Next, reactions containing 100 fmol dgRNA100 or dgRNA100+30A and Triman in MgCl_2 buffer were incubated on 32 °C for 10 min, 100 min and ON (Figure 2.4.2.1 C). It was observed that longer incubation time resulted in shorter products that were eventually completely degraded.

In the above-mentioned assays, 100-nt and 130-nt-long RNA templates were used to test Triman activity (Figure 2.4.2.1 A-C). To explore if the enzyme's activity depends on the length of RNA templates, also siRNAs were used as Triman substrates. Triman was incubated with various small 5' ^{32}P labeled RNA templates: RNA69, RNA172, RNA71 for 10 min and 100 min. Reactions were analyzed on polyacrylamide-urea gels and imaged by phosphor imaging (Figure 2.4.2.1 D). This assay showed that Triman was also competent to degrade short RNA templates (22-30 nucleotides).

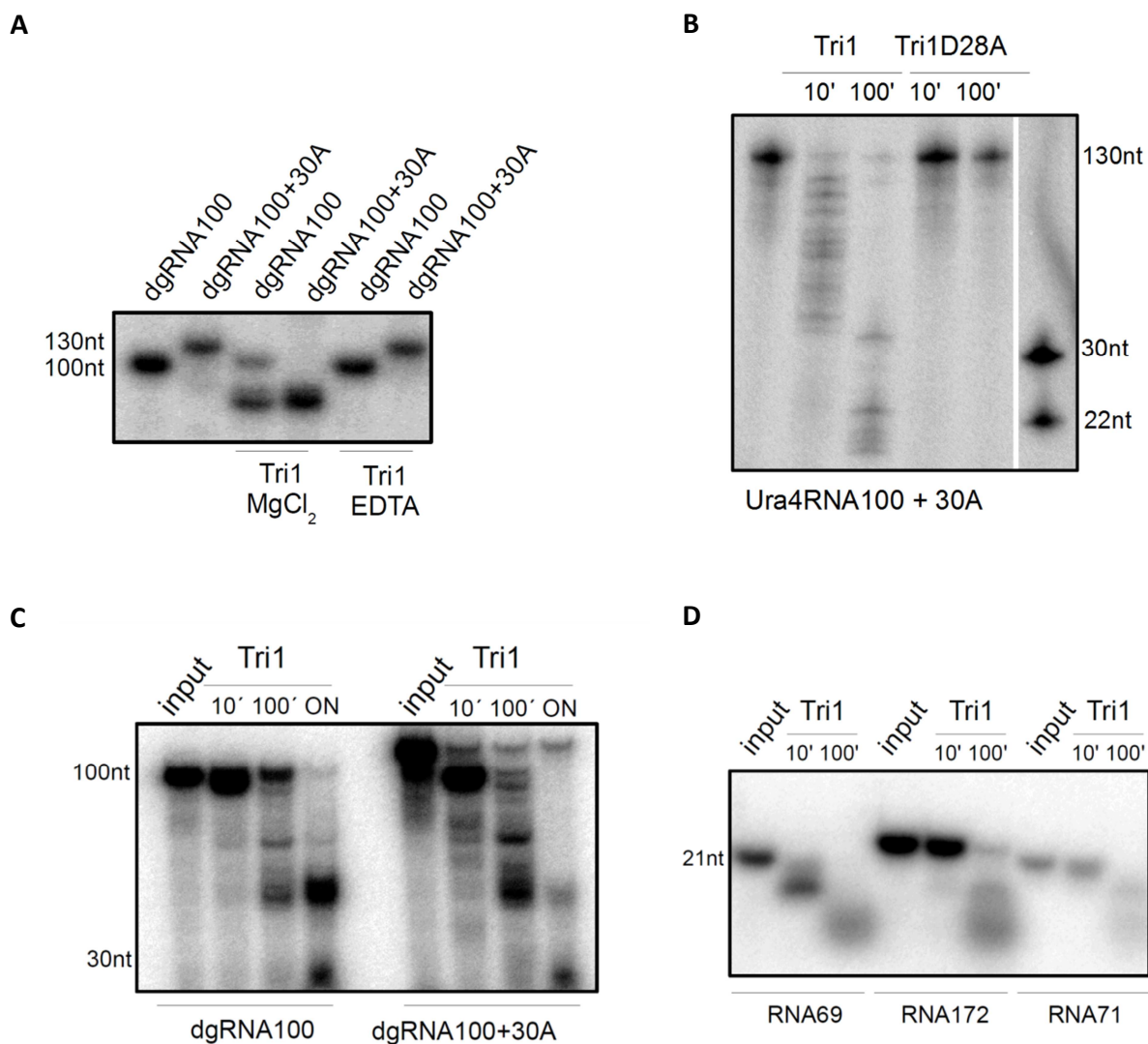


Figure 2.4.2.1. Reconstitution of Triman activity on 5'³²P labeled single-stranded RNA templates *in vitro*. Reactions were separated on polyacrilamide-urea gels and imaged by phosphor imaging. (A) Gel showing Triman activity on dgRNA100 or dgRNA100+30A in a buffer containing either Mg²⁺ or EDTA. (B) Gel showing Triman and TrimanD28A activity on Ura4RNA100+30A templates. D28A mutation abolished the nuclease activity. (C) Gel showing Triman activity on dgRNA100 or dgRNA100+30A for 10min, 100 min and ON. Longer incubation time resulted in more RNA degradation. (D) Gel showing Triman activity on small RNAs RNA69, RNA172, RNA71. Triman activity is not dependent on the length of RNA template.

In the reconstitution assays of Triman activity, specific intermediate degradation products were often observed (Figure 2.4.2.1 B, Figure 2.4.2.1 D). This suggested that RNA secondary structure might inhibit nuclease activity of Triman. Therefore, Triman activity was probed on 100-nt-long double-stranded RNA template (dsUraRNA100) and 22-nt-long double-stranded RNA template (dsRNA71). 100 fmol of 5' 32 P labeled dsUraRNA100 (Figure 2.4.2.2 A) or dsRNA71 (Figure 2.4.2.2 B) was incubated with Triman in $MgCl_2$ buffer at 32 °C for 10 min and 100 min. It was observed that Triman was not able to degrade neither 100-nt-long dsRNA templates nor 22-nt-long double-stranded siRNAs.

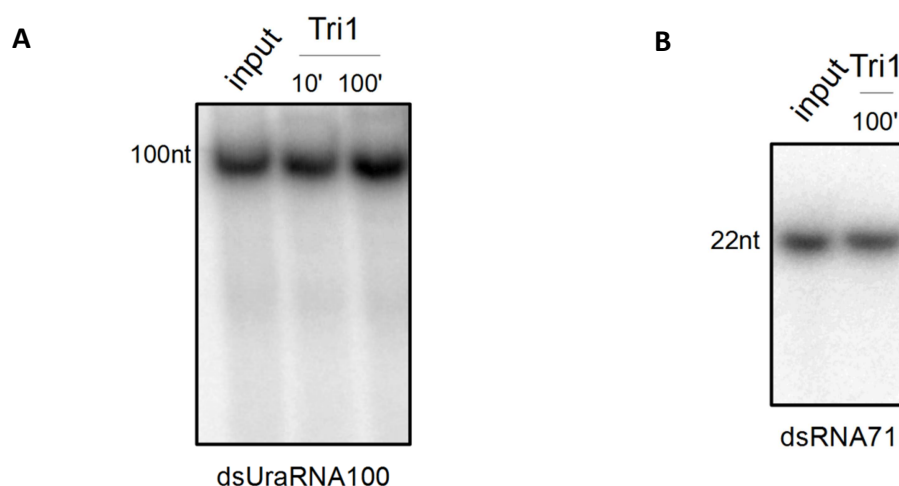


Figure 2.4.2.2. Reconstitution of Triman activity on 5' 32 P labeled double-stranded RNA templates in *vitro*. Reactions were separated on polyacrilamide-urea gels and imaged by phosphor imaging. (A) Gel showing Triman activity on 100nt long double-stranded RNA template *dsUraRNA100*. Incubation time is indicated. (B) Gel showing Triman activity on 22 –nt-long double-stranded RNA template *dsRNA71*.

The above-described assays demonstrated that Triman is a Mg^{2+} -dependent nuclease which degrades only single-stranded RNA templates (Figure 2.4.2.1, Figure 2.4.2.2). The 'ladder' shaped degradation pattern of Triman activity (Figure 2.4.2.1 B) and the conservation of the active site with CAF1 family proteins, suggested that Triman is an exonuclease. To validate that Triman is an exonuclease and not an endonuclease, Triman activity was tested on RNA templates that do not contain free 2' hydroxyl (OH) group on the 3' end.

To obtain the 3' modified RNA-template, β -elimination reaction was performed. 20 pmol of RNA72 was subjected to oxidation and β -elimination reaction. Triman activity was reconstituted by incubating 1 pmol of 22-nt-long RNA72 or β -eliminated RNA72 with 2 μ l of Triman in a 10 μ l reaction containing MgCl_2 buffer for 100 min at 32 °C. Reactions were mixed with formamide, analyzed on polyacrylamide-urea gel and visualized by staining with SybrGold (Figure 2.4.2.3 A). Nuclease activity was not observed on oxidized and β -eliminated RNA72 which had 3' monophosphate.

Similarly, Triman was incubated with 1 pmol of RNA72 and with RNA templates that contained 2-O-methyl-groups (2'Ome) on each nucleotide: RNA-2Ome1 or RNA_2Ome2, in MgCl_2 buffer for 100 min at 32 °C (Figure 2.4.2.3 B). While RNA72 that has free 2' OH group was degraded, 2-O-methyl containing RNAs were not degraded. These results confirmed that Triman is indeed 3'-5' exonuclease.

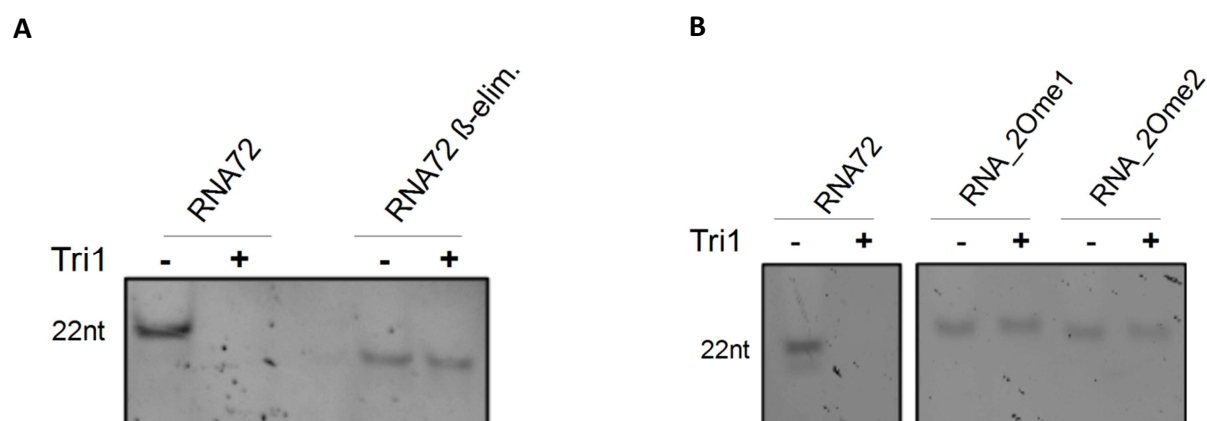


Figure 2.4.2.3. Triman requires free 2'OH group for the activity which confirms it is a 3'-5' exonuclease. (A) SybrGold stained polyacrylamide-urea gel showing Triman activity on single-stranded RNA72 and β -eliminated RNA72. (B) SybrGold stained polyacrylamide-urea gels showing Triman activity on RNA72 and RNA templates which have 2'Ome modification on each nucleotide (RNA-2Ome1 and RNA_2Ome2).

2.5 Argonaute acts as a ruler for the final length of small RNA

Triman *in vitro* reconstitution assays showed that Triman does not generate RNAs of a defined length; longer incubation time of Triman and RNA templates resulted in more degradation products (Chapter 2.4.2). Thus, the specificity for the final length is determined by another factor. Previously it was shown that in Ago1-D580A slicer mutant, Ago1-associated sRNAs remain double-stranded (Buker et al. 2007; Halic & Moazed 2010). Moreover, this Ago1-D580A-bound ds-siRNAs had a broader length distribution than the ones bound to the slicer-competent wt Argonaute (Halic & Moazed 2010). This and the above-mentioned assays suggested that Ago1 binds longer Dicer-generated small RNA duplexes. After the release of the passenger strand, longer Ago1-bound small RNA guide undergoes trimming reaction of the 3' end by Triman.

To reconstitute this final trimming step *in vitro*, an assay was performed where resin-bound Argonaute, loaded with RNAs of various lengths, was incubated with Triman. By using resin-bound Argonaute, it was possible to wash away RNAs that were not loaded onto Argonaute. First, 10 pmol of RNA72 (22ntRNA), RNA172 (30ntRNA) and RNA184 (26ntRNA) were radioactively labelled on the 5' end by PNK for 30 min at 37 °C. All following steps were performed by incubating the reactions at 32 °C in thermomixer.

Labeled small RNA molecules were loaded onto resin-bound Ago1; around 2 µl of the resin-bound Argonaute (50-200 ng) was incubated with 1 µl of 5' ³²P labeled RNAs (50 fmol) in a 10 µl reaction containing MgCl₂ buffer and 1 µl RNase inhibitor for 2 h. After loading, unbound small RNAs were washed away by adding 1 ml of the washing buffer (25 mM Hepes 7.5, 2 mM MgCl₂, 2 mM DTT, 0.02 % NP40, 100 mM NaOAc), pipetting the reactions 4 times up and down, centrifugation for 2 min at 14000 g and removing the supernatant from the resin-bound Argonaute. The washing step was repeated 2 times. Then, 2 µl of Triman, or alternatively 2 µl of RNase-free water (control reaction), was added to the resin-bound Argonaute that is loaded with sRNAs and incubated for 90 min. Also, the reactions containing only RNAs and Triman were mixed and incubated. As a control for non-specific binding of small RNAs to the resin, reactions containing resin alone and RNAs were mixed. small RNAs were extracted by adding phenol-

chloroform, ethanol-precipitated and analyzed on 18 % polyacrylamide-urea gel. Phosphor imaging was used to detect RNAs (Figure 2.5.1 A, Figure 2.5.1 B).

It was observed that incubation of the resin-bound Argonaute that was loaded with 30-nt-long sRNA with Triman resulted in generation of a specific product migrating around 22 nt (Figure 2.5.1 A). Incubation of free 30-nt-long sRNA with Triman, as expected, resulted in a complete degradation of small RNA. Unspecific binding of small RNAs to the resin was not observed. In contrast to the reaction containing 30-nt-long sRNAs, incubation of the resin-bound Argonaute loaded with 22-nt-long RNA with Triman did not change the length of small RNA – it remained 22-nt-long (Figure 2.5.1 A).

Similar result was observed when resin-bound Argonaute was incubated with 26-nt-long RNA and Triman (Figure 2.5.1 B). In this reaction also a specific product of the size of 22-nt was observed. These observations were in an agreement with the sequencing data of Argonaute-associated sRNAs and indicated that Argonaute indeed acts as a protective factor and determines the final length of small RNA which is 22 nucleotides.

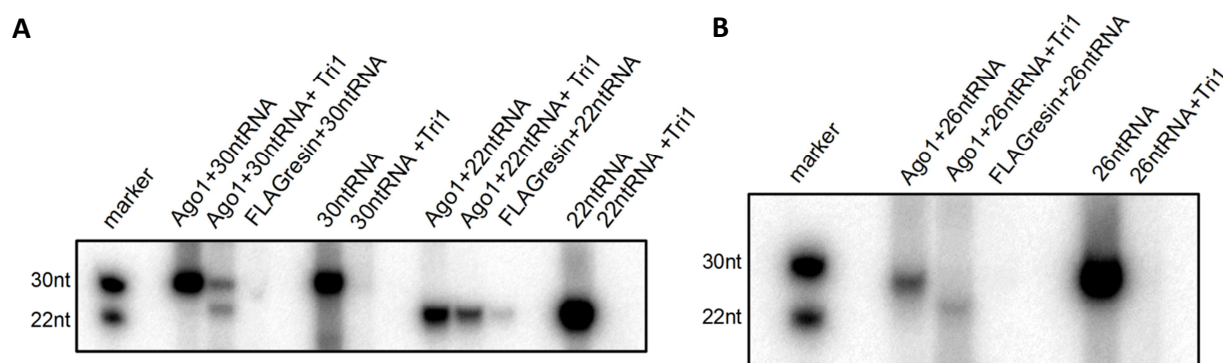


Figure 2.5.1. Argonaute acts as a ruler for the final length of small RNAs. Triman activity on Argonaute-associated single-stranded RNA templates that are (A) 30- and 22-nt-long and (B) 26-nt-long. Small RNAs were 5' ³²P labeled, loaded onto resin-bound Argonaute and unbound fraction was washed away. Argonaute-associated small RNAs were incubated with Triman. Reactions were separated on polyacrylamide-urea gels and imaged by phosphor imaging. Incubation of Argonaute-associated small RNAs that are longer than 22 nt with Triman results in a generation of a mature 22-nt-long small RNAs.

To determine whether Triman is able to process very long Ago1-bound RNA molecules, an assay employing 63-nt-long RNA (*RNA63*) was performed. 100 fmol of 5' ^{32}P labeled *RNA63* was mixed with FLAG-Ago1 to enable loading of RNA onto Ago1 for 1 h at 32 °C. After incubation, Triman was added and reaction was incubated for an additional 1 h at 32 °C.

A product of a mature size around 22-23 nt was formed in a reaction containing *RNA63*, Argonaute and Triman (Figure 2.5.2, lane 5). In contrast, in a control reaction which contained Ago1 and *RNA63* no signal was observed (Figure 2.5.2, lane 4). Moreover, when *RNA63* and Triman were mixed without Argonaute, signal of the specific size was not observed (Figure 2.5.2, lane 3). This assay showed that Triman is also able to trim longer RNA molecules that are bound to Argonaute. The observed signal of trimmed Argonaute associated sRNA was very weak due to inefficient binding of long RNA onto Argonaute.

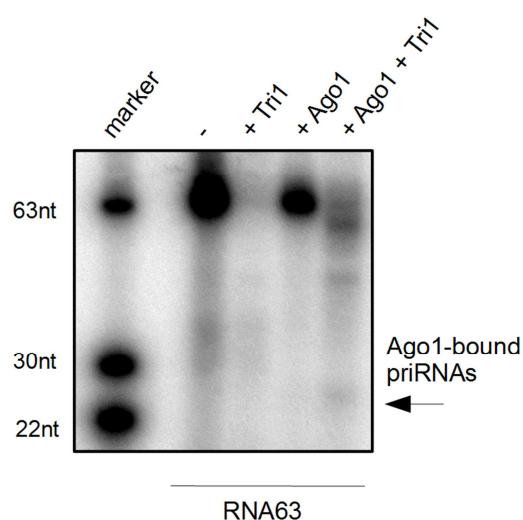


Figure 2.5.2. Triman activity on Argonaute-associated 5' ^{32}P labeled 63-nt-long RNA template. Reactions were separated on polyacrilamide-urea gels and imaged by phosphor imaging. Only in the presence of Argonaute product of the mature size of 22-23 nt was generated.

2.6 Triman processes longer priRNA precursors purified from *dcr1Δtri1Δ* cells

In the next assay, we reconstituted Triman activity on longer priRNA precursors that are bound onto Argonaute in *dcr1Δtri1Δ* cells. Therefore, Argonaute with copurifying RNAs was purified from *dcr1Δtri1Δ* cells and incubated with 50-200 ng of Triman for 90 min on 32 °C. Ago1-copurifying RNAs were recovered by phenol-chloroform, ethanol-precipitated, and dephosphorylated using CIP (NEB). Subsequently, dephosphorylated RNAs were 5' ³²P labeled and analyzed on 18 % polyacrylamide-urea gel.

It was previously shown that agarose beads, which are used for protein purification, bind also some RNAs from the cell lysate (Halic & Moazed 2010). These nonspecifically copurifying RNAs that are not bound by Argonaute were thus also observed on the polyacrylamide-urea gel and were marked by black arrows (Figure 2.6.1 A). It was observed that Triman was trimming longer priRNA precursors that were associated with Argonaute in *dcr1Δtri1Δ* cells to the mature size of 22-nt (Figure 2.6.1 A, red box). Other, nonspecifically copurifying RNAs that are binding to the resin and are not bound by Argonaute (Halic & Moazed 2010) were not degraded (Figure 2.6.1 A, black arrows). This assay illustrates that Triman is specifically degrading Argonaute-associated sRNAs and indicates that Triman is recruited by Argonaute.

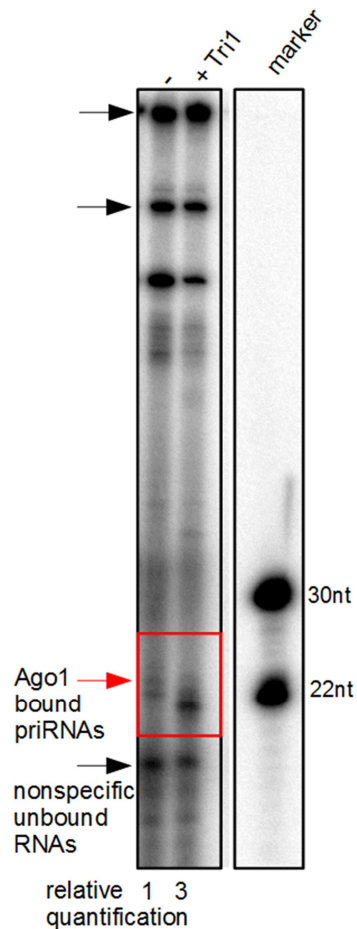


Figure 2.6.1. Triman processes longer Argonaute-associated RNA precursors purified from *dcr1Δtri1Δ* cells. Argonaute-copurifying RNAs were incubated with Triman, 5' 32 P labeled, separated on polyacrilamide-urea gels and imaged by phosphor imaging. Triman activity was specific to Argonaute-associated small RNAs (red-box and red arrow) (Halic & Moazed 2010). Black arrows denote nonspecific-copurifying RNAs that are binding to the resin, but are not associated with the Argonaute (Halic & Moazed 2010). Five different replicates were used for quantification.

2.7 Triman overexpression generates more small RNAs *in vivo*

Next, we asked whether Triman overexpression (Tri1OE) would result in generation of more priRNAs *in vivo*. To do that, we overexpressed Triman from the strong *nmt1* promotor in *dcr1Δ* cells (*dcr1Δ*+Tri1OE). FLAG-Ago1 was purified from wild-type, *dcr1Δ*, *dcr1Δ*+Tri1OE, and *dcr1Δtri1Δ* cells using anti-FLAG-M2 agarose beads. Argonaute-associated small RNAs were phenol-chloroform extracted and dephosphorylated using CIP (NEB). After resuspending

precipitated small RNAs in RNase-free water, they were ^{32}P labeled on 5' end and separated on polyacrylamide-urea gel (Figure 2.7.1 A). It was observed that Tri1OE resulted in production of several-fold more Argonaute-associated priRNAs, indicating that trimming represents limiting step in the course of priRNA biogenesis. Furthermore, sequencing of Argonaute-associated small RNAs showed that when Triman is overexpressed, both priRNAs and siRNAs are 1 nucleotide shorter (Figure 2.7.1 B).

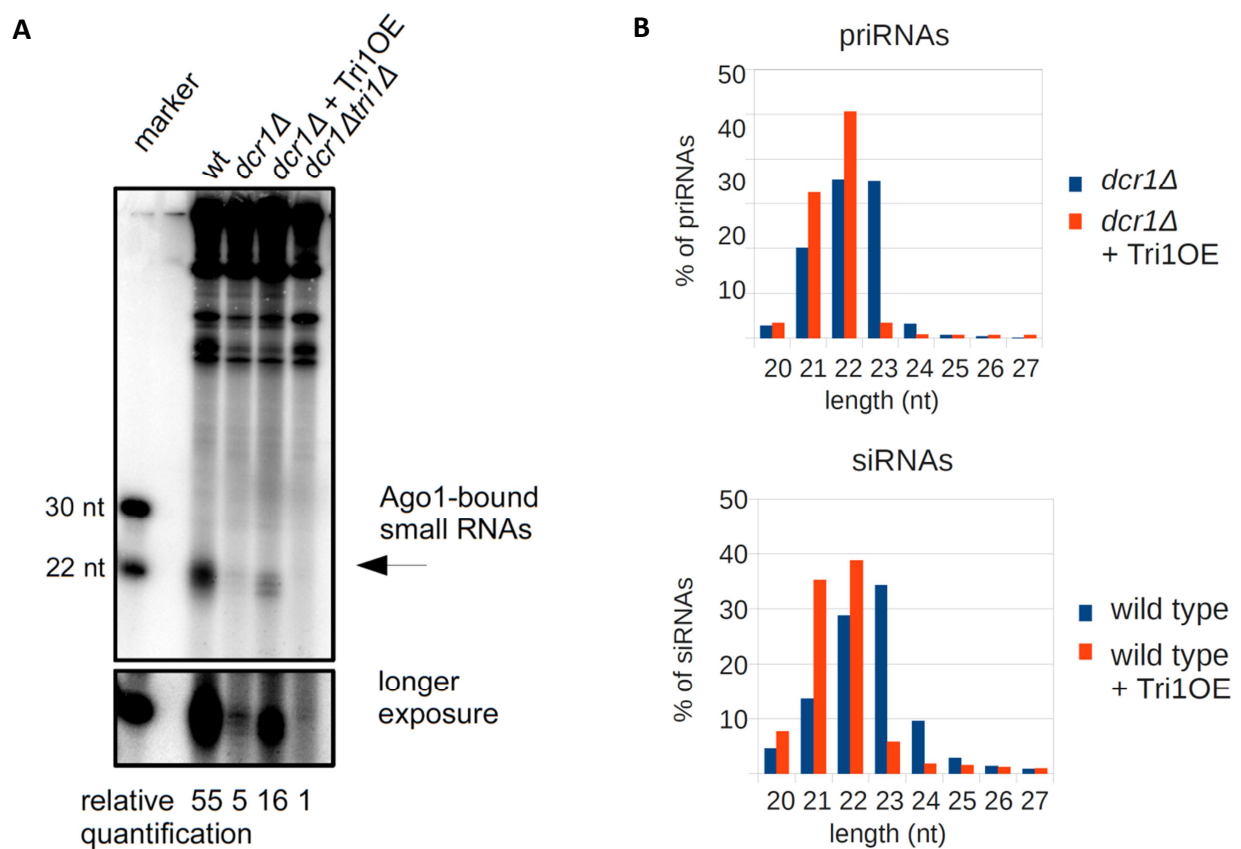


Figure 2.7.1. Triman overexpression generates more small RNAs (A) Triman overexpression (Tri1OE) results in generation of several-fold more Argonaute –associated priRNAs. Polyacrilamide-urea gel showing 5' ^{32}P labeled Argonaute-associated RNAs purified from wild-type, *dcr1Δ*, *dcr1Δ*+Tri1OE, and *dcr1Δtri1Δ* cells. Bands were visualized by phosphor imaging. Lower panel shows longer exposure of Argonaute-associated small RNAs. Tri1OE denotes Triman overexpression. The assay was performed in two independent replicates which were used for

quantification. (B) Length distribution of Argonaute-associated small RNAs from indicated strains. Both siRNAs and priRNAs are longer in cells with overexpression of Triman.

2.8 Argonaute and Triman cooperate to generate small RNAs

To test the interaction between Argonaute and Triman, *in vitro* co-immunoprecipitation assay was performed (see Chapter 4.2.3.3). It was observed that FLAG-Ago1 interacts with HA-Triman that was bound to HA-resin (Figure 2.8.1, lane 1). Unspecific binding of FLAG-Ago1 to HA-resin was not observed (Figure 2.8.1, lane 2). This indicated that Argonaute recruits Triman to process Ago1-bound small RNAs.

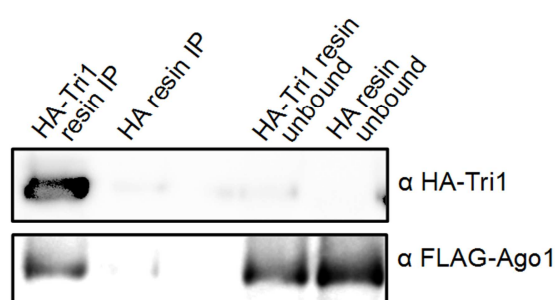


Figure 2.8.1. *In vitro* co-immunoprecipitation assay showing that Argonaute directly interacts with Triman. FLAG-Argonaute was incubated with the resin-bound HA-Triman (HA-Tri1 resin IP) and with the HA-resin alone as a control for unspecific binding (HA resin IP). Reactions were separated on polyacrilamide gel and Western blott was performed. FLAG-Ago1 was only binding to the resin-bound HA-Triman, but not to the resin alone.

To further explore the interaction of Argonaute and Triman, a mass spectrometry (MS) analysis of FLAG-Argonaute purifications was employed. FLAG-Ago1 was purified utilizing low salt lysis buffer (50 mM Hepes pH 7.6, 150mM M NaOAc, 5 mM Mg(OAc)₂, 1 mM EGTA, 1 mM EDTA, 0.1% (v/v) NP-40, Protease inhibitor cocktail tablets) and coffee grinder. MS analysis showed that Triman is one of the proteins which co-purifies with Argonaute (Table 5.1). Overall, these data indicated that Triman is recruited to Argonaute in order to process Ago1-associated sRNAs to the final length.

2.9 Trimming is important for the stability of Ago1:sRNA complex

Next we asked if the trimming activity is important for the stability of Ago1:sRNA complex. Therefore, the stability of binding of RNAs of various lengths onto Argonaute was tested. 22- and 30-nt-long single-stranded small RNAs were 5' ^{32}P labeled. First, 50 fmol of radioactively labeled small RNAs were loaded onto resin-bound FLAG-Argonaute (50-200 ng) in a 10 μl reactions containing MgCl_2 buffer and 1 μl RNase inhibitor for 30 min at 32 °C. After loading, unbound small RNAs were washed away 2 times by adding 1 ml of washing buffer, pipetting the reactions 4 times up and down, centrifugation for 2 min at 1 4000 g and removing the supernatant from the resin-bound Argonaute. Argonaute-associated small RNAs were incubated at 32 °C. The stability of the complex was assayed in the intervals of 40 minutes – small RNAs that dissociated from the resin-bound Argonaute were washed away every 40 min by addition of 100 μl of washing buffer and centrifugation for 2 min at 1 4000 g to remove the supernatant from the resin-bound Argonaute. Washing step was done two times and washes were collected and ethanol-precipitated. All fractions were analyzed on the polyacrylamide-urea gel and the bands were visualized by phosphor imaging (Figure 2.9.1). While 22-nt-long small RNAs remained stably bound to Argonaute, 30-nt-long and longer small RNA precursors dissociated very fast.

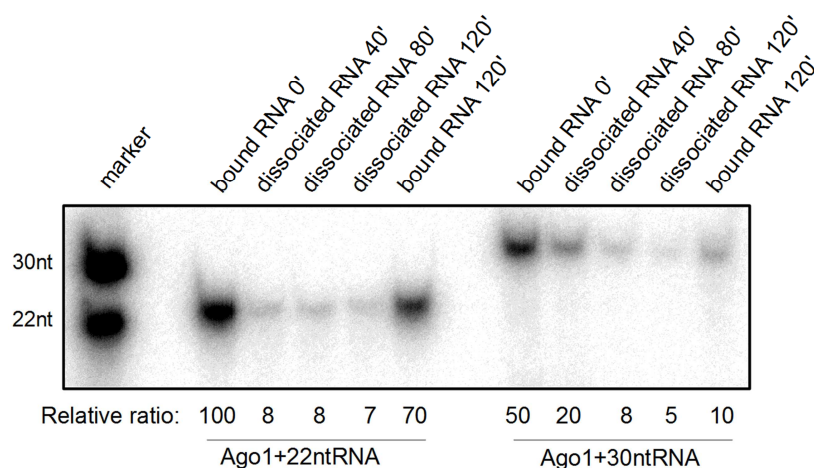


Figure 2.9.1. Argonaute does not associate stably with 30-nt-long small RNAs. Resin-bound FLAG-Argonaute was loaded with 22- or 30-nt-long small RNAs, and small RNAs that dissociated from resin-bound Argonaute were washed away every 40 min. Reactions were separated on polyacrylamide-urea gel and imaged by phosphor imaging.

2.10 Trimming is important for the Argonaute-slicer activity

In order to investigate whether the length of small RNA is important for the slicing activity of Argonaute, an Argonaute slicer assay was reconstituted *in vitro* (Figure 2.10.1 A). Argonaute was loaded with small RNA guides of different lengths and incubated with the 5' ^{32}P labeled target RNA. While Argonaute loaded with 22-nt-long small RNA was efficiently slicing the complementary target, Argonaute loaded with 24- and 26-nt-long small RNAs showed 7-fold and 10-fold decreased slicing activity. In addition, the stability of the interaction of 22-nt, 24-nt, 26-nt, and 30-nt-long sRNAs with Argonaute was investigated (Figure 2.10.1 B). It was observed that Argonaute stably associated with RNAs of 22-nt, 24-nt and 26-nt, thus the observed defect in slicing of the corresponding Ago1:sRNA complexes was not a result of inefficient binding. 30-nt-long RNA was not stably associated with Argonaute.

These results indicated that longer RNA guides cannot efficiently guide Argonaute to slice complementary targets.

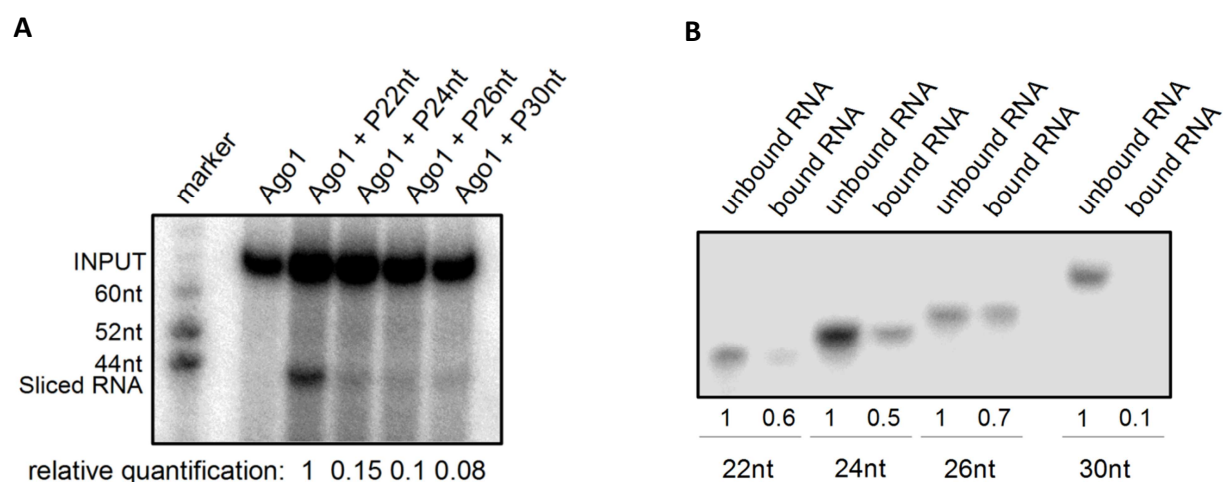


Figure 2.10.1. *In vitro* reconstitution of Argonaute slicer activity. (A) FLAG-Ago1 was loaded with small RNA guides *RNA22*, *RNA24*, *RNA26* and *RNA30*, following addition of 5' ^{32}P labeled-target RNA. The sliced product migrates around 44-nt. (B) Argonaute stably associates with 22-, 24-, and 26-nt-long small RNAs, but not with the 30-nt-long sRNAs. 5' ^{32}P labeled RNAs of different lengths were loaded onto FLAG-Ago1 that was bound to the resin. After loading, unbound sRNAs were washed away and Ago1-associated small RNAs were incubated for 2h. After incubation, unbound RNAs were washed away and analyzed on the gel together with the sRNAs which remained bound to Ago1.

2.11 Triman is a general factor involved in biogenesis of siRNAs and priRNAs

In order to obtain deeper understanding on the involvement of Triman in small RNA generation, deep-sequencing data of Argonaute-associated small RNAs was further analyzed. As already described in Chapter 2.3, in *tri1Δ* cells both Ago1-associated priRNAs and siRNAs were longer (Figure 2.3.1 B - C). This effect was observed for small RNAs that were mapping to various genomic regions – centromeric region, mRNAs, rRNA (Figure 2.11.1 A – D). This indicated that Triman acts as a general factor and is required for biogenesis of all siRNAs and piRNAs in *S. pombe*.

In analysis, sequencing reads were normalized to the number of reads and to the total quantity of Argonaute-associated sRNAs (Figure 2.11.1 E). To estimate total quantity of Ago1-associated small RNAs, FLAG-Argonaute from wt, *tri1Δ*, *rrp6Δ*, *tri1Δrrp6Δ*, *dcr1Δrrp6Δ*, *dcr1Δ* and *dcr1Δtri1Δ* was purified. Copurifying RNAs were extracted, 5^{32}P labeled and analyzed on polyacrilamide-urea gel. The total quantity of Ago1-associated small RNAs were estimated based on three biological replicates. It was observed that in *tri1Δ* cells, Ago1-associated small RNAs were reduced around 2-fold (Figure 2.11.1 E). In *dcr1Δ* cells, where only priRNAs are bound onto Ago1, they were around 10-fold reduced. In *dcr1Δtri1Δ* cells, where also priRNAs are not produced, Ago1-associated sRNAs were around 100-fold reduced. These observations indicated that Triman is a general factor involved in biogenesis of priRNAs and siRNAs.

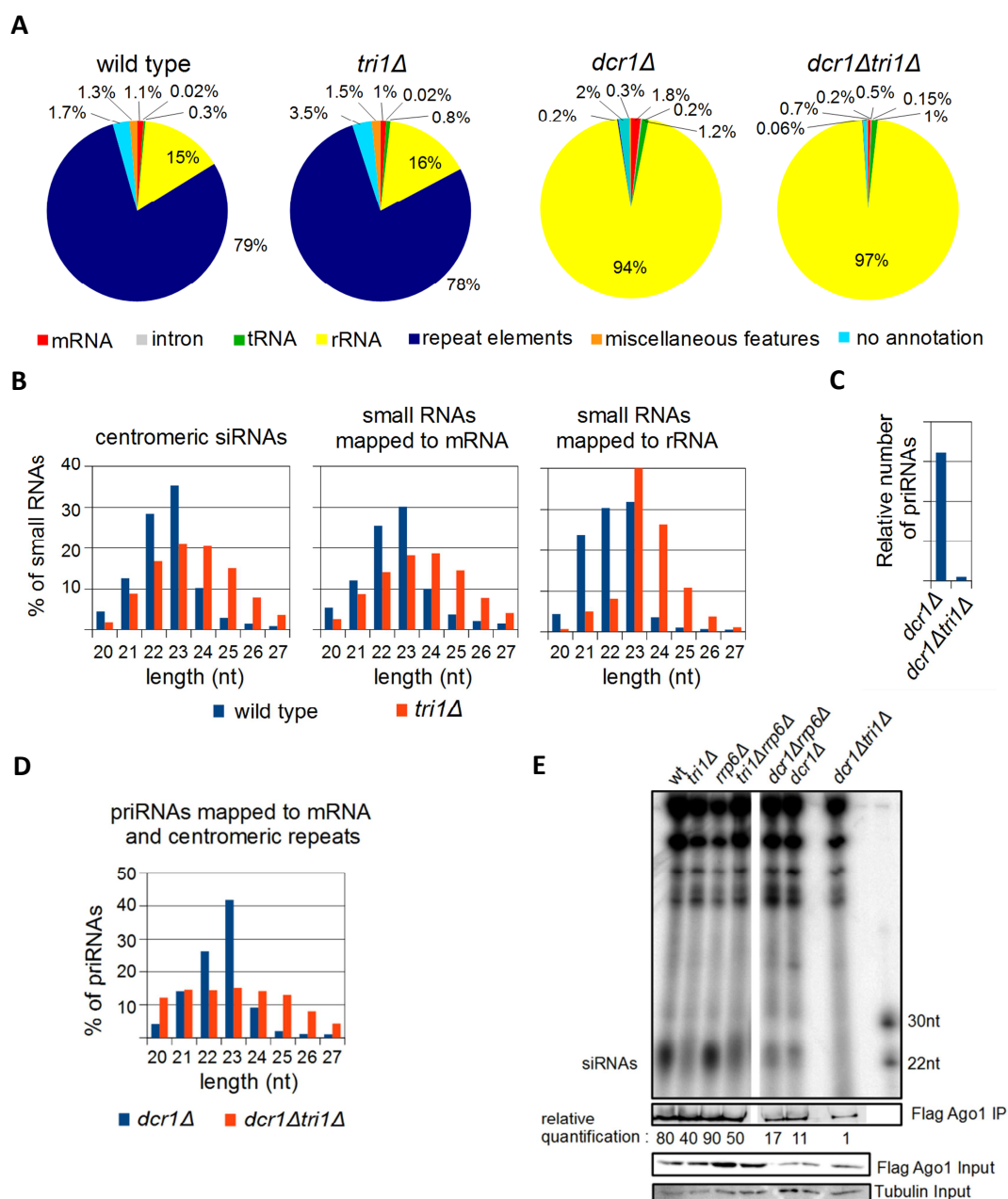


Figure 2.11.1. High-throughput sequencing of Ago1-associated small RNAs from indicated cells. (A) Pie charts showing percentages for the individual RNA classes relative to the total number of reads in each strain. (B) Length distribution of Ago1-associated small RNAs from wt and *tri1Δ* cells mapping to centromeric region, mRNA and rRNA. (C) Relative number of priRNAs mapping to mRNA and centromeric repeats is more than 20-fold reduced in *dcr1Δtri1Δ* cells. (D) Length distribution of priRNAs from *dcr1Δ* and *dcr1Δtri1Δ* cells mapping to mRNAs and centromeric repeats. In *dcr1Δtri1Δ* cells priRNAs have broader length distribution which corresponds their distribution in total RNA fraction. (E) Polyacrilamide-urea gel showing 5^{32}P labeled RNAs copurifying with Ago1 from indicated strains. Quantification is based on 3 biological replicates. Lower panels show western blot detection of FLAG-Ago1 in immunoprecipitated (IP) and total cell lysate (Input). Tubulin was used as a loading control.

2.12 Triman is not required for maintenance of centromeric heterochromatin

Is trimming required for maintenance of centromeric heterochromatin? To investigate that, a silencing assay on 5-fluoro-orotic acid (5-FOA) and thiabendazole (TBZ) plates were performed. Our strains contained *ura4⁺* reporter gene inserted in the centromeric *dg* repeats (*otr1R::ura4⁺*). Silencing state of a reporter gene inserted in centromeric region indicates maintenance of heterochromatin. If reporter gene is expressed, and cells are plated on media containing FOA, toxic product is generated and cells show a growth defect. It was observed that *tri1Δ* cells were functional in maintenance of centromeric heterochromatin, as they did not show growth defect on FOA plates (Figure 2.12.1 A). Similar result was observed when silencing assay was performed on plates containing TBZ (Figure 2.12.1 B). TBZ is a microtubule depolymerizing drug and mutants which have segregation defect also show growth defect on media containing TBZ. Overall, silencing assays indicated that Triman is not required for maintenance of centromeric heterochromatin.

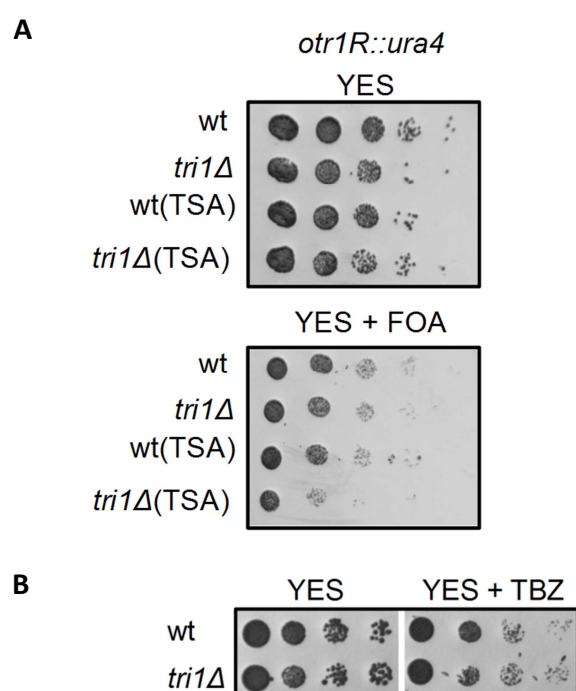


Figure 2.12.1. Silencing assay showing *tri1Δ* cells are functional in maintaining silencing of pericentromeric heterochromatin, but have a defect in establishment (Related to Chapter 2.13). (A) Log-phased wt and *tri1Δ* strains were ten-fold serially diluted and spotted onto non-selective plates (YES) or selective plates (YES containing 5-FOA) to estimate the expression of *otr1R::ura4⁺*. In an establishment assay, cells were grown on trichostatin (TSA) for 24 h, following 24 h recovery on rich media and spotting on 5-FOA. (B) Log-phased wt and *tri1Δ* strains were five-fold serially diluted and spotted onto non-selective plates (YES) or selective plates containing TBZ.

In the sequencing data of Argonaute-associated small RNAs, a 1.5- and 2-fold reduction of centromeric *dg* and *dh* sRNAs was observed in *tri1Δ* cells (Figure 2.12.2 A - B). This was also in a correlation with the results obtained by splinted ligation assay (Figure 2.2.1 C).

In order to quantify the levels of H3K9me in *tri1Δ* cells, an H3K9me chromatin immunoprecipitation sequencing (ChIPseq) and ChIP-qPCR was performed. It was observed that in *tri1Δ* cells, H3K9me levels at centromeric *dg* repeats were around 20 % reduced (Figure 2.12.2 C). Deep-sequencing data of Ago1-associated small RNAs demonstrated that the most sensitive element in *tri1Δ* cells was *IRC3* element where small RNAs were almost completely abolished (Figure 2.12.2 D, upper panel). However, heterochromatin structure at this region was not disrupted as H3K9me levels were only slightly reduced (Figure 2.12.2 D, lower panel). The levels of H3K9me probably stay intact because heterochromatin is able to spread from neighboring *dg* repeats to the surrounding region. This data indicated that Triman is involved in the final processing of small RNAs, however due to the high amounts of siRNAs generated at the pericentromeric repeats, cells are still able to maintain centromeric heterochromatin.

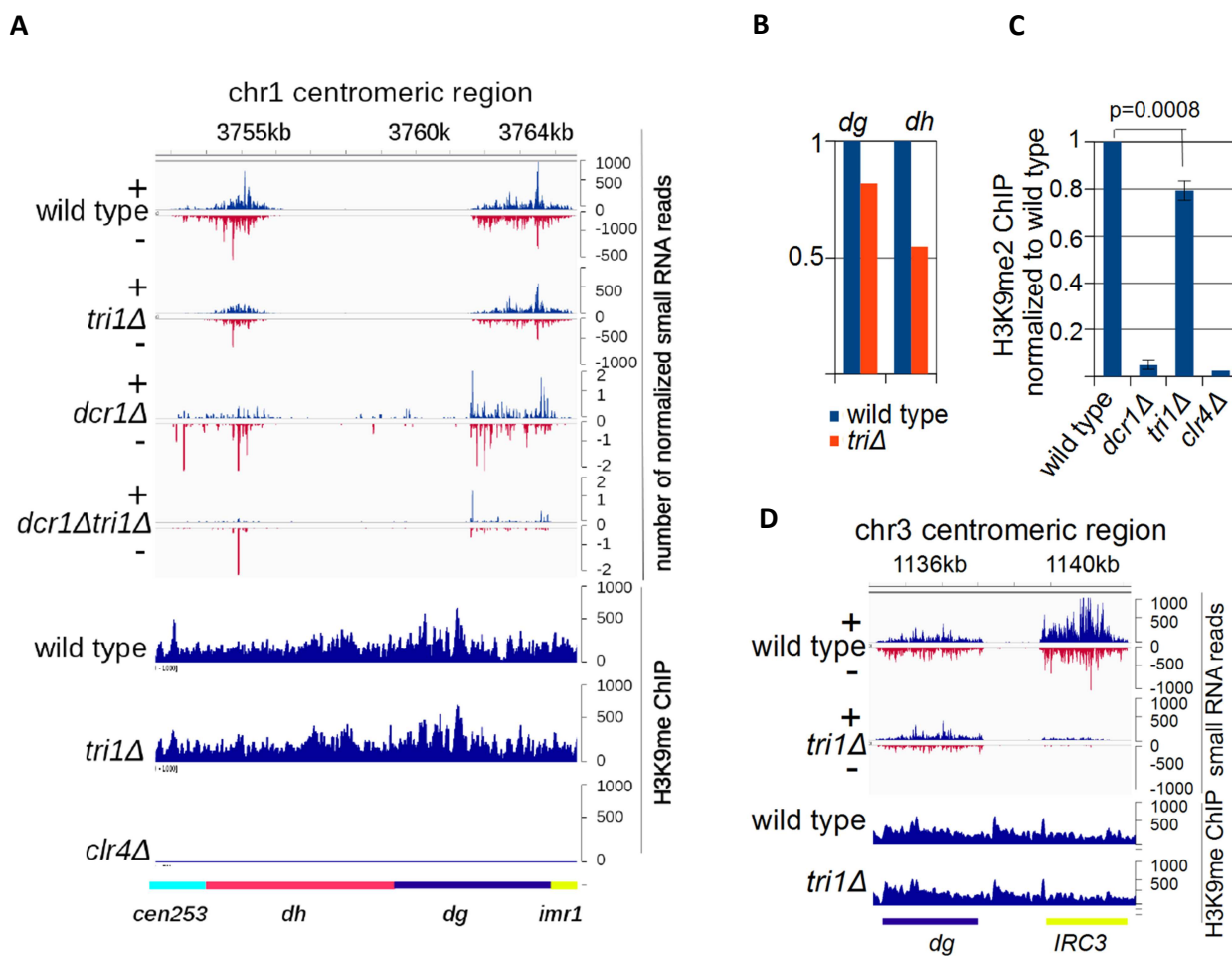


Figure 2.12.2. Triman is not required for maintenance of centromeric heterochromatin. (A) Small RNA reads (upper panel) and ChIPseq reads (lower panel) were plotted over centromeric region of chromosome 1. Scale bars on the right denote small RNA read numbers normalized per one million reads and to the total number of Ago1-associated small RNAs. (B) Quantification of centromeric *dg* and *dh* siRNAs in wild-type and *tri1Δ* cells. (C) ChIP experiment showing H3K9me at centromeric *dg* repeats in indicated strains. Quantification is based on six independent biological replicates. Error bars indicate standard deviations. (D) Small RNA reads (upper panel) and ChIPseq reads (lower panel) were plotted over *dg* and *IRC* elements on chromosome 3. Scale bars on the right denote small RNA read numbers normalized per one million reads and to the total number of Ago1-associated small RNAs.

2.13 Triman is important for establishment of pericentromeric heterochromatin

In order to investigate the function of Triman in establishment of centromeric heterochromatin by silencing assay, it was necessary to perturb existing heterochromatin. This was possible by treating cells with the histone deacetylase (HDAC) inhibitor trichostatin A (TCA). Histone deacetylation is a prerequisite for histone methylation. Thus, by interfering with the removal of acetyl groups of histones, H3K9me and heterochromatin formation is also disabled (Ekwall et al. 1997). Cells in exponential growth phase were treated with TCA, recovered for 24 hours on rich media, plated on 5-FOA plates and incubated on 32 °C for 2-3 days (Figure 2.12.1 A). More than a 10-fold defect in heterochromatin re-establishment was observed in *tri1Δ* cells in comparison to wt cells, which were fully functional in re-establishment (Figure 2.12.1 A). This indicated that Triman might have a role in initiation of heterochromatin formation at centromeric region.

To validate the result obtained by silencing assay, a re-establishment experiment was performed. For this assay, it was necessary to create mutant strain that was completely abolished of siRNAs, priRNAs and heterochromatin, after which subsequently each deleted component was re-introduced. Therefore, a strain that had deletion of Clr4, the sole H3K9 methyltransferase in *S. pombe*, Dcr1 that generates siRNAs, and Tri1 to abolish priRNAs as well, was created by mating. Subsequently, *clr4⁺* and *dcr1⁺* genes were reintroduced on a plasmid in *clr4Δdcr1Δtri1Δ* strain and in the control *clr4Δdcr1Δ* strain. The ability of cells to re-establish heterochromatin was investigated by silencing assay, relative levels of *dg* transcripts measured by RT-qPCR and H3K9me2 ChIP.

Silencing assay showed that reintroduction of *clr4⁺* and *dcr1⁺* genes in *clr4Δdcr1Δtri1Δ* strain could not re-establish silencing, as these cells showed high sensitivity to microtubule-destabilizing agent TBZ (Figure 2.13.1 A). In contrast, reintroduction of *clr4⁺* and *dcr1⁺* genes in the control *clr4Δdcr1Δ* strain resulted in low sensitivity to TBZ and indicated that these cells were able to re-establish silencing (Figure 2.13.1 A).

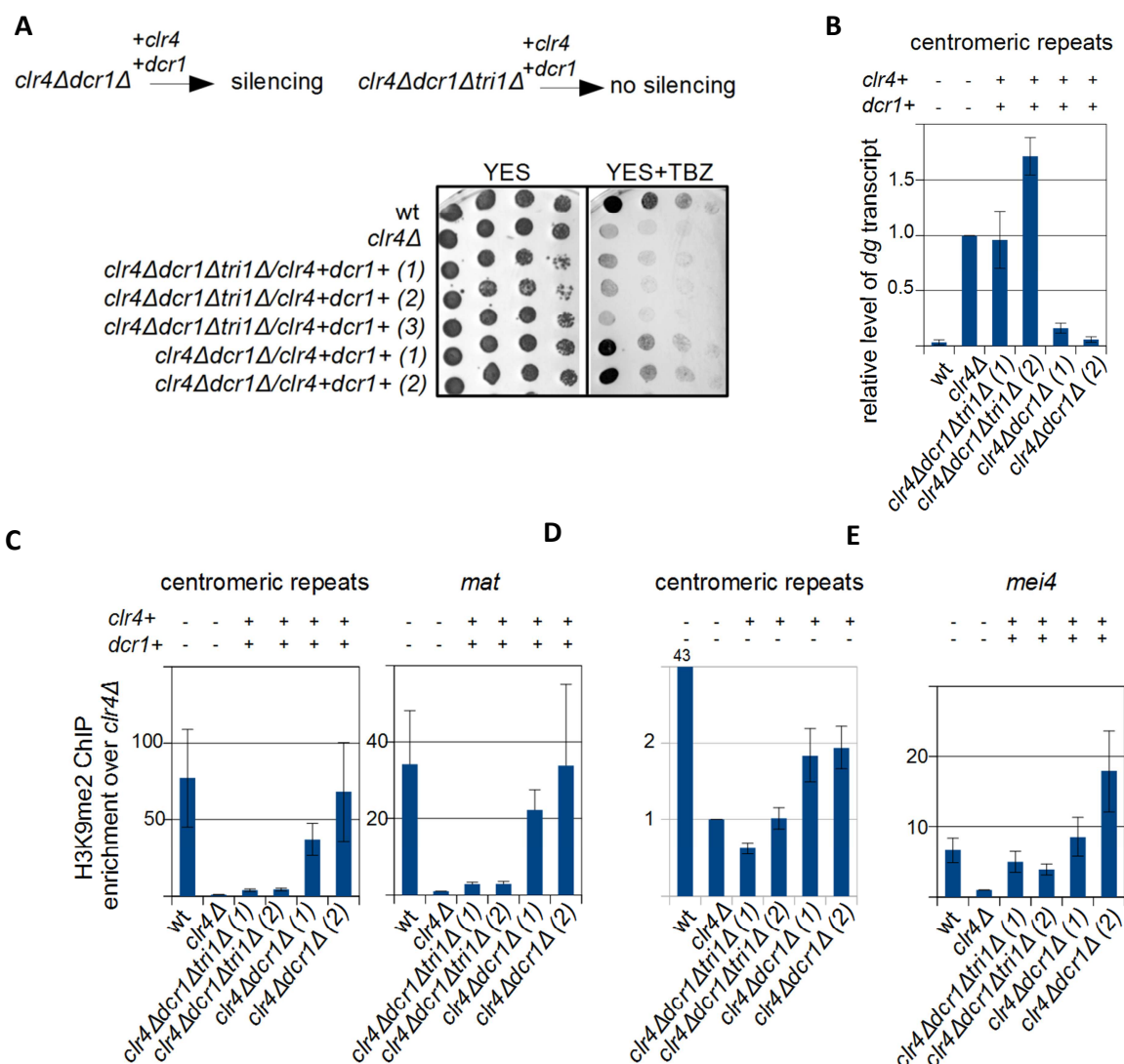


Figure 2.13.1. Triman is required for establishment of centromeric heterochromatin. (A) Silencing assay showing that reintroduction of $clr4^+$ and $dcr1^+$ genes in $clr4\Delta dcr1\Delta tri1\Delta$ strain could not re-establish silencing. Log-phased strains were five-fold serially diluted and spotted onto non-selective plates (YES) or selective plates containing TBZ. (B) Quantification of centromeric dg transcripts in indicated strains by RT-qPCR. $clr4\Delta dcr1\Delta tri1\Delta$ cells could not re-establish silencing of dg repeats after reintroduction of $clr4^+$ and $dcr1^+$ genes. Error bars indicate standard deviations. (C) ChIP experiment showing that H3K9me levels were not re-established at centromeric dg repeats and mat locus in $clr4\Delta dcr1\Delta tri1\Delta$ cells after reintroduction of $clr4^+$ and $dcr1^+$ genes. (D) ChIP experiment showing that priRNAs can establish low levels of H3K9me at dg repeats. After $clr4^+$ was reintroduced into $clr4\Delta dcr1\Delta$ cells, where only priRNAs are present, very low levels of H3K9me were established. (E) ChIP experiment showing that Triman is not required for establishment of H3K9me at $mei4$. Error bars indicate standard deviations.

To further explore if Triman is important for establishment of centromeric heterochromatin, levels of *dg* transcripts were measured by RT-qPCR. It was observed that in *clr4Δdcr1Δtri1Δ/clr4⁺dcr1⁺* cells centromeric repeats were not silenced and their levels were upregulated similar as in *clr4Δ* cells (Figure 2.13.1 B). However, when *clr4⁺* and *dcr1⁺* genes were reintroduced in the control *clr4Δdcr1Δ* cells, silencing was restored and the *dg* levels were reduced comparable to the levels in wt cells (Figure 2.13.1 B). Similar results were obtained by H3K9me ChIP. In the *clr4Δdcr1Δtri1Δ/clr4⁺dcr1⁺* cells, H3K9me level at centromeric *dg* repeat was not restored, but in *clr4Δdcr1Δ/clr4⁺dcr1⁺* cells H3K9me was comparable to wt levels (Figure 2.13.1 C). These results demonstrated that Triman is required for establishment of silencing and heterochromatin formation at centromeric region.

At *S. pombe* mating-type (*mat*) region, RNAi-mechanism is not required for maintenance of heterochromatin, but is required for establishment. In the absence of RNAi-mechanism, heterochromatin can be established by Atf1/Pcr1 mechanism, but very inefficiently and at slow rate (Hall et al. 2002; Jia et al. 2004). In order to investigate whether Triman is also important for establishment of silencing at *mat* locus, H3K9me levels at *mat* loci were also assayed. It was observed that in *clr4Δdcr1Δtri1Δ/clr4⁺dcr1⁺* cells heterochromatin could not be established at *mat* locus (Figure 2.13.1 C). In contrast, in *clr4Δdcr1Δ/clr4⁺dcr1⁺* cells H3K9me levels were established at levels comparable to wt cells. These results show that Triman is an important factor in establishment of centromeric heterochromatin and heterochromatin at *mat* locus.

It was previously suggested that priRNAs play an important role in initiation of heterochromatin formation (Halic & Moazed 2010). To directly test that, *clr4⁺* was reintroduced in *clr4Δdcr1Δtri1Δ* cells which lack siRNAs and priRNAs (Figure 2.13.1 D). It was observed that H3K9me levels were not reestablished in *clr4Δdcr1Δtri1Δ/clr4⁺* cells, indicating that small RNAs are required for initial heterochromatin formation. When *clr4⁺* was reintroduced into *clr4Δdcr1Δ* cells, where only priRNAs are present, very low levels of H3K9me were observed to be above background level (Figure 2.13.1 D). This demonstrated that antisense priRNAs originating from centromeric repeats could nucleate siRNA generation and heterochromatin formation.

Previously, it was demonstrated that H3K9 methylation can be detected at a subset of meiotic genes, including *mei4*, during vegetative phase of the cell cycle (Hiriart et al. 2012; Zofall et al. 2012). The observed H3K9me establishment and maintenance at a subset of loci is not dependent on RNAi, rather it occurs through recruitment of CLRC via Mmi1 surveillance mechanism (Zofall et al. 2012; Tashiro et al. 2013). Consistent with this, it was observed that priRNAs are not important for establishment of heterochromatin at *mei4* locus, as H3K9me was formed even in *clr4Δdcr1Δtri1Δ/clr4+dcr1+* cells (Figure 2.13.1 E). Therefore, priRNAs and Triman are dispensable for heterochromatin formation at this locus.

2.14 Triman is important for formation of heterochromatin islands

H3K9me mapping across the fission yeast genome revealed around 30 additional islands of heterochromatin (Zofall et al. 2012; Hiriart et al. 2012; Tashiro et al. 2013). These heterochromatin islands are found at the open reading frames or 3' ends of meiotic genes and ncRNAs (Zofall et al. 2012). At a subset of islands, heterochromatin is generated through Mmi1 surveillance machinery, and it was established in an RNAi-dependent mechanism (Zofall et al. 2012). To address if Triman and 3' end processing is important for RNAi and H3K9me at heterochromatin islands, deep sequencing data of Ago1-associated small RNAs was additionally analyzed. It was observed that in *tri1Δ* cells, small RNAs were reduced at a subset of islands, for example at *mcp5* and *SPAC8C9.04c* a 1.4- and 3-fold reduction was observed (Figure 2.14.1 A - B). Argonaute-associated small RNAs in *tri1Δ* cells were not only reduced at heterochromatin islands, but also had broader length distribution characteristic for *tri1Δ* cells, for example at *mcp5* island (Figure 2.14.1 C).

Also, as determined by ChIP and ChIP-sequencing, in *tri1Δ* cells H3K9me levels were abolished or reduced at several islands, for example *mcp5*, *SPAC8C9.04c*, *vps29*, *RNA.394*, *eno1* (Figure 2.14.1 D- E). In contrast, it was demonstrated that H3K9me is established independently of RNAi-machinery at *mei4* island (Zofall et al. 2012; Hiriart et al. 2012; Tashiro et al. 2013). As expected, at this island a defect in H3K9me in *tri1Δ* cells was not observed (Figure 2.14.1 D, right panel). These results demonstrate that trimming is important for siRNA generation and H3K9me at a subset of heterochromatin islands in fission yeast.

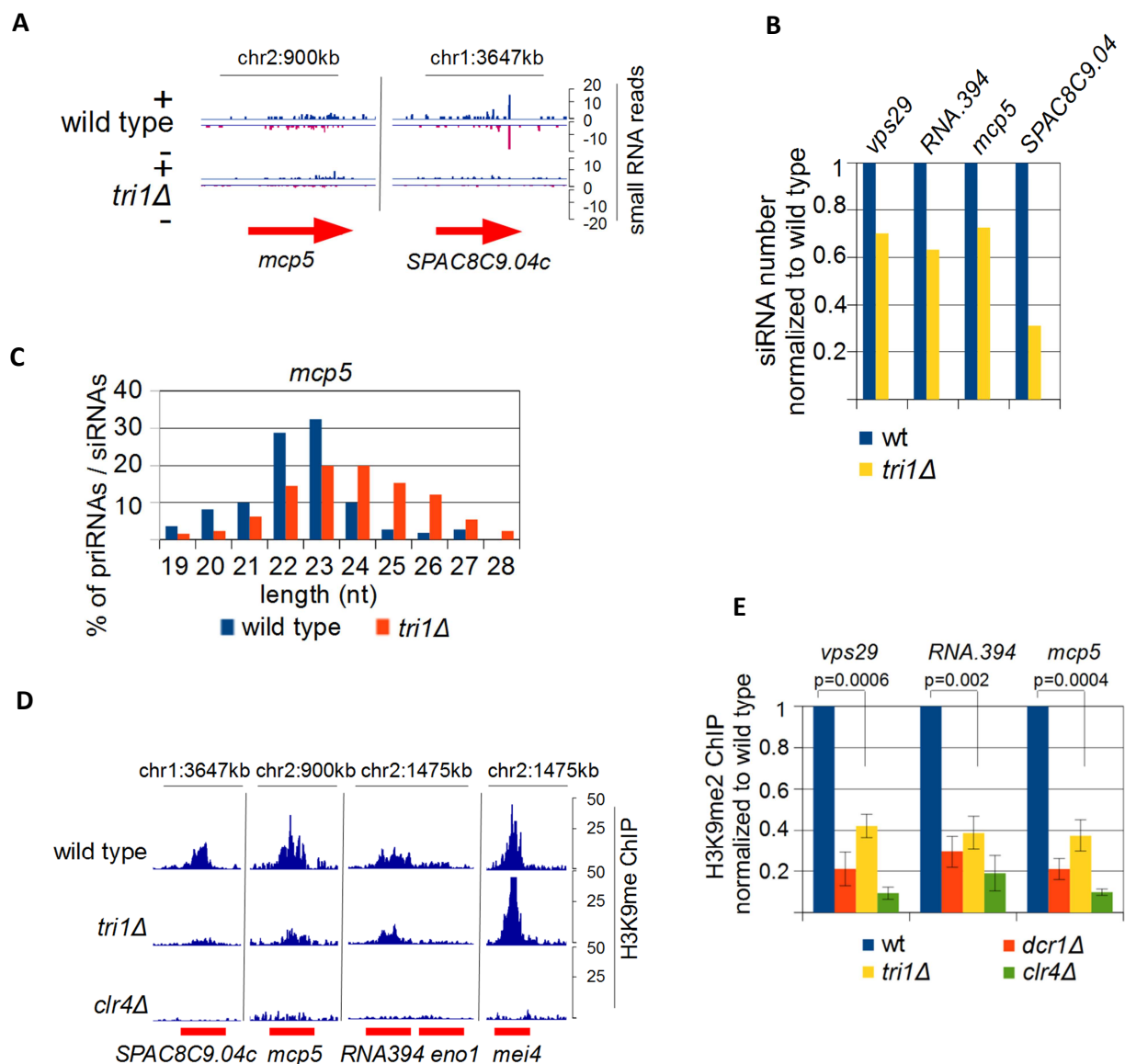


Figure 2.14.1. Triman is required for maintenance of facultative heterochromatin. (A) Small RNA reads from wt and *tri1*Δ cells were plotted over *mcp5* and *SPAC8C9.04c* loci. Scale bars on the right denote small RNA read numbers normalized per one million reads and to the total number of Argonaute-associated small RNAs. (B) Diagram showing number of Argonaute-associated small RNAs at indicated loci in wild-type and *tri1*Δ strains. (C) Length distribution of Argonaute-associated small RNAs in wt and *tri1*Δ cells at *mcp5* locus. (D) H3K9me ChIP sequencing experiment from indicated strains. ChIPseq reads were plotted over genes where facultative heterochromatin is formed in a Triman-dependent manner. At *mei4* H3K9me is not dependent on Triman. (E) ChIP experiment from indicated strains showing H3K9me at indicated loci is generated in a Dicer- and Triman-dependent way.

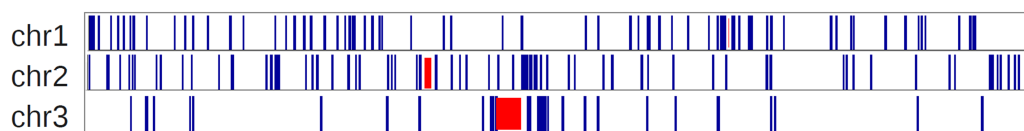
2.15 In *rrp6* Δ cells RNAi is nucleated at various clusters in a Triman/priRNA dependent manner

In our screen where splinted ligation assay was used to detect potential nucleases involved in the biogenesis of priRNAs, it was observed that Argonaute-associated centromeric *dg* transcripts in *dcr1* Δ *rrp6* Δ cells accumulated almost 10-fold more than in *dcr1* Δ cells (Figure 2.1.1 D). This indicated that Rrp6 subunit of exosome, which is involved in degradation of antisense transcripts, is involved in priRNA degradation. To elucidate the function of Rrp6 in the context of RNAi and to see if high levels of antisense RNAs that accumulate in *rrp6* Δ cells could nucleate RNAi at ectopic loci, high-throughput sequencing of Argonaute-associated small RNAs from *rrp6* Δ , *tri1* Δ *rrp6* Δ , *rrp6* Δ *dcr1* Δ cells was performed.

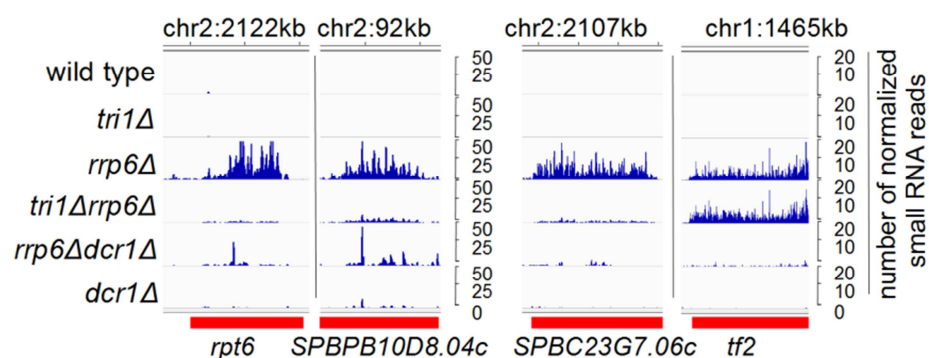
We and Yamanaka et al. (2013) have observed that in *rrp6* Δ cells, siRNAs are generated from various genomic clusters that are usually not targeted by RNAi (Figure 2.15.1 A - C). Genes that nucleated RNAi in *rrp6* Δ cells were scattered over three *S. pombe* chromosomes (Figure 2.15.1 A). It was observed that RNAi was not nucleated uniformly at all genomic regions. Genes that are surrounding pericentromeric region on the chromosome 1 and 3 nucleated RNAi more often than the genes in other regions. The same was not observed for the pericentromeric region on the chromosome 2. RNAi nucleation was also more frequent near the mating type region on the chromosome 2. This indicated that genes located in the proximity of constitutive heterochromatin can nucleate RNAi more frequently than on other regions. However, many genes which trigger RNAi are not localized near heterochromatic regions indicating that RNAi can nucleate anywhere in the genome.

At some genes, RNAi nucleation in *rrp6* Δ cells was Triman-dependent; for example at *SPBPB10D8.04c*, *rpt6*, *SPBC23G7.06c* small RNAs were abolished in *tri1* Δ *rrp6* Δ cells (Figure 2.15.1 B). The inability of siRNA generation in cells lacking Triman indicated that priRNAs are loaded onto and guide Argonaute to these clusters to nucleate RNAi. However, at some loci, deletion of Triman resulted only in a reduction of small RNAs (*med17*, *mug21*, *erg6*) (Figure 2.15.1 C) or had no significant effect on small RNA generation (*tf2*, *myo2*) (Figure 2.15.1 B – C, right panels).

A



B



C

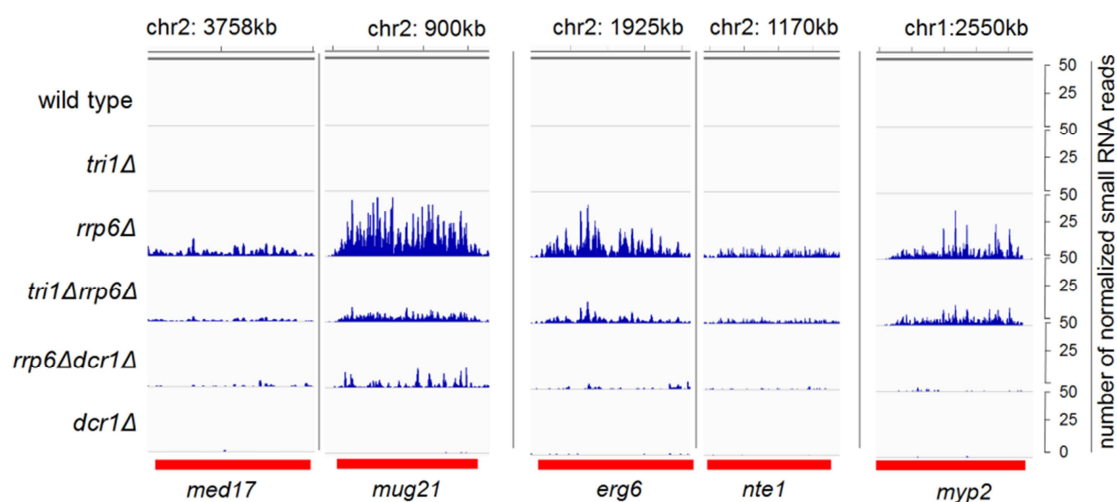


Figure 2.15.1. In *rrp6Δ* cells RNAi targets various genomic clusters across *S. pombe* genome. (A) Map showing 490 genes that nucleate RNAi in *rrp6Δ* cells (2-fold increase, >10 reads) (blue bars) scattered over three *S. pombe* chromosomes. Red bars depict centromeric heterochromatin. (B), (C) High-throughput sequencing of Argonaute-associated small RNAs from indicated cells. Small RNA reads from indicated cells were plotted over targeted genes (denoted by red lines below the peaks). Scale bars on the right denote small RNA read numbers normalized per one million reads and to the total number of Argonaute-associated small RNAs.

It was observed that in *rrp6Δ* cells more than 10 % of Argonaute-associated sRNAs map to mRNAs (Figure 2.15.2 A - B). In contrast, in wild-type cells 1 % of sRNAs map to protein coding genes (Figure 2.11.1 A). The genes targeted by RNAi in *rrp6Δ* cells included various developmental genes, proteosomal subunit, as well as transposon Tf2 (Figure 2.15.1 B - C, Table 5.2).

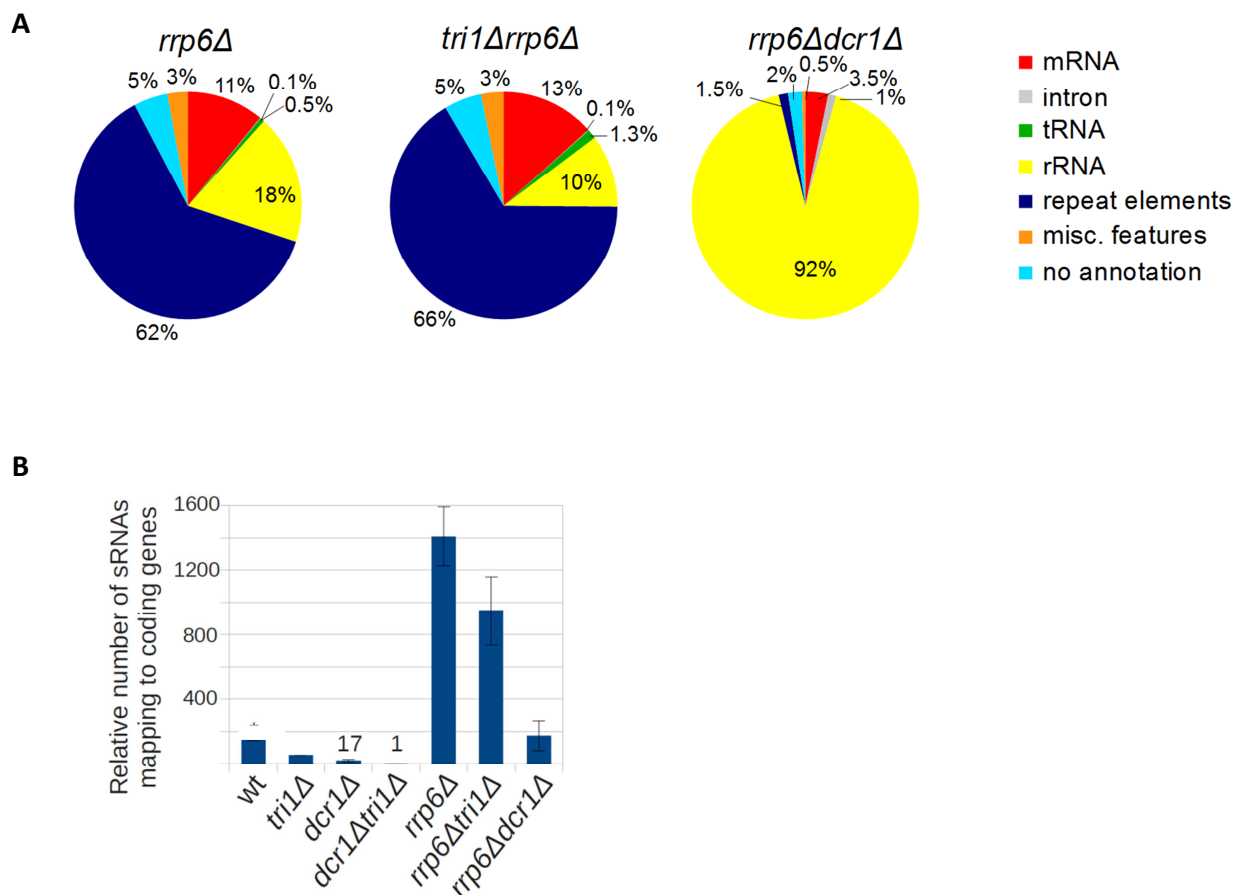


Figure 2.15.2. Rrp6 protects mRNAs from RNAi. High-throughput sequencing of Argonaute-associated small RNAs from indicated cells. (A) Pie charts showing percentages of the indicated RNA classes relative to the total number of reads in each strain. (B) Relative number of small RNAs mapping to protein coding genes in indicated cells. Small RNAs originating from mRNA transcripts are highly increased in *rrp6Δ* background.

In order to see whether siRNA generation in *rrp6Δ* cells establishes heterochromatin, an H3K9me ChIP was performed. H3K9me was detected at clusters targeted by RNAi, for example at genes *SPBPB10D8.04c*, *rpt6*, *SPBC23G7.06c* (Figure 2.15.1 B, Figure 2.15.3 A).

Next, we asked whether Triman is necessary to establish observed heterochromatin formation in *rrp6Δ* cells. Studying *de novo* establishment of pericentromeric heterochromatin required deletion of genes from several pathways and their subsequent reintroduction (Chapter 2.12). Here, using ectopic RNAi nucleation in *rrp6Δ* background, the investigation of *de novo* establishment of H3K9me was possible without the need to deplete preexisting heterochromatin and RNAi factors.

It was observed that in *tri1Δrrp6Δ* cells, siRNA generation was abolished at majority of clusters, for example at *rpt6*, *SPBPB10D8.04c*, *SPBC23G7.06c* (Figure 2.15.1 B, Table 5.2). As expected, H3K9me was also not established at these loci in the absence of Triman in *rrp6Δ* cells (Figure 2.15.3 A). As already stated, Triman deletion had only slight or no effect on siRNA levels at some clusters. Although at *tf2* and *myo2*, siRNAs were not affected by deletion of Triman in *rrp6Δ* cells (<2-fold reduction) (Figure 2.15.1 B – C, right panels), H3K9me was abolished. This further supports the finding that longer small RNAs are not completely functional and that final trimming is required for heterochromatin establishment.

These results indicated that accumulation of antisense transcript can result in RNAi targeting. Next, we wanted to explore if increase of antisense *in trans* can nucleate RNAi and heterochromatin formation. Thus, antisense to *rpt6* gene was cloned into pREP plasmid and overexpressed in wild-type, *dcr1Δ*, *tri1Δ*, *clr4Δ* cells. By ChIP it was observed that plasmid based expression of antisense to *rpt6* established small levels of H3K9me in a Dicer- and Triman-dependent way (Figure 2.15.3 C).

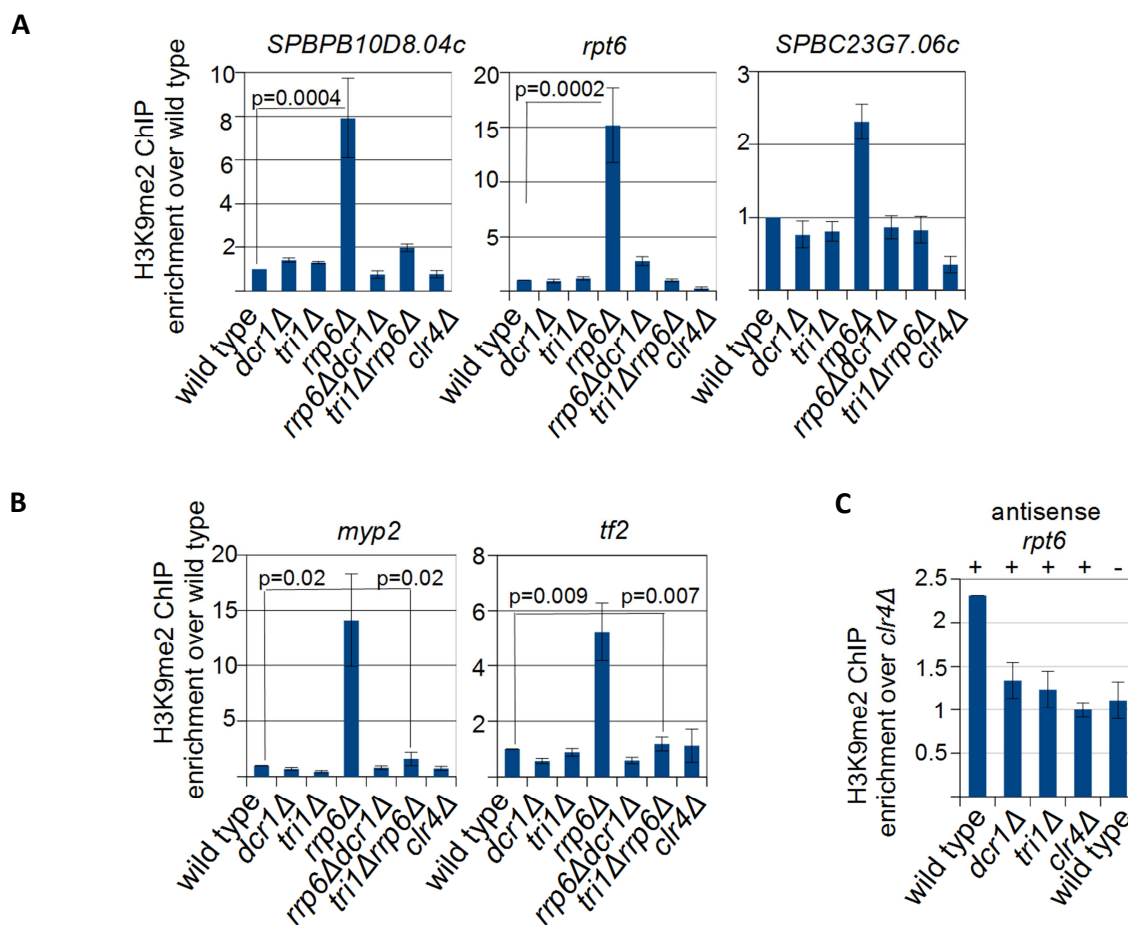


Figure 2.15.3. H3K9me ChIP showing that in *rrp6Δ* cells heterochromatin is established in a Triman- and Dicer- dependent way at indicated genes. Six independent biological replicates were used for quantification. Error bars indicate standard deviation; *p* value was calculated using Student's test. (A) H3K9me was abolished at *SPBPB10D8.04c*, *rpt6*, *SPBC23G7.06c* in *tri1Δrrp6Δ* cells, where also siRNAs were abolished. (B) H3K9me was abolished at *myp2* and *tf2* in *tri1Δrrp6Δ* cells, although the levels of siRNAs were not affected. (C) ChIP assay showing that plasmid based overexpression of antisense to *rpt6* gene resulted in H3K9me in a Dicer- and Triman- dependent way.

In addition to protein coding genes and transposons, in *rrp6Δ* cells RNAi also targeted rDNA (Figure 2.15.4 A). The observed siRNA generation was only slightly alleviated in *tri1Δrrp6Δ* cells (Figure 2.15.4 B, upper panel), but H3K9me was abolished to a level observed in wild-type cells (Figure 2.15.4 B, lower panel). This indicated that in *rrp6Δ* cells, RNAi also targets rDNA and induces heterochromatin in a Triman-dependent way.

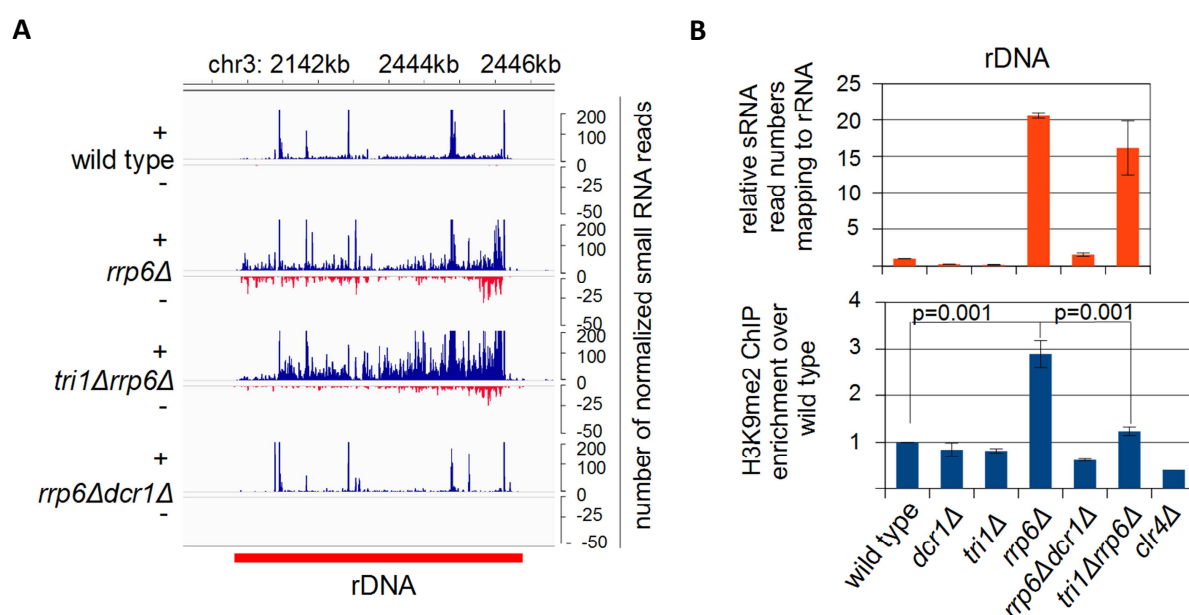


Figure 2.15.4. In *rrp6Δ* cells RNAi targets rDNA. (A) High-throughput sequencing of Argonaute-associated small RNAs from indicated cells. Small RNA reads were plotted over 25S rDNA locus. Scale bars on the right denote small RNA read numbers normalized per one million reads and to the total number of Argonaute-associated small RNAs. (B) Upper panel shows relative number of normalized small RNA reads from indicated strains at rDNA locus. Lower panel shows H3K9me ChIP at rDNA locus. In *rrp6Δ* cells, heterochromatin was established at rDNA in Triman- and Dicer-dependent way. Three independent biological replicates were used for quantification. Error bars indicate standard deviation; p value was calculated using Student's test.

Furthermore, we asked whether nucleation of RNAi and establishment of H3K9me at ectopic loci in *rrp6Δ* cells have functional role in silencing of targeted genes. Therefore, the levels of sense and antisense transcripts of *rpt6* and *SPBC23G7.06c* genes were quantified using qPCR (Figure 2.15.5). These genes were chosen because they nucleated RNAi and H3K9me in *rrp6Δ* cells in priRNA/Triman dependent manner (Figure 2.15.1 B, Figure 2.15.3 A). It was observed that in

strains with deletions of RNAi factors in *rrp6Δ* cells, where RNAi targeting and H3K9me is abolished, significant upregulation of the transcripts was not observed compared to *rrp6Δ* cells (Figure 2.15.5).

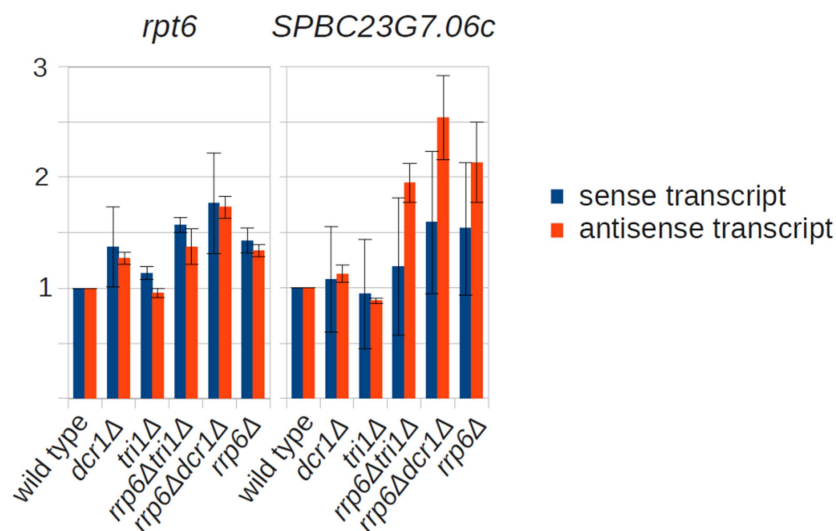


Figure 2.15.5. RNAi does not reduce RNA levels in *rrp6Δ* cells. Quantification of sense and antisense transcripts at *rpt6* and *SPBC23G7.06c* by qPCR in indicated cells. In *rrp6Δ* cells RNAi targets *rpt6* and *SPBC23G7.06c* genes and induces establishment of H3K9me. However, the established heterochromatin is not sufficient to induce functional silencing of the transcripts, as in double mutants of RNAi factors and Rrp6 significant upregulation of the transcripts is not observed.

Furthermore, it was shown that genes which are targeted by RNAi in *rrp6Δ* cells are also targeted by RNAi in wild-type *S. pombe* cells under varied growth conditions (Yamanaka et al. 2013). This suggested that *S. pombe* uses RNAi as a mechanism of gene regulation as a response to changing environmental conditions. To test this observation, as well as to determine whether RNAi nucleation in changing environmental conditions is dependent on Triman, cells were grown in media containing low concentrations of nitrogen or glucose. The levels of H3K9me in different mutant strains were then assessed by H3K9me ChIP experiment.

ChIP experiments under varied growth conditions had high variations between biological replicates for *tri1Δ* sample. In low nitrogen, significant enrichment of H3K9me in wild-type cells

was not observed at *Tf2* and *myp2* (<2-fold enrichment over *clr4Δ*) (Figure 2.15.6 A). However, in low nitrogen heterochromatin was established in Dicer-dependent manner at *rpt6*, *SPBC23G7.06c* and *lys1* (Figure 2.15.6 B). Although high variations between biological replicates for *triΔ* sample were observed, H3K9me at these genes was not abolished in cells lacking Triman. Moreover, *triΔ* cells had elevated levels of H3K9me. This indicates that Triman might have some unknown role at those genes.

In low glucose, H3K9me was detected in wild-type cells at some genes, for example at *SPBC23G7.06c* and *rpt6* (Figure 2.15.6 C). The observed heterochromatin was abolished in both *dcr1Δ* and *tri1Δ* cells, although higher variations were again observed for *tri1Δ* sample. This indicated that RNAi might indeed have a role at those loci in wild-type cells cultured in low glucose conditions.

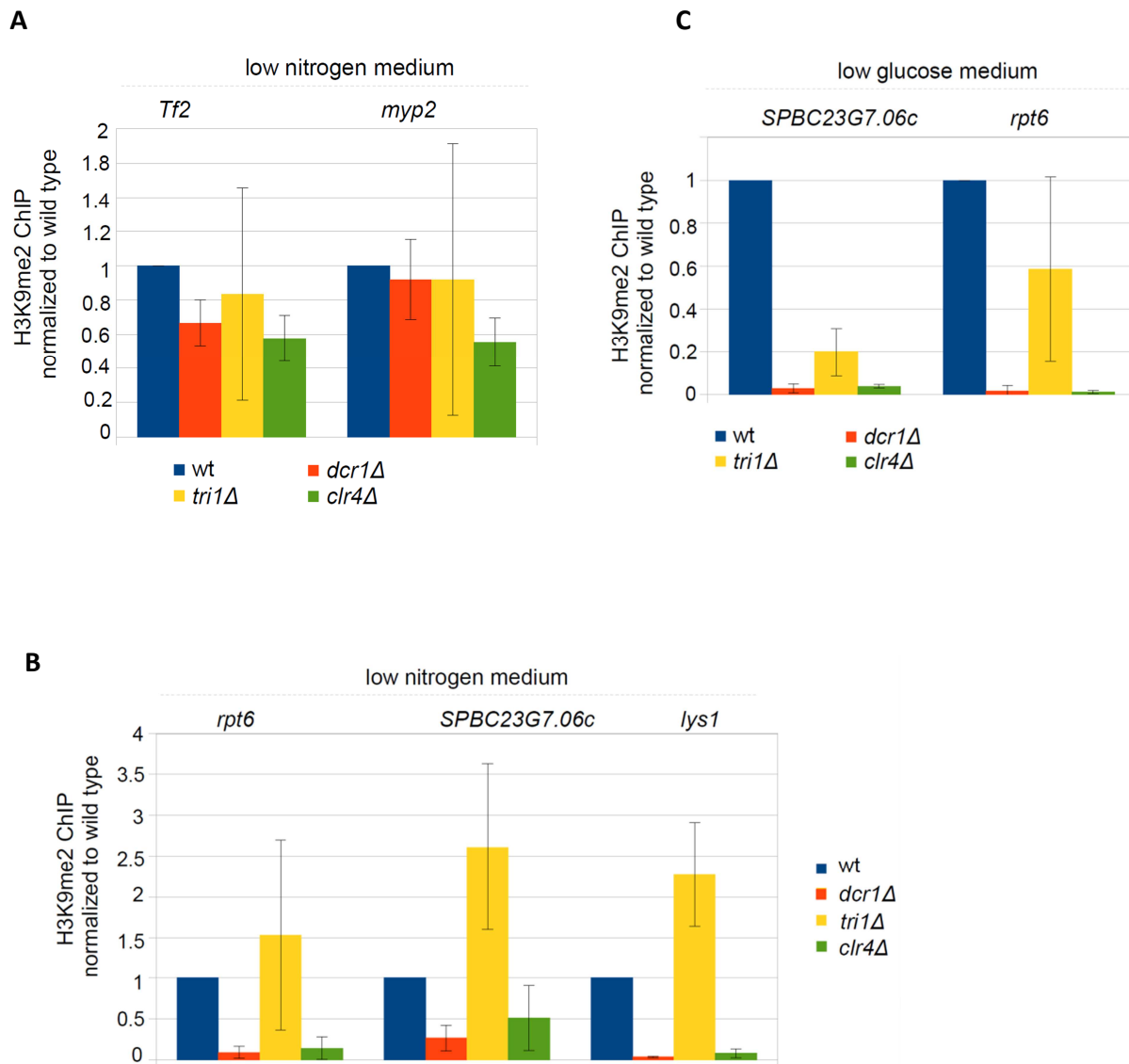


Figure 2.15.6. H3K9me ChIP in indicated strains grown under varied growth conditions. (A) In low nitrogen, establishment of heterochromatin was not observed at *Tf2* and *myp2* in indicated strains. Six independent biological replicates were used for quantification. Error bars indicate standard deviation. (B) In low nitrogen, establishment of heterochromatin was observed in wild-type cells at *rpt6*, *SPBC23G7.06c* and *lys1*. H3K9me was dependent on Dicer but not on Triman. Two independent biological replicates were used for quantification. Error bars indicate standard deviation. (C) In low glucose, establishment of heterochromatin was observed in wild-type cells at *SPBC23G7.06c* and *rpt6* genes. Two independent biological replicates were used for quantification. Error bars indicate standard deviation.

3 DISCUSSION

3.1 Triman is required for the biogenesis of priRNAs and mature siRNAs

Previously, a class of Argonaute-associated small RNAs called priRNAs (Halic & Moazed 2010) has been identified in fission yeast. These small RNAs are generated independently of Dicer- and RDRC-activity, and it was suggested that they function in initiating the positive-feedback loop of siRNA generation and heterochromatin formation (Halic & Moazed 2010). However, little was known about how they are generated. priRNAs are degradation products originating from various genomic regions. Because Argonaute slicer activity is not required for priRNA biogenesis, both 5' and 3' ends are most probably generated by the activity of unknown nucleases.

Here, by employing splinted ligation as a screening method, new players in the course of priRNA biogenesis have been identified. In *dcr1Δrrp6Δ* cells, Argonaute-associated *dg* priRNAs were more than 10-fold increased. This revealed the role of the nuclear exosome Rrp6 in degradation of priRNAs. In *dcr1ΔSPBC29A10.09cΔ* cells, Argonaute-associated *dg* priRNAs were not detectable by splinted ligation. This immediately suggested an important role of this previously uncharacterized gene in the biogenesis of priRNAs. By employing deep-sequencing of Argonaute-associated small RNAs, it was observed that in *SPBC29A10.09cΔ* cells not only Argonaute-associated priRNAs were longer, but also siRNAs. This indicated that *SPBC29A10.09c* is involved in trimming of small RNAs in fission yeast and thus it was named Triman. Additionally, in cells lacking Triman both priRNAs and siRNAs were reduced. While priRNA reduction was around 10-fold, siRNAs were around 2-fold reduced (Figure 2.1.2).

Even previously published data indicated the existence of a distinct mechanism for generation of small RNAs of mature length in fission yeast. Because *S. pombe* Dicer lacks PAZ domain, the produced double-stranded RNAs have a greater size range in comparison to PAZ-containing Dicers (Colmenares et al. 2007). Also, deep-sequencing data of Argonaute-associated small RNAs from slicer-defective Ago1-D580A indicated the existence of a trimming enzyme (Halic & Moazed 2010). In this slicer defective Ago1, small RNAs remain double-stranded. It was

observed that these centromeric dsAgo1-D580A-associated small RNAs also had a broader length distribution, similarly as in *triIΔ* cells. Hence, the finding that Triman is responsible for shaping the length of both Argonaute-associated priRNAs and siRNAs was in an agreement with the aforementioned data.

3.2 Triman is a CAF1 family 3'-5' exonuclease

Triman belongs to the CAF1 family of proteins, which are mainly deadenylases. The active site is highly conserved in higher eukaryotes (Table 5.1) and consists of four conserved residues, three aspartates (D) and a glutamate (E), which adopt a DEDD fold. These amino acids are important for coordinating two magnesium ions that are involved in the catalysis.

Indeed, biochemical characterization has shown that Triman is a Mg^{2+} -dependent 3'-5' exonuclease (Figure 2.4.2.1, Figure 2.4.2.2). Triman was able to degrade both short and long single-stranded RNA templates, and longer incubation time generally resulted in more degradation. Also, Triman was not able to degrade double-stranded small RNAs. To exclude the possibility that Triman is an endonuclease, activity was tested on β -eliminated and 2'-O-methyl modified RNA-templates. It was observed that for Triman activity a free 2' OH group is needed and 3' modified RNAs were not degraded. This confirmed that Triman is not an endonuclease but 3'-5' exonuclease.

3.3 The final processing of 3' end is a conserved process in small RNA biogenesis

Because Triman belongs to the highly conserved CAF1 family of exonucleases, Triman homologs might play a similar role in biogenesis of small RNAs in other organisms. Biogenesis of Dicer-independent priRNAs shows great similarity to the biogenesis of Dicer-independent piRNAs in the germline of animal cells (Aravin et al. 2007; Ghildiyal & Zamore 2009). Steps of piRNA biogenesis have been recapitulated in the lysate from silkworm ovary-derived cell line (Kawaoka et al. 2011). It was observed that following loading onto Piwi protein, piRNA

precursor undergoes trimming on 3' end. Although the trimming enzyme has not been identified, it was observed it is a Mg^{2+} dependent exonuclease (Kawaoka et al. 2011). Some miRNAs are also subjected to the final 3' end processing. It was shown that maturation of Dicer-dependent miRNA-like sRNA (miR-1) requires QIP, a 3'-5' exonuclease in *Neurospora* (Lee et al. 2010; Xue et al. 2012). Furthermore, in *Drosophila* a 3'-5' exoribonuclease Nibbler is responsible for the 3' end trimming of more than one quarter miRNAs (Han et al. 2011; Liu et al. 2011). In addition, human homolog of Triman is poly(A)-specific ribonuclease (PARN). Recently it was found that PARN is responsible for the final step of maturation of miR-451, a highly conserved erythropoietic miRNA in vertebrates (Yoda et al. 2013). Primary miR-451 has a hairpin structure and it is processed by Drosha in the nucleus. But, unlike canonical miRNAs, further processing bypasses Dicer (Cifuentes et al. 2010; Cheloufi et al. 2010; Yang et al. 2010). Instead pre-miRNA-451 is directly loaded onto Ago2 which slices its 3' arm. This generates 30-nt-long intermediate which is immediately trimmed by PARN on the 3' end to generate mature miR-451 (Yoda et al. 2013). These examples demonstrate that trimming of 3' end is a conserved mechanism in the course of biogenesis of diverse small RNAs.

3.4 Argonaute and Triman cooperate to generate priRNAs and siRNAs

Because Triman would completely degrade RNAs after longer incubation time (Figure 2.4.2.1), it became evident that also another factor is involved in generation of small RNA of mature size. Functional assays, mass spectrometry analysis of Argonaute purifications and *in vitro* co-immunoprecipitation indicated that Argonaute and Triman cooperate to generate small RNAs of mature length. In a course of small RNA biogenesis, Argonaute binds longer double-stranded RNA precursors. After the removal of the passenger strand, Argonaute-associated guide strand is trimmed to the mature length by Triman. In this process, Argonaute acts as a ruler for the final size of small RNA.

Furthermore, sequencing data of Argonaute-associated small RNAs showed that in cells lacking Triman, all siRNAs and priRNAs are longer: centromeric sRNAs, sRNAs mapping to mRNAs, sRNAs mapping to rRNA. These data showed that Triman determines the length of all

Argonaute-associated small RNAs and acts as a general factor involved in biogenesis of priRNAs and siRNAs.

Moreover, overexpression of Triman resulted in production of several-fold more Argonaute-associated priRNAs, indicating that trimming represents limiting step in the course of priRNA biogenesis. Also, sequencing of Argonaute-associated small RNAs revealed that in Triman overexpression, both priRNAs and siRNAs are 1 nucleotide shorter. This indicated that high cellular levels of Triman would result in removal of additional nucleotide from Argonaute-associated small RNAs.

3.5 Trimming is important for the stability of the complex between Ago1 and small RNA and for the proper Argonaute-slicing activity

In order to address if the length of small RNA guide is important for the stability of the complex Ago1:small RNA, *in vitro* assay where Argonaute was loaded with small RNAs of various lengths was performed. While 22-nt, 24-nt, and 26-nt-long small RNAs were stably associated with Argonaute, 30-nt long and longer small RNAs were dissociating at high rate. This indicates that the final shaping of Argonaute-associated small RNAs is important for the formation of stable complex between Argonaute and its small RNA guide. Longer 3' end of small RNA probably does not accommodate very well in the PAZ domain of Argonaute, causing weaker binding and rapid dissociation.

Argonaute slicing activity is important for siRNA generation and heterochromatin formation in fission yeast. Our *in vitro* reconstitution of Argonaute slicer activity demonstrated that longer small RNAs cannot efficiently guide Argonaute to slice cognate targets. Complex containing 22-nt-long small RNA with Argonaute was efficient in slicing of complementary target, but only 2 nt longer sRNA showed around 7-fold less efficiency. Therefore, the final 3' trimming of Argonaute-associated small RNAs is important for their function in efficient guiding Argonaute to slice complementary targets.

3.6 priRNA and siRNA trimming is required for *de novo* heterochromatin assembly

What are the functional consequences of Triman deletion for *S. pombe* cells? It was observed that Ago1-associated centromeric *dg* and *dh* small RNAs are 1.5 and 2-fold reduced in *tri1Δ* cells. This indicated that 3' end trimming is important for proper siRNA biogenesis. However, *tri1Δ* cells were able to maintain the levels of pericentromeric heterochromatin as H3K9me levels were only around 20 % reduced. In wild-type cells majority of Ago1-associated small RNAs (around 80 %) originate from pericentromeric region. In *tri1Δ* cells, around 20 % of centromeric siRNAs were still 22-nt-long (Figure 2.11.1 B). Since pericentromeric siRNAs are produced in vast amount, even in deletion of Triman threshold level of mature size sRNAs that are able to maintain heterochromatin were still produced.

Furthermore, siRNAs were almost completely abolished at *IRC3* repeat element which flanks *dg* and *dh* repeats on chromosome 3. But, *tri1Δ* cells were able to maintain functional H3K9me levels at *IRC3*, which demonstrated that heterochromatin is still able to spread from *dg* repeats to the surrounding region.

Next, involvement of Triman on establishment of heterochromatin formation was explored. By treating cells with TSA, inhibitor of histone deacetylases, it was possible to perturb existing heterochromatin. While treated wild-type cells could reestablish functional heterochromatin, *tri1Δ* cells showed a defect in reestablishment of centromeric heterochromatin as determined by growth assay. This indicated that Triman might be involved in the initiation of silencing and prompted us to validate these results and to perform reestablishment assay.

In the reestablishment assay, *clr4⁺* and *dcr1⁺* genes were reintroduced into *clr4Δdcr1Δtri1Δ* cells, where heterochromatin, siRNAs and priRNAs are abolished. As a control, *clr4⁺* and *dcr1⁺* were also reintroduced into *clr4Δdcr1Δ* cells. It was observed that *clr4Δdcr1Δtri1Δ/clr4⁺dcr1⁺* cells were not able to establish functional pericentromeric heterochromatin, in contrast to the *clr4Δdcr1Δ/clr4⁺dcr1⁺* control cells. Also, in *clr4Δdcr1Δtri1Δ/clr4⁺dcr1⁺* cells pericentromeric *dg* transcripts were upregulated in contrast to control cells. This indicated that Triman is required

for establishment of siRNA generation and heterochromatin formation at pericentromeric region in *S. pombe*.

Previously, it was suggested that priRNAs play an important role in initiating siRNA amplification and heterochromatin generation (Halic & Moazed 2010). Here, *clr4*⁺ was reintroduced into *clr4Δdcr1Δtri1Δ* cells which lack heterochromatin, siRNAs and priRNAs. It was observed that H3K9me levels were not reestablished at centromeric *dg* repeats in *clr4Δdcr1Δtri1Δ/clr4*⁺ cells. This indicated that Clr4 cannot be recruited to pericentromeric region in the absence of small RNAs and that RNAi precedes H3K9methylation. In contrast, reintroduction of *clr4*⁺ in *clr4Δdcr1Δ* cells, where only priRNAs are present, established very low levels of H3K9me reestablishment at centromeric *dg* repeats.

These experiments demonstrated that high levels of antisense priRNAs generated at pericentromeric region can nucleate very low levels of H3K9me which could initiate siRNA generation and establishment of heterochromatin at *dg* repeats.

3.7 Triman is important for H3K9me at heterochromatin islands

Several groups have observed that H3K9 methylation can be detected at loci outside of major constitutive heterochromatin domains involving pericentromeric, subtelomeric and mating type region in *S. pombe* (Zofall et al. 2012; Hiriart et al. 2012; Tashiro et al. 2013). This additional heterochromatin islands comprise meiotic mRNAs and ncRNAs that are suppressed in vegetative growth phase. It was suggested that the islands represent analogy to facultative heterochromatin in higher eukaryotes (Zofall et al. 2012). However, it was observed that heterochromatin at reported islands does not restrict Pol II access or has an influence on the transcript levels of the corresponding island, arguing against that comparison (Egan et al. 2014). H3K9 methylation at a subset of islands occurs in an Mmi1-dependent mechanism. Also, heterochromatin formation at several islands has been reported to be also dependent on RNAi factors (Zofall et al. 2012). Here, it was observed that in *tri1Δ* cells, Argonaute-associated small RNAs are reduced at several heterochromatin islands that are dependent on RNAi-machinery (Figure 2.14.1 A, B). Remaining Ago1-associated small RNAs in *tri1Δ* cells were also longer. In addition, by ChIP-sequencing it

was observed that H3K9 methylation was abolished or reduced in *tri1Δ* cells at several islands, for example *mcp5*, *SPAC8C9.04c*, *vps29* (Figure 2.14.1 D,E). In contrast, deletion of *tri1⁺* had no effect on H3K9me on islands which are reported to be RNAi-independent, such as *mei4*.

This indicated that Triman is required for heterochromatin formation at RNAi-dependent heterochromatin islands in fission yeast. At these islands, small RNAs are generated in an around 10.000-fold lower quantity compared to the pericentromeric region. Hence, a small defect in 3' end processing results in a substantial defect in a generation of small RNAs and as a consequence, in an inappropriate H3K9methylation. This occurs most likely because of improper slicing ability of Argonaute complex that is loaded with longer small RNA (Chapter 2.10). Overall, these observations imply that a possible mechanism which regulates formation of heterochromatin islands as a response to changing environment might involve the 3' end processing of Argonaute-associated small RNAs. At constitutive heterochromatin domains, vast production of small RNAs ensures that there is always a sufficient fraction of sRNAs generated of mature size, which are thus capable of ensuring proper heterochromatin maintenance.

3.8 In *rrp6Δ* cells RNAi is nucleated at euchromatic loci in priRNA/Triman-dependent manner

In eukaryotes, a multi-protein complex exosome is involved in processing, turnover and surveillance activities of various RNA targets. It's substrates range from rRNAs, snRNAs and mRNAs to cryptic unstable transcripts (CUTs) (Gudipati et al. 2012). Fission yeast genome is, as other eukaryotic genomes, widely transcribed with vast number of ncRNAs and antisense transcripts being produced (Dutrow et al. 2008). This necessities the existence of mechanisms which are responsible for RNA quality control of spurious transcription, which mainly involve the exosome.

Rrp6 is a 3'-5' exonuclease associated with the exosome in fission yeast. It was shown to be important for quality control of various RNA transcripts (Gudipati et al. 2012) and also implicated to act with Clr4 to suppress antisense transcripts originating from euchromatic region (Zhang et al. 2011). At pericentromeric region of fission yeast, it acts in a parallel way to RNAi

to silence pericentromeric transcripts (Murakami et al. 2007; Bühler et al. 2007; Reyes-Turcu et al. 2011; Zhang et al. 2011).

Here, in a screen for potential nucleases involved in biogenesis of priRNAs it was observed that centromeric *dg* transcripts accumulated in *dcr1Δrrp6Δ* cells more than 10-fold (Figure 2.1.1 D). This indicated that Rrp6 might have a role in degradation of priRNAs and is consistent with the finding that Rrp6 has a role in degradation of many antisense transcripts (Houseley et al. 2006).

To elucidate the function of Rrp6, high-throughput sequencing of Argonaute-associated small RNAs from *rrp6Δ* cells was performed. We and Yamanaka et al. (2013) have observed that in *rrp6Δ* cells, RNAi targets various loci across the genome (Figure 2.15.1, Figure 2.15.2, Table 5.2). The genes that were targeted by RNAi comprised many developmental genes, proteasomal subunit and ncRNAs (Yamanaka et al. 2013). Moreover, observed siRNA production was accompanied by H3K9me (Figure 2.15.3, Figure 2.15.4 B).

The observed ectopic RNAi nucleation in *rrp6Δ* cells has enabled us a dissection for factors required for RNAi establishment without the need to 'erase' preexisting heterochromatin and RNAi. High-throughput sequencing of Argonaute-associated small RNAs revealed that in *rrp6Δtri1Δ* cells, at most loci small RNAs were not generated and H3K9me was not established (for example at *rpt6*, *SPBPB10D8.04c*, *SPBC23G7.06c*). This indicated that in *rrp6Δ* cells, Triman is required to generate priRNAs which guide Argonaute to establish siRNA amplification and heterochromatin formation at ectopic targets. Furthermore, by overexpressing antisense to *rpt6* gene *in trans*, it was observed that small levels of H3K9me were established in wild-type cells in Dicer- and Triman-dependent manner (Figure 2.15.3 C). These results indicate that antisense RNAs can be processed into priRNAs that can initiate siRNA production and heterochromatin formation.

At some loci, small RNA generation in *rrp6Δtri1Δ* cells was only alleviated or not affected. For example at *tf2* and *myo2* siRNAs were not affected by deletion of Triman in *rrp6Δ* cells. Nevertheless, deletion of Triman abolished H3K9me also at these loci. This indicated that at these targets, RNAi is initiated by some other, priRNA-independent mechanism. However,

Triman is still required to generate adequate amounts of siRNAs of the mature size which are capable of guiding Argonaute to establish heterochromatin at these loci.

To find out whether nucleation of RNAi and establishment of H3K9me at ectopic loci in *rrp6Δ* cells results in active silencing of targeted genes, the levels of sense and antisense transcripts of two genes (*rpt6* and *SPBC23G7.06c*) that nucleated RNAi in *rrp6Δ* were quantified. It was observed that by deleting RNAi factors or *Clr4* in *rrp6Δ* cells, which abolishes RNAi targeting and H3K9me, the transcript levels were not significantly upregulated compared to *rrp6Δ* cells (Figure 2.15.5). This indicated that low levels of H3K9me which are established in *rrp6Δ* cells are not sufficient to restrict RNA polymerase II and induce functional silencing. However, in this experiment only 2 genes were investigated. Also, at *rpt6* gene in *rrp6Δdcr1Δ* cells a slight increase of transcripts can be observed in comparison to the single mutants. Therefore, the possibility that very low fluctuations in transcripts levels could have a significant effect *in vivo* cannot be excluded. In Yamanaka et al. (2013) it was shown that cells lacking RNAi factors or *Clr4* in a combination with *rrp6Δ* showed upregulation of the transcripts when compared to the single mutants. This observation was shown for several genes (*mug5*, *mcp3*, *mek1* and *SPCC1442.04c*) and indicated that in *rrp6Δ* cells RNAi establishes functional silencing. Our data is not in an agreement with this observation and the differences might result because not the same genes were investigated. However, the levels of established H3K9me at ectopic loci in *rrp6Δ* cells are much lower than those found at constitutive heterochromatin at pericentromeric regions (Figure 2.15.3, Figure 2.12.2 A), indicating that they might not result in functional silencing. This would be also in an agreement with the finding that at heterochromatin islands comprising meiotic genes, small levels of H3K9me do not result in functional silencing of the targeted genes (Egan et al. 2014).

Furthermore, it was reported that loci targeted by RNAi in *rrp6Δ* cells could be targeted by RNAi in wild-type cells under varied growth conditions that cells experience in environment (Yamanaka et al. 2013). This suggested that *S. pombe* uses RNAi as a mechanism of gene regulation in response to changing conditions. In our ChIP experiments, in low nitrogen a significant enrichment of H3K9me in wild-type cells was not observed at *tf2* and *myo2* (<2-fold enrichment over *clr4Δ*) (Figure 2.15.6 A). However, at some genes small levels of H3K9me were established in Dicer-dependent manner (*rpt6*, *SPBC23G7.06c*, *lys1*) (Figure 2.15.6 B). Although

triΔ samples showed particularly high variations between biological replicates, the observed establishment seemed to be independent of Triman. Moreover, in *triΔ* cells H3K9me levels were even higher. This indicated that Triman might have some other, unknown role at those genes. In low glucose, H3K9me was detected in wild-type cells at some genes, for example at *SPBC23G7.06c* and *rpt6* (Figure 2.15.6 C). The observed heterochromatin was abolished in both *dcrlΔ* and *tri1Δ* cells, although higher variations were again observed for *tri1Δ* sample. This indicated that RNAi might indeed have a role at those loci in wild-type cells cultured in low glucose conditions. It would be interesting to see whether heterochromatin observed in cells grown in carbon-limiting conditions has a functional role in silencing by assessing the corresponding transcript levels and RNA polymerase II occupancy.

The ectopic RNAi targeting in *rrp6Δ* cells indicates that exosome-mediated RNA quality control is required for the protection of the genome from spurious RNAi. If the exosome machinery is disrupted, accumulation of antisense transcripts and priRNAs lead to ectopic RNAi nucleation and heterochromatin formation at a subset of protein-coding genes and ncRNAs. At some regions, priRNAs are not able to induce RNAi and heterochromatin establishment. This indicates that other factors might be necessary in a process of establishment or on the possible presence of antagonizing factors at these loci. Overall, the results presented here indicate that accumulated antisense priRNAs can act with Argonaute as a surveillance mechanism. This represents one possible host cell pathway that can recognize repetitive and foreign DNA elements. A similar mechanism has been proposed in *C. elegans*, where 21U-RNAs bound to Piwi protein PRG-1 scan for and initiate siRNA amplification and H3K9me of foreign sequences (Shirayama et al. 2012; Lee et al. 2012; Bagijn et al. 2012; Tashiro et al. 2013; Ashe et al. 2012). This indicates that mechanistically similar pathways might exist in different organisms as a defense mechanism to nucleate silencing of transposons and foreign sequences.

3.9 The model of Triman-dependent priRNA biogenesis and RNAi nucleation

priRNAs are degradation products originating from various genomic regions. They are processed by an unknown mechanism to create longer priRNA precursors, which are loaded onto Argonaute. Triman is recruited to the Ago1:priRNA complex to generate the 3' end of priRNA. priRNAs in turn can guide Argonaute to nucleate RNAi specifically at pericentromeric region because it is bidirectionally transcribed. This leads to siRNA amplification and subsequent heterochromatin generation.

siRNAs are generated by an Rdp1- and Dicer-activity, however Dicer-products are longer than the mature siRNAs. Longer double-stranded Dicer-generated siRNA precursors are loaded onto Argonaute, passenger strand is sliced by the Argonaut's slicer activity and removed. Triman is recruited to the Ago1:siRNA complex to trim the 3' end of Argonaute-bound siRNA. This final maturation step is important for generation of mature Ago1:siRNA complex which is capable of slicing the cognate target and heterochromatin establishment.

In a case antisense levels in a cell are perturbed, Argonaute is able to bind them and induce RNAi to the targeted locus in a priRNA/Triman dependent-way.

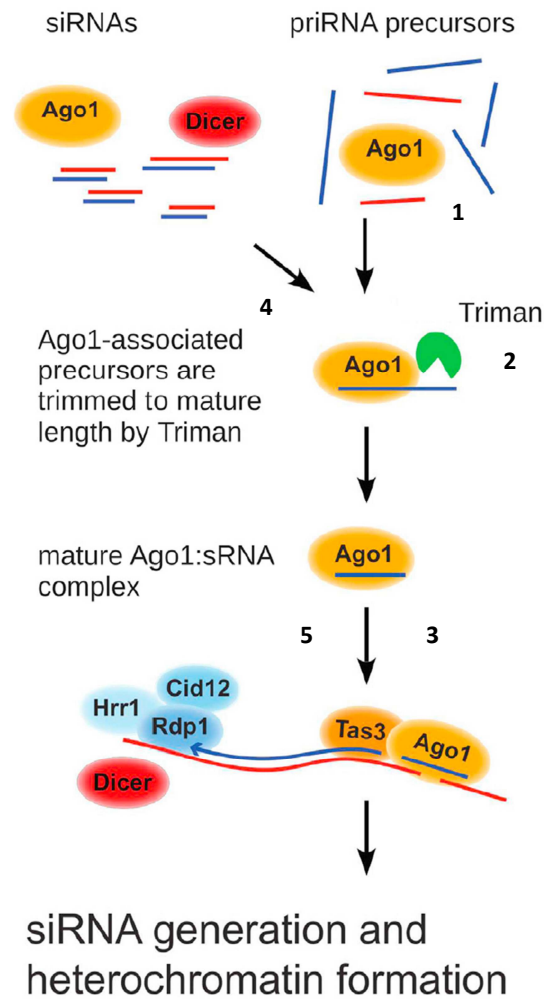


Figure 3.9.1. Model representing biogenesis of Dicer-independent priRNAs which nucleate siRNA amplification and heterochromatin formation. (1) Argonaute binds priRNA precursors in a process of transcriptome surveillance. (2) Argonaute loaded with longer priRNAs recruits Triman to process the 3' end of small RNA. (3) Mature Ago1:priRNA complex will be targeted to the pericentromeric region which is bidirectionally transcribed, and induce siRNA amplification. (4) siRNAs are generated by Dicer, loaded onto Argonaute, and following release of the passenger strand, processed on the 3' end by Triman. (5) Once heterochromatin-independent siRNAs accumulate, they initiate positive-feedback loop of siRNA amplification and heterochromatin formation.

4 MATERIALS AND METHODS

4.1 Materials

4.1.1 Consumables and Chemicals

Chemicals used in this study were purchased from Bio-Rad (Hercules, USA), Roth (Karlsruhe, Germany), Merc (Darmstadt, Germany), Qiagen (Hilde, Germany), Roche (Basel, Switzerland), and Sigma-Aldrich (Munich, Germany).

DNA oligonucleotides were synthesized by Metabion (Martinsried, Germany), Thermo Scientific and Biotex (Berlin, Germany). Enzymes, dNTPs and molecular weight markers were purchased from New England Biolabs (Ipswich, USA), Invitrogen (Darmstadt, Germany) and Fermentas (Burlington, USA).

4.1.2 Oligonucleotides

Table 4.1.2.1. Oligonucleotides used in this study.

Oligonucleotides used for RT-qPCR and ChIP	Oligonucleotide sequence (5' → 3')
110A.TDH1_F	CCAAGCCTACCAACTACGA
110A.TDH1_R	AGAGACGAGCTTGACGAA
110E.DHE_F	GCCCATTTCATCAAACGAGTC
110E.DHE_R	GATTCGGCACCTTTGTCATT
110F.DGF_F	CTGCGGTTACCCCTTAACAT
110F.DGF_R	CAACTGCGGATGGAAAAAGT
207_RPT6_F	GAGAATCCATTCGAGGTCCA
207_RPT6_R	AATGCAAACATACCGGCTTC
214_23G7_F	GTCATTGACGTTGACGTTGG
214_23G7_R	CAATCGCTTCGTACCAAAT
194_B10_F	TGCGATTGCTTTAGGCTTTT
194_B10_R	CGCGTTAATTGCTTGATAA

113_25S_F	TTTCTCCTTCTCGGGGATT
113_25S_R	AACACCACTTTCTGGCCATC
RNA oligonucleotides used in <i>in vitro</i> assays	
RNA61	AAAGUAGAGGUAAGAACAGUA
RNA70	UACUGUUCUUACCUCUACUUU
RNA71	GCGAGCGAGGCAAAGAACAAGA
RNA72_22nt	UUGUUCUUUUGCCUCGCUCGCUG
RNA172_30nt	UGAAAGCUUUAGUUGAUACGUCCACGGACA
RNA_26nt	UGGUACCAAAGCUCGAACAUAUAAAAA
RNA69	UUUACUGUUCUUACCUCUACU
RNA172_26nt	UGAAAGCUUUAGUUGAUACGUCCACG
RNA172_24nt	UGAAAGCUUUAGUUGAUACGUCCA
RNA_2Ome1	chol-[UCUUAAAUCAGCUUUCAAAAUACGAGAAACCU] 2'O – Methyl -RNA
RNA_2Ome2	chol-[CAUCACGUACGCGGAAUACUUCGAAAUGUCC]] 2'O – Methyl -RNA
Splinted ligation oligonucleotides	
94.Ligation primer	CGCTTATGACATTCCdd
93A.dg	GAATGTCATAAGCGATTGTGACGAGGCACATTCCTTA
93B.dg	GAATGTCATAAGCGAATTTGACGAGGCACATTCCTTA
93C.dh1	GAATGTCATAAGCGCAGGAGTTGCGCAAACGAAGTTA
93D.dg	GAATGTCATAAGCGACCGAGTGCAAATGCTTTTGTA
93E.dg	GAATGTCATAAGCGCTGACTTGGCTTGTCTTCTGTA
93F.dg	GAATGTCATAAGCGGGCATAGCGATGATAGTTCTA
93G.dg	GAATGTCATAAGCGAGGCATAGCGATGATAGTTCTA
93H.dh1	GAATGTCATAAGCGGACGATAAGCAGGAGTTGCGCA
Oligonucleotides used for high-throughput sequencing	
3' adaptor oligonucleotide (miRNA Cloning Linker-1 from IDT)	rApp/CTGTAGGCACCATCAAT/3ddC
5' adaptor oligonucleotide	GUUCAGAGUUCUACAGUCCGACGAUC
RT oligo	ATT GAT GGT GCC TAC AG
P5	AATGATACGGCGACCACCGACAGGTTTCAGAGTTCTACAGTCCGACGATC
158A1	CAAGCAGAAGACGGCATACGAGGATCCATTGATGGTGCCTACAG
158B1	CAAGCAGAAGACGGCATACGACAGCTGATTGATGGTGCCTACAG
158C1	CAAGCAGAAGACGGCATACGATCTAGAATTGATGGTGCCTACAG
158D1	CAAGCAGAAGACGGCATACGAATCGATATTGATGGTGCCTACAG

158E1	CAAGCAGAAGACGGCATACGAGCGACTATTGATGGTGCCTACAG
158F1	CAAGCAGAAGACGGCATACGACCAGTCATTGATGGTGCCTACAG
158G1	CAAGCAGAAGACGGCATACGAAGTATGATTGATGGTGCCTACAG
158H1	CAAGCAGAAGACGGCATACGATACGCGATTGATGGTGCCTACAG
RNA synthesis oligonucleotides	
130F.	GCTGGGACAGCAATATCGTA
130F_30A.	TTTTTTTTTTTTTTTTTTTTTTTTTTTTTTTTTTGCTGGGACAGCAATATCGTA
130R.	AGGATTACGACCAGCTCCAT
130R_30A.	TTTTTTTTTTTTTTTTTTTTTTTTTTTTTTTTTTAGGATTACGACCAGCTCCAT
130FT7.	GCGTAATACGACTCACTATAGGGGCTGGGACAGCAATATCGTA
130RT7_2.	GCGTAATACGACTCACTATAGGGAGGATTACGACCAGCTCCAT
54.dg100	GCGTAATACGACTCACTATAGGGCTTCGTTTATATCGCTAACAAGAA ATC
49.dg30A	TTTTTTTTTTTTTTTTTTTTTTTTTTTTTTTTTTTCATCTCCATTCTTGTCAT TAT
49.dg	CATCTCCATTCTTGTCATTAT
272F.	GCGTAATACGACTCACTATAGGGCATGATGATGACGATTACAGTCCG TGGAC
272R.	CGTGATGTAACCTTGATGAAAGCTTTAGTTGATACGTCCACGGACTGT AATCGTCATCATCATGCCCTATAGTGAGTCGTATTACGC
290F_65nt.	GCGTAATACGACTCACTATAGGGTATGATGATGACGATTACAGTCCG TGGACGTATCAACTAAAGCTTTCATCAAGTTACATCACA
290R_65nt.	TGTGATGTAACCTTGATGAAAGCTTTAGTTGATACGTCCACGGACTGT AATCGTCATCATCATACCCCTATAGTGAGTCGTATTACGC

4.1.3 Plasmids

Table 4.1.3.1. List of plasmids.

Plasmid number	Name
p379	pREP nmt1_FLAG_Tri1
p381	pREP nmt1_Tri1
p393	pREP nmt1_FLAG_Tri1D28A
p348	pREP clr4promotor_clr4_clr4terminator
P474	pJR1U dcr1promotor_dcr1_dcr1terminator

4.1.4 Strains

Table 4.1.4.1. List of strains.

<i>S. pombe</i> strains	Genotype
SP65	<i>h+ otr1R(SphI)::ura4+ ura4-DS/E leu1-32 ade6-M210 nat::FLAG-Ago1</i>
SP136	<i>h+ otr1R(SphI)::ura4+ ura4-DS/E leu1-32 ade6-M210 nat::FLAG-Ago1 tri1Δ::Kan</i>
SP34	<i>h+ otr1R(SphI)::ura4+ ura4-DS/E leu1-32 ade6-M210 nat::FLAG-Ago1 dcr1Δ::hph</i>
SP141	<i>h+ otr1R(SphI)::ura4+ ura4-DS/E leu1-32 ade6-M210 nat::FLAG-Ago1 dcr1Δ::hph tri1Δ::Kan</i>
SP504	<i>h+ otr1R(SphI)::ura4+ ura4-DS/E leu1-32 ade6-M216 his7-366 nat::FLAG-Ago1 rrp6Δ::Kan</i>
SP549	<i>h+ otr1R(SphI)::ura4+ ura4-DS/E leu1-32 ade6-M210 nat::FLAG-Ago1 tri1Δ::hph rrp6Δ::Kan</i>
SP520	<i>h+ imr1R(NcoI)::ura4+ ura4-D18 leu1-32 ade6-M216 kan::FLAG-Ago1 rrp6Δ::nat dcr1Δ::hph</i>
SP613	<i>ade6-M210 leu1-32 ura4-D18 tri1Δ::Kan dcr1Δ::hph clr4Δ::nat (1)</i>
SP614	<i>ade6-M210 leu1-32 ura4-D18 tri1Δ::Kan dcr1Δ::hph clr4Δ::nat (2)</i>
SP615	<i>ade6-M210 leu1-32 ura4-D18 tri1Δ::Kan dcr1Δ::hph clr4Δ::nat (3)</i>
SP622	<i>ade6-M210 leu1-32 ura4-D18 dcr1Δ::hph clr4Δ::nat (1)</i>
SP623	<i>ade6-M210 leu1-32 ura4-D18 dcr1Δ::hph clr4Δ::nat (2)</i>
SP613+p348	<i>ade6-M210 leu1-32 ura4-D18 tri1Δ::Kan dcr1Δ::hph clr4Δ::nat (1) + clr4⁺</i>
SP614+p348	<i>ade6-M210 leu1-32 ura4-D18 tri1Δ::Kan dcr1Δ::hph clr4Δ::nat (2) + clr4⁺</i>
SP615+p348	<i>ade6-M210 leu1-32 ura4-D18 tri1Δ::Kan dcr1Δ::hph clr4Δ::nat (3) + clr4⁺</i>
SP622+p348	<i>ade6-M210 leu1-32 ura4-D18 dcr1Δ::hph clr4Δ::nat (1) + clr4⁺</i>
SP623+p348	<i>ade6-M210 leu1-32 ura4-D18 dcr1Δ::hph clr4Δ::nat (2) + clr4⁺</i>
SP613+p348+ p474	<i>ade6-M210 leu1-32 ura4-D18 tri1Δ::Kan dcr1Δ::hph clr4Δ::nat (1) + clr4⁺ + dcr1⁺</i>
SP614+p348+ p474	<i>ade6-M210 leu1-32 ura4-D18 tri1Δ::Kan dcr1Δ::hph clr4Δ::nat (2) + clr4⁺ + dcr1⁺</i>
SP615+p348+ p474	<i>ade6-M210 leu1-32 ura4-D18 tri1Δ::Kan dcr1Δ::hph clr4Δ::nat (3) + clr4⁺ + dcr1⁺</i>
SP622+p348+ p474	<i>ade6-M210 leu1-32 ura4-D18 dcr1Δ::hph clr4Δ::nat (1) + clr4⁺ + dcr1⁺</i>
SP623+p348+ p474	<i>ade6-M210 leu1-32 ura4-D18 dcr1Δ::hph clr4Δ::nat (2) + clr4⁺ + dcr1⁺</i>
<i>E. coli</i> strains	
XL1-blue	<i>RecA1 endA1 gyrA96 thi-1 hsdR17 supE44 relA1 lac [F' proAB lacIqZ ΔM15 Tn10(Tetr)]</i>
BL21(DE3) Star	<i>F-ompT hsdSB(rb-, mB-) gal dcm rne l31</i>

4.1.5 Antibodies

Table 4.1.5.1. List of antibodies.

Name	Source	Dilution
anti-FLAG M2 antibody	Sigma	1:5000
HA-probe Antibody	Santa Cruz	1:200
anti-mouse IgG-HRP	Santa Cruz	1:2000
α tubulin Antibody	Santa Cruz	1:1000
goat anti-rat IgG-HRP	Santa Cruz	1:3000
Anti-Histone H3 (di methyl K9) antibody [1220]	AbCam	

4.1.6 Buffers, solutions and media

Table 4.1.6.1. List of buffers, solutions and media.

Name	Composition
LB (<i>E. coli</i> media)	10 g/l tryptone, 5 g/l Yeast extract, 10 g/l NaCl
YES (<i>S. pombe</i> media)	5 g/l Yeast extract, 30 g/l glucose, 0,225 g/l of amino acids (leucine, adenine, histidine, lysine)
EMMC - leucine (<i>S. pombe</i> media)	20 g/l glucose, 12,4 g/l EMM without dextrose, 0,226 g/l adenine, 0,226 g/l uracil, 0,226 g/l histidine
EMMC + low glucose	5 g/l glucose, 12,4 g/l EMM without dextrose, 0,226 g/l adenine, 0,226 g/l uracil, 0,226 g/l histidine
EMMC - nitrogen	20 g/l glucose, 12,4 g/l EMM without dextrose, 0,226 g/l adenine, 0,226 g/l histidine, 0,226 g/l leucine, 0,226 g/l lysine, 0,226 g/l uracil
In vitro RNA synthesis	
Transcription buffer	40 mM Tris pH 7.6, 2 mM spermidine, 6 mM MgCl ₂ , 0.01% Triton X100, 10 mM DTT
Splinted ligation	
	20 mM Hepes (pH 7.5) and 80 mM KCl
10xT4 RNA ligation buffer without ATP	500 mM Tris-HCl pH 7.5, 100 mM MgCl ₂ , 100 mM DTT, 600 μ g/ml BSA
Periodate oxidation/ β-elimination of RNA	
5Xborax/boric acid buffer	148 mM borax, 148 mM boric acid pH 8.6
RNA purification	
<i>Lysis buffer for RNA</i>	300 mM NaOAc pH 5.2, 10 mM EDTA, 1 % SDS
In vitro Triman assays	
MgCl ₂ buffer	25 mM Hepes (pH 7.5), 2 mM MgCl ₂ , 2 mM DTT, 0.02% NP-40

Washing buffer	25 mM Hepes 7.5, 2 mM MgCl ₂ , 2 mM DTT, 0.02 % NP40, 100 mM NaOAc
Protein purification	
1.5 M lysis buffer	50 mM Hepes (pH 7.6), 1.5 M NaOAc, 5 mM Mg(OAc) ₂ , 1 mM EGTA, 1 mM EDTA, 0.1% (v/v) Nonidet P-40 (NP-40) and protease inhibitors (Protease inhibitor cocktail tablets, Roche).
150 mM lysis buffer	50 mM Hepes (pH 7.6), 150 mM NaOAc, 5 mM Mg(OAc) ₂ , 1 mM EGTA, 1 mM EDTA, 0.1% (v/v) Nonidet P-40 (NP-40) and protease inhibitors (Protease inhibitor cocktail tablets, Roche, Complete, EDTA free).
Elution buffer	lysis buffer containing 0.2 mg/ml 3xFLAG peptide and 5% (v/v) glycerol
Western blot	
Amido-black solution	7.5 % HOAc, 20% EtOH, 0.1 % amido-black
Destaining solution	50 % EtOH, 5 % HOAc
Blotting buffer	20 % methanol, 48 mM Tris base, 39 mM glycine, 0.037 % SDS
1× TBS-T buffer	50 mM Tris-Cl, pH 7.5, 150 mM NaCl, 0.05% Tween 20
ChIP	
Lysis buffer	50 mM Hepes (pH 7.6), 1.5 M NaOAc, 5 mM Mg(OAc) ₂ , 1 mM EGTA, 1 mM EDTA, 0.1% (v/v) Nonidet P-40 (NP-40) and protease inhibitors (Protease inhibitor cocktail tablets, Roche).
ChIP elution buffer	50 mM Tris-HCl pH 8.0, 10 mM EDTA, 1% SDS

4.2 Methods

4.2.1 Working with *S. pombe* cells

4.2.1.1 Strain construction

Strains used in the study are generated either by PCR-based gene targeting or mating technique and are described in Table 4.1.4.1. In strains containing gene deletion, a coding region was replaced with an antibiotic-resistance cassette. Transformants were plated onto YES plates and after an overnight incubation replica plated onto selective YES plates containing 100-200 mg/ml of corresponding antibiotic. Positive transformants that grew on selective plates were screened by PCR and confirmed by sequencing. Strains containing plasmids were grown on EMMC media lacking corresponding selective marker (EMMC-leu-(ura)). Heterochromatin establishment assay was performed as previously described (Reyes-Turcu et al. 2011). *tri1Δdcr1Δclr4Δ* and *dcr1Δclr4Δ* strains were generated by mating and genes *clr4+* and *dcr1+* were reintroduced on plasmids (p348 and p474, see Table 4.1.3.1).

4.2.1.2 Silencing assays

Log-phased cultures were tenfold or fivefold serially diluted in a way that highest density spot contained 1×10^5 cells. 3 μ l of each were spotted onto non-selective (N/S), 5-fluoro-orotic acid (5-FOA, 1g/l 5-FOA), and TBZ (15 or 20 mg/ml) plates. Cells were grown for 2-3 days at 32 °C and imaged. In heterochromatin establishment assay, cells were treated with trichostatin (TSA, 35 mg/ml) and incubated on 32 °C for 24 h, following recovery for 24 h in YES media prior to spotting on 5-FOA plates.

4.2.2 Nucleic acid analysis

4.2.2.1 Purification of total RNA

10 ml of yeast cultures were grown to mid-exponential phase ($OD_{600} = 1.0 - 1.5$). Pellets were resuspended in 500 μ l of *Lysis buffer for RNA* (300 mM NaOAc pH 5.2, 10 mM EDTA, 1 % SDS) following addition of 500 μ l acid phenol-chloroform and incubation for 10 min at 65 °C with occasional vortexing. Samples were centrifuged for 15 min at 15 000 g at room-temperature and aqueous (top) phase was ethanol-precipitated. Purified samples were resuspended in RNase-free water, normalized to the same concentration and around 50 μ l of samples were treated with DNase I (Roche) for 30 min at 37 °C, following denaturation of the enzyme for 10 min at 37 °C. After the addition of 400 μ l of phenol-chloroform and 400 μ l of NaOAc (300 mM, pH 5.2), samples were centrifuged for 15 min at 15 000 g at room-temperature and RNAs were ethanol-precipitated. RNAs were dissolved in RNase-free water and quantified by RT-qPCR.

Reverse transcription (RT) reaction was done from 100 ng of total RNA using Superscript III (Invitrogen) and 1 pmol of DNA oligo (corresponding to the interested transcript) according to standard manufacturer's instructions.

4.2.2.2 Quantitative PCR (qPCR)

QPCR was performed using TOptical thermocycler (Biometra) with DyNAmo Flash SybrGreen qPCR Kit (Biozym). qPCR was done in a 10 µl reaction volumes containing 1xDyNAmo Flash SybrGreen Mix, 0.4 µM forward and reverse primers, and the template. For quantification of the extent of H3K9me over genomic regions of interest, 3 µl of IP sample (500 ng – 800 ng of DNA) obtained from H3K9-ChIP experiment or 3 µl of IN sample was added to qPCR mix as a template. In a case pericentromeric transcript levels were assessed, total RNA was purified, reverse transcribed, and cDNA obtained from RT or –RT control (to detect contamination, dimer formation, or presence of genomic DNA) reaction was used as a template in qPCR reaction. Two technical duplicates were pipetted in a 96-well plate (4titude). QPCR parameters were: initial denaturation at 95 °C for 3 minutes, followed by 46 cycles of denaturation at 95 °C for 10 seconds, annealing at 59 °C for 20 seconds and elongation at 72 °C for 15 seconds. Oligonucleotides used for RT-qPCR and ChIP are listed in the Table 4.1.2.1.

4.2.2.3 *In vitro* RNA synthesis

In vitro RNA synthesis was performed as previously described (Colmenares et al. 2007) and was performed to generate small RNA templates used in Triman activity assays. 160 U of T7 RNA polymerase (NEB) was used to transcribe 0.5 µg of template DNA in a 50 µl reaction containing transcription buffer (40 mM Tris pH 7.6, 2 mM spermidine, 6 mM MgCl₂, 0.01% Triton X100, 10 mM DTT), 4 mM ATP and CTP, 2 mM GTP and UTP, 40 U RNasin (Promega). Reactions were incubated at 37 °C for 2 h, following treatment with 10U of RNase-free DNase I (Sigma) for 30 min at 37 °C. Transcription products were phenol-chloroform extracted and ethanol-precipitated with glycogen.

4.2.2.4 Radioactive labeling of small RNAs

RNA templates (used in *in vitro* assays, Argonaute-copurifying RNAs, oligonucleotides used in splinted ligation assays) were radioactively labeled on 5' with [γ -³²P]-ATP using T4

polynucleotide kinase (PNK, Roche) for 30 min at 37 °C. Reactions were run through Microspin G25 column (GE Healthcare) to remove unincorporated isotope.

Prior radioactive labeling, RNAs that were loaded onto Ago1 *in vivo* were first dephosphorylated on 5' end using Calf intestinal alkaline phosphatase (CIP, NEB) for 30 min at 37 °C

4.2.2.5 Splinted ligation

Splinted ligation reaction was used for detection of Argonaute-associated *dg* small RNAs and was performed as previously described (Halic & Moazed 2010; Maroney et al. 2008). Argonaute-associated small RNAs were extracted from purified endogenously tagged FLAG-Ago1 (see chapter protein purification) by phenol-chloroform and ethanol-precipitated.

Ligation oligonucleotide was 5' radioactively labeled with [γ -³²P]-ATP using PNK (Roche). A mix containing ligation oligonucleotide and bridge oligonucleotide in a buffer containing 20 mM Hepes (pH 7.5) and 80 mM KCl was prepared and target RNA (200 ng) was added in a total reaction of 18 μ l. Reactions were first denatured at 95 °C for 1 min and annealed at 65 °C for 2 min and 37 °C for 10 min. Then 2 μ l of ligation mix containing 10 x ligation buffer and 10 U of T4 DNA ligase (NEB) were added to each reaction. Ligation was performed for 1 h at 35 °C and T4 DNA ligase was heat inactivated at 70 °C for 10 min. The radioactive label from unligated ligation oligo was removed using 0.5 μ l of CIP. Samples were analyzed on 18 % denaturing polyacrylamide-urea gels and the bands visualized using phosphor imaging. List of used oligos can be found in the Table 4.1.2.1.

4.2.2.6 Periodate oxidation/ β -elimination of RNA

Approximately 20 pmol of RNA72 was mixed with 6 μ l 5Xborax/boric acid buffer (148 mM borax, 148 mM boric acid pH 8.6) and 3.75 μ l NaIO₄ solution (200 mM in water) for 30 min at room temperature.

6 μ l of glycerol was added to the reaction to quench unreacted sodium periodate by incubating for 10 min. Then, 2.5 μ l of 2 M NaOH was added and incubated at 45 °C for 90 min (β -elimination).

The reaction was spun through Microspin G-25 Columns (GE Healthcare) and RNA was precipitated by ethanol. Protocol was provided by Dr. Klaus Förstemann.

4.2.2.7 High throughput sequencing

Small RNA libraries were prepared as previously described (Halic & Moazed 2010). FLAG-Ago1 was purified from endogenously tagged strains (see chapter protein purification) from around 2.5 l of cells pelleted at OD ~ 2. After the final washing step, 500 µl of NaOAc (300 mM, pH 5.2) and 500 µl of phenol-chloroform was added to the resin-bound FLAG-Argonaute to extract copurifying RNAs. Samples were briefly vortexed, centrifuged for 15 min at 15 000 g at 20 °C, and supernatant was ethanol-precipitated overnight.

Precipitated samples were resuspended in a formamide-loading dye and separated on 18 % polyacrylamide-urea gel. Each sample was run on a separate gel to avoid cross contamination. RNAs were visualized by staining with SybrGold and Ago1-associated sRNAs were excised from the gel according to the size (18–30 nucleotides) from other resin-copurifying RNAs. Size-selected sRNAs were eluted from the gel by incubating the crushed gel in 500 µl NaOAc pH 5.2 and 500 µl phenol-chloroform on 4 °C overnight with rotation. Samples were then transferred into Phase Lock Gel tubes, following centrifugation for 15 min at 15 000 g at 20 °C and upper-lawyer was ethanol-precipitated.

Small RNAs were dissolved in 13 µl of RNase-free water. 3' ligation reaction was performed in a 10 µl reaction containing 7 µl of small RNAs, 1 µl 10xT4 RNA ligation buffer without ATP (500 mM Tris-HCl pH 7.5, 100 mM MgCl₂, 100 mM DTT, 600 µg/ml BSA), 5 U RNasin (Promega), 2 mM preadenylated 3' adaptor oligonucleotide and 5 U T4 RNA ligase (Promega) for 2 h at 20 °C.

Reactions were then mixed with formamide-loading dye and separated on 18 % polyacrylamide-urea gel. 3' ligated Ago1-associated sRNAs were excised from the gel according to the size (37–45 nucleotides). Excised gel pieces were eluted from the gel by incubating the crushed gel in 500 µl NaOAc pH 5.2 and 500 µl phenol-chloroform as described above. After ethanol-precipitation, 3' ligated products were resuspended in 7.5 µl of RNase-free water.

5' ligation was performed by mixing 7.5 µl of 3' ligated sRNAs with 2 pmol 5' adaptor oligonucleotide (GUUCAGAGUUCUACAGUCCGACGAUC), 5 U RNasin (Promega), 0.06 mg BSA, 5 U T4 RNA ligase (Promega) in 10 µl ligation buffer (commercially supplied with T4 RNA ligase, containing ATP) and incubating at 20 °C for 2 hr.

Total 5' ligation reaction (10 µl) was used for reverse-transcription (RT) and mixed with 1 µl of 3' RT oligo (ATT GAT GGT GCC TAC AG), 4 µl 5x First strand buffer (Invitrogen), 2 µl DTT (100 mM), 1 µl dNTP mix (10 mM each), and 2 µl of RNase-free H₂O. 1 µl aliquot was taken as a negative RT control, and 1 µl Superscript III (Invitrogen) was added to the rest of the reaction. RT was performed by incubation for 1 h at 42 °C, followed by treatment with RNase H (15 min at 37 °C and enzyme deactivation 10 min at 75 °C).

To determine the cycle number necessary for amplification of generated cDNAs, a small scale, test PCR was performed and analyzed on 3 % agarose gel. Then, PCR was performed using Illumina P5 and Illumina P7 oligo with inserted barcodes (P158A1–P158H1) for 14–20 cycles. PCR parameters were 1 cycle of initial denaturation at 94 °C for 2 min, followed by necessary cycle numbers (14-20) of 94 °C for 15 sec, 60 °C for 30 sec, and 72 °C for 30 sec, and a final extension step of 72 °C for 4 min.

PCR products were concentrated using SpeedVac (Thermo Scientific) and purified on 10 % agarose gels. Small aliquots of gel-purified PCR products were analyzed on agarose gels along with corresponding aliquots of 100 bp DNA ladder to quantify the samples. Solexa sequencing was performed at the Gene Center (Illumina Genome Analyzer IIX; LaFuge). The quality of the libraries was checked by the Agilent 2100 Bioanalyser.

Data analysis was performed by Mario Halic. Illumina reads that matched to the first 6 nt of the 3' linker were selected. Small RNA reads in the size range 18-29 nt were mapped to the *S. pombe* genome allowing 3 nucleotides mismatch of the small RNA reads to the genome using Maq (<http://maq.sourceforge.net>) and Novoalign (<http://www.novocraft.com>). Reads mapping to multiple locations were randomly assigned. Datasets were normalized to number of reads per million sequences. Additionally, datasets were normalized to total amounts of small RNAs that were associated with Ago1 in corresponding strains as determined by Ago1 pulldowns and

quantification of Argonaute-associated small RNAs. One rRNA sequence was removed from data analysis. Genome sequence and annotation that are available from the *S. pombe* Genome Project (http://www.sanger.ac.uk/Projects/S_pombe/) were used. The data was displayed using Integrative Genomics Viewer (IGV) (<http://www.broad.mit.edu/igv>). Sequenced strains are listed in Table 5.3.

4.2.2.8 Triman activity assays

Each *in vitro* assay is described in the result section of the corresponding assay. In general, around 50-200 ng of FLAG-Triman or FLAG-TrimanD28A was used and incubated with 100 fmol 5' ³²P labeled small RNAs that were generated by *in vitro* transcription or purchased. Corresponding sequences of RNA templates are listed in the Table 4.1.2.1. In a case Argonaute-associated sRNAs were used to test Triman activity, around 100-500 ng of extracted copurifying RNAs were used. All reactions were run on 18 % polyacrylamide-urea gels and imaged by phosphor imaging.

4.2.2.9 Argonaute slicer assay

In reconstitution of Argonaute-slicer activity *in vitro*, FLAG-Argonaute was purified from *dcr1ΔtriΔ* cells utilizing bead beater and 1.5 M Lysis buffer (see protein purification). 100 ng of purified FLAG-Ago1 was loaded with 10 fmol small RNA guides: *RNA22*, *RNA24*, *RNA26*, or *RNA30* in a reaction containing *MgCl₂* buffer for 1 h at 32 °C. Then, 50 fmol of 5' ³²P labeled 130-nt target RNA (generated by *in vitro* RNA synthesis, chapter 4.2.2.3) was added to the reactions and incubated for 2 h at 32 °C. Reactions were separated on 18% polyacrylamide-urea gels and imaged by phosphor imaging.

The stability of the complex of Argonaute and small RNA guides of different sizes was performed by incubating 100 fmol of 5' ³²P labeled *RNA22*, *RNA24*, *RNA26*, or *RNA30* with resin-bound FLAG-Ago1 in a reaction containing *MgCl₂* buffer for 30 min at 32 °C. After loading, reactions were washed two times by adding 1 ml of *Washing buffer* and centrifugation for 1 min at 1500 g to remove unloaded RNAs. Reactions were then incubated for 2 h at 32 °C, following 2 washing steps with 100 μl of wash buffer. Washes (representing dissociated RNAs)

were ethanol-precipitated. Argonaute-bound RNAs were extracted by phenol-chloroform and ethanol-precipitated. All fractions were analyzed on 18 % polyacrylamide-urea gels and imaged by phosphor-imaging.

4.2.3 Protein analysis

4.2.3.1 Protein affinity purification

Protein expression and purification was performed by using *S. pombe* as the host and 3xHA or 3xFLAG peptides as protein purification tags. Proteins were either over-expressed from PREP1 plasmids or endogenous genes were tagged. Cell lysis was done by grinding in a coffee grinder with dry ice for 10 min (Buker et al. 2007), or using a MP Biotech bead beater. In a case lysis was done using coffee grinder, cells were prepared by re-suspending in 0.25 volumes of lysis buffer and frozen by dropping into liquid nitrogen, and after lysis additional 1 volume of lysis buffer was added. Standard lysis buffer was named *1.5 M Lysis buffer* and contained 50 mM Hepes (pH 7.6), 1.5 M NaOAc, 5 mM Mg(OAc)₂, 1 mM EGTA, 1 mM EDTA, 0.1% (v/v) Nonidet P-40 (NP-40) and protease inhibitors (Protease inhibitor cocktail tablets, Roche, Complete, EDTA free). When lysis was done for mass spectrometry analysis, *150 mM lysis buffer* (50 mM Hepes pH 7.6, 150 mM NaOAc, 5 mM Mg(OAc)₂, 1 mM EGTA, 1 mM EDTA, 0.1% (v/v) NP-40, Protease inhibitor cocktail tablets) was used and lysis was done utilizing coffee grinder.

Lysates were transferred in 50-ml Falcone tubes and spun at 7 000 g for 15 min. Supernatant was collected and incubated with prewashed anti-FLAG-M2 agarose beads (Sigma) or anti-HA on 4 °C for 2-3 h. The beads with immobilized protein were loaded onto Bio-Rad polyprep column and washed with 20 column volumes of lysis buffer. Chaperone proteins were removed by adding 1 mM ATP in the last two washes. Elution was done in five fractions using elution buffer (lysis buffer containing 0.2 mg/ml 3xFLAG peptide and 5% (v/v) glycerol) and aliquots were flash frozen in liquid nitrogen.

4.2.3.2 Western blotting

Proteins of interest were separated by SDS-gel electrophoresis and transferred to methanol-preactivated polyvinylidene fluoride (PVDF) membrane (Millipore). The transfer was done using The Trans-Blot SD semi-dry transfer cell (Bio-Rad) according to the manufacturer's instructions. The proteins on the blotted membranes were detected by staining with a solution containing amido-black (7.5 % HOAc, 20% EtOH, 0.1 % amido-black) following destaining (50 % EtOH, 5 % HOAc). Then, membranes were washed in 1× TBS-T buffer (50 mM Tris-Cl, pH 7.5, 150 mM NaCl, 0.05% Tween 20) and incubated in 5 % milk for 1 h on room temperature or overnight on 4 °C.

For the detection of FLAG-tagged proteins, the membrane was incubated in a 1:5000 solution of horseradish peroxidase-conjugated anti-FLAG M2 antibody (Sigma) in 1x TBS-T for 1 h at room temperature. The detection of HA-tagged proteins was done in a 1:200 solution of HA-probe Antibody (Santa Cruz) for 1 h at room temperature, following 3 short washing steps with 1 x TBS-T and incubation with the horseradish peroxidase-conjugated goat-anti-mouse IgG-HRP (Santa Cruz, 1:2000). For detection of tubulin, the same procedure was done utilizing α tubulin Antibody (Santa Cruz, 1:1000) and goat anti-rat IgG-HRP (Santa Cruz, 1:3000).

The proteins were detected using the ECL solution (Thermo Scientific) and imaged using LAS-3000 Mini Camera (FujiFilm).

4.2.3.3 *In-vitro* co-immunoprecipitation assay

100-200 ng of resin bound HA-Triman was incubated with 100-200 ng of FLAG-Ago1 in a reaction containing 25 mM Hepes pH 7.5, 2 mM MgCl₂, 2 mM DTT, 0.02 % NP-40 for 1.5 h at room temperature. Also, FLAG-Ago1 was mixed with the HA-resin alone as a control for the unspecific binding of Ago1 to the HA-resin. At the end of incubation time, resin was pelleted at 1400 g for 3 min and supernatant (resin unbound) was separated from resin fraction. Resin was further washed with 200 μ l buffer containing 25 mM Hepes pH 7.5, 2 mM MgCl₂, 2 mM DTT, 0.02% NP-40 and 100 mM NaOAc. After washing, resin was again pelleted at 1400 g for 3 min,

and wash fraction was discarded. Washing step was repeated two more times. Reactions were loaded on polyacrylamide-gel and analyzed by western-blot using horseradish peroxidase-conjugated anti-FLAG M2 (Sigma, 1:1000), or HA-probe Antibody (Santa Cruz, 1:200) and goat anti-mouse IgG-HRP (Santa Cruz, 1:2000).

4.2.3.4 Chromatin immunoprecipitation (ChIP) assay

ChIP assays were carried as described (Huang & Moazed 2003). In standard experiments, yeast cells were grown in YES medium. In the ChIP experiments of cells grown in varied growth conditions, cells were grown in the low nitrogen medium (EMMC-nitrogen) or low glucose medium (EMMC+0.5 % glucose). 50 ml of cultures at OD₆₀₀ of 1.0–1.3 were cross-linked with 1% or 3% formaldehyde at room temperature for 15 min. Quenching was done by treatment with glycine (125 mM) for 5 min. Cells were washed twice with water and resuspended in 500 µL *1.5 M Lysis buffer* with freshly added protease inhibitors (Protease inhibitor cocktail tablets, Roche, Complete, EDTA free), 1 mM PMSF and 0.8 mM DTT. Lysis was done using a MP Biotech bead beater three times for 30 sec. 700 µL of lysis buffer was added to dilute lysates and sonication was performed in 15 ml sonification tubes (Sumilon) using Bioruptor UCD-200 (Diagenode) program for 35 cycles (30 sec sonication, 30 sec pauses). Chromatin supernatant was obtained by spinning the lysate at 15 000 g for 15 min. Samples were normalized according to the RNA concentration and 20 µL of supernatant was used for input DNA. Dimethylated H3K9 antibody (H3K9me2, Abcam no. Ab1220) was immobilized on magnetic resin Dynabeads Protein A (Novex, Life Technologies), for 15 min at room temperature. Immunoprecipitation was performed by adding supernatants and incubation at 4 °C for 2 h. Beads with immobilized protein were washed 5 times with lysis buffer and eluted with 150 µL of *Chip elution buffer* (50 mM Tris-HCl pH 8.0, 10 mM EDTA, 1% SDS) at 65 °C for 15 min. Also, *Chip elution buffer* was added to the input samples to a final volume of 150 µl. Eluted samples were treated with RNase A for 30 min at 37 °C, following addition of Proteinase K and incubation at 65 °C overnight to reverse the crosslinks. DNA was purified by phenol-chloroform method and ethanol-precipitated. Samples were resuspended in 200 µl of water and further quantified using qPCR. Each set of experiments was performed at least in three different biological replicates.

5 APPENDIX

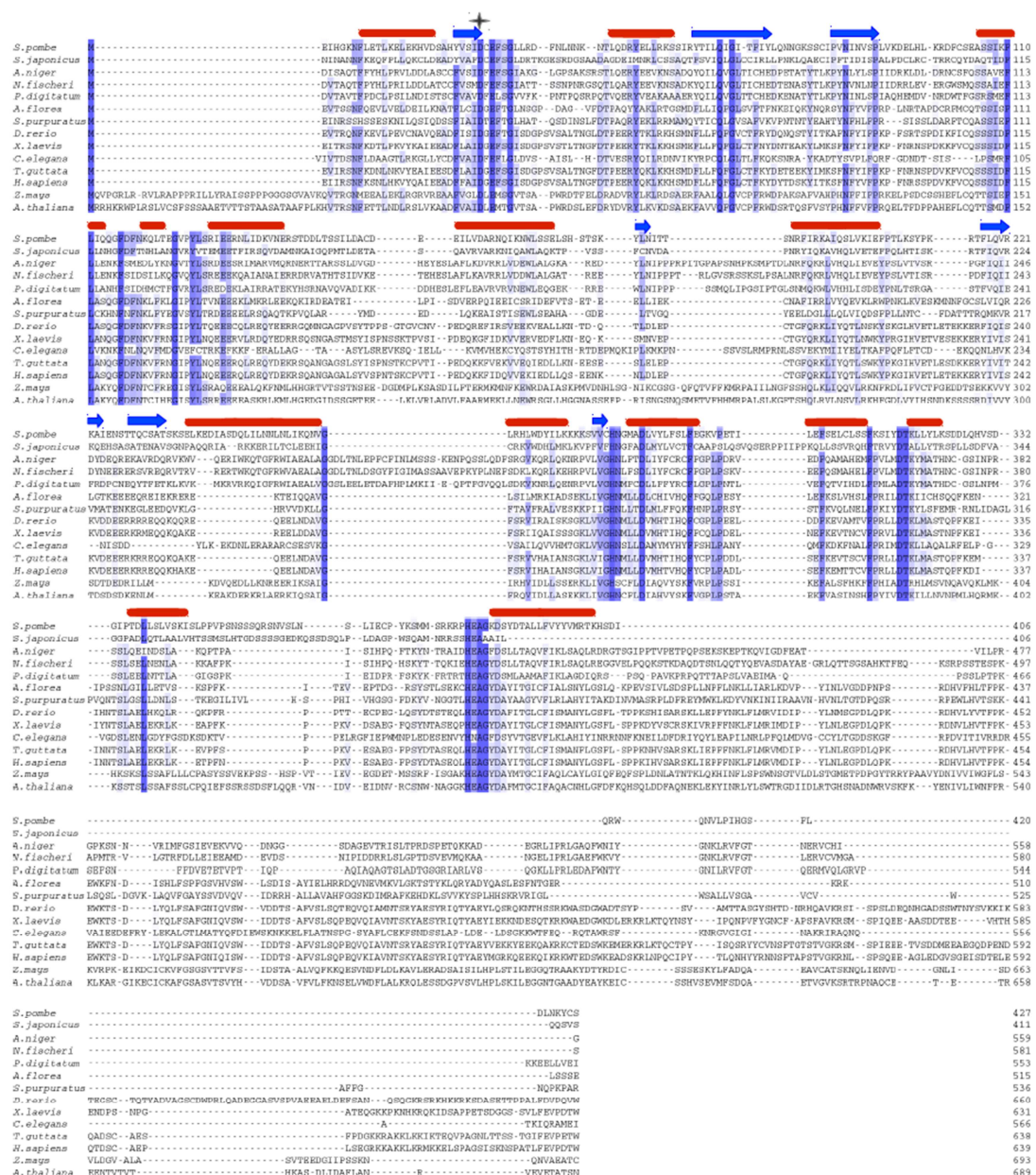


Figure 5.1. TrimD28A is conserved in eukaryotes. The sequence conservation is marked by color from not conserved (white) to highly conserved (dark violet). Secondary structure elements are shown above sequence. Blue arrows represent β -strands; red cylinders represent α -helices. TrimD28A is an activity mutant and the mutation is represented by black star

Table 5.1. Mass-spectrometry analysis of proteins co-purifying with Flag-Argonaute.

Argonaute IP	Unique peptides	Coverage %	Unique peptides	Coverage %
Ago1	53	66	48	62
Tas3	19	49	15	35
Chp1	23	29	1	1
Arb1	19	55	2	7
Arb2	4	22	0	0
Triman	3	3	2	3

Table 5.2. RNAi targets various genomic clusters in *rrp6Δ* cells. Listed genes had more than 100 reads per million and had siRNA enrichment of more than 5-fold compared to wild-type cells.

- denotes that in *tri1Δrrp6Δ* cells siRNA generation was abolished
- +/- denotes that in *tri1Δrrp6Δ* cells siRNA generation was reduced
- + denotes that in *tri1Δrrp6Δ* cells siRNA generation was not significantly affected
(less than 2-fold reduction in siRNA generation as compared *rrp6Δ* cells)

Gene	Chromosome	Start	End	siRNAs in <i>tri1Δ</i> cells
<i>SPAC977.14c</i>	Chromosome 1	59715	60770	-
<i>rps2202 / SPAC5D6.01</i>	Chromosome 1	1511797	1512189	-
<i>rds1 / SPAC343.12</i>	Chromosome 1	1668071	1669279	-
<i>myp2 / SPAC4A8.05c</i>	Chromosome 1	2547351	2553665	+
<i>SPAC4A8.06c</i>	Chromosome 1	2554013	2555749	+/-
<i>SPAP7G5.03</i>	Chromosome 1	3736955	3739106	-
<i>lys1 SPAP7G5.04c</i>	Chromosome 1	3739162	3743421	-
<i>rad50 / SPAC1556.01c</i>	Chromosome 1	3791831	3795856	-
<i>mug21 / SPBC216.02</i>	Chromosome 2	898075	900981	-
<i>SPBC21B10.03c</i>	Chromosome 2	1667059	1669434	-
<i>erg6 / SPBC16E9.05</i>	Chromosome 2	1923986	1925122	+/-
<i>SPBC18E5.10</i>	Chromosome 2	2092851	2094277	-
<i>SPBC23G7.06c</i>	Chromosome 2	2106448	2108786	-
<i>rpt6 / SPBC23G7.12c</i>	Chromosome 2	2121530	2122783	-
<i>SPBC1711.07</i>	Chromosome 2	2146256	2147698	-
<i>fab1 / SPBC3E7.01</i>	Chromosome 2	2653545	2659343	+/-
<i>spt16 / SPBP8B7.19</i>	Chromosome 2	3671459	3674518	+/-
<i>srb4 / SPBC31F10.04c</i>	Chromosome 2	3757531	3759284	-
<i>gyp2 / SPCC1259.11c</i>	Chromosome 3	1053866	1056028	+/-
<i>nte1 SPCC4B3.04c</i>	Chromosome 3	1168730	1172786	+/-
<i>SPCC4B3.03c</i>	Chromosome 3	1173490	1175529	+
<i>Rhp26 / SPCP25A2.02c</i>	Chromosome 3	1179636	1182557	+/-
<i>SPCC1442.04c</i>	Chromosome 3	1774200	1775429	+
<i>Tjf2</i>				+

Table 5.3. List of sequenced strains with the corresponding number of aligned reads.

Genotype	Aligned reads in millions
wild type	28
<i>tri1Δ</i>	27
<i>dcr1Δ_1</i>	26
<i>dcr1Δ_2</i>	2.9
<i>dcr1Δ_3</i>	1.6
<i>dcr1Δtri1Δ_1</i>	12
<i>dcr1Δtri1Δ_2</i>	3.3
<i>rrp6Δ_1</i>	8.7
<i>rrp6Δ_2</i>	5.3
<i>rrp6Δdcr1Δ_1</i>	2.7
<i>rrp6Δdcr1Δ_2</i>	3.7
<i>rrp6Δdcr1Δ_3</i>	3.7
<i>rrp6Δdcr1Δ_4</i>	3
<i>rrp6Δtri1Δ_1</i>	4.5
<i>rrp6Δtri1Δ_2</i>	5.6
<i>rrp6Δtri1Δ_3</i>	8.4
ChIP_wild type	1.7
ChIP_ <i>tri1Δ</i>	2.2
ChIP_ <i>clr4Δ</i>	0.9

6 REFERENCES

- Allshire, R.C. et al., 1994. Position effect variegation at fission yeast centromeres. *Cell*, 76(1), pp.157–169. Available at: <http://www.sciencedirect.com/science/article/pii/0092867494901805> [Accessed December 23, 2014].
- Aravin, A.A. et al., 2008. A piRNA pathway primed by individual transposons is linked to de novo DNA methylation in mice. *Molecular cell*, 31(6), pp.785–99. Available at: <http://www.pubmedcentral.nih.gov/articlerender.fcgi?artid=2730041&tool=pmcentrez&rendertype=abstract> [Accessed September 7, 2014].
- Aravin, A.A., Hannon, G.J. & Brennecke, J., 2007. The Piwi-piRNA pathway provides an adaptive defense in the transposon arms race. *Science (New York, N.Y.)*, 318(5851), pp.761–4. Available at: <http://www.ncbi.nlm.nih.gov/pubmed/17975059> [Accessed February 15, 2015].
- Ashe, A. et al., 2012. piRNAs can trigger a multigenerational epigenetic memory in the germline of *C. elegans*. *Cell*, 150(1), pp.88–99. Available at: <http://www.pubmedcentral.nih.gov/articlerender.fcgi?artid=3464430&tool=pmcentrez&rendertype=abstract> [Accessed July 14, 2014].
- Audergon, P.N.C.B. et al., 2015. Restricted epigenetic inheritance of H3K9 methylation. *Science*, 348(6230), pp.132–135. Available at: <http://www.pubmedcentral.nih.gov/articlerender.fcgi?artid=4397586&tool=pmcentrez&rendertype=abstract> [Accessed April 3, 2015].
- Bagijn, M.P. et al., 2012. Function, targets, and evolution of *Caenorhabditis elegans* piRNAs. *Science (New York, N.Y.)*, 337(6094), pp.574–8. Available at: <http://www.pubmedcentral.nih.gov/articlerender.fcgi?artid=3951736&tool=pmcentrez&rendertype=abstract> [Accessed February 25, 2015].
- Batista, P.J. et al., 2008. PRG-1 and 21U-RNAs interact to form the piRNA complex required for fertility in *C. elegans*. *Molecular cell*, 31(1), pp.67–78. Available at: <http://www.pubmedcentral.nih.gov/articlerender.fcgi?artid=2570341&tool=pmcentrez&rendertype=abstract> [Accessed March 2, 2015].
- Bayne, E.H. et al., 2010. Stc1: A Critical Link between RNAi and Chromatin Modification Required for Heterochromatin Integrity. *Cell*, 140(5), pp.666–677. Available at: <http://www.pubmedcentral.nih.gov/articlerender.fcgi?artid=2875855&tool=pmcentrez&rendertype=abstract> [Accessed March 17, 2015].

- Bernard, P. et al., 2001. Requirement of heterochromatin for cohesion at centromeres. *Science (New York, N.Y.)*, 294(5551), pp.2539–42. Available at: <http://www.sciencemag.org/content/294/5551/2539.abstract> [Accessed March 23, 2015].
- Bernstein, E. et al., 2001. Role for a bidentate ribonuclease in the initiation step of RNA interference. *Nature*, 409(6818), pp.363–6. Available at: <http://www.ncbi.nlm.nih.gov/pubmed/11201747> [Accessed January 22, 2015].
- Brennecke, J. et al., 2008. An epigenetic role for maternally inherited piRNAs in transposon silencing. *Science (New York, N.Y.)*, 322(5906), pp.1387–92. Available at: <http://www.pubmedcentral.nih.gov/articlerender.fcgi?artid=2805124&tool=pmcentrez&rendertype=abstract> [Accessed December 26, 2014].
- Brennecke, J. et al., 2007. Discrete small RNA-generating loci as master regulators of transposon activity in *Drosophila*. *Cell*, 128(6), pp.1089–103. Available at: <http://www.ncbi.nlm.nih.gov/pubmed/17346786> [Accessed February 10, 2015].
- Bühler, M. et al., 2007. RNAi-dependent and -independent RNA turnover mechanisms contribute to heterochromatic gene silencing. *Cell*, 129(4), pp.707–21. Available at: <http://www.ncbi.nlm.nih.gov/pubmed/17512405> [Accessed February 24, 2015].
- Buker, S.M. et al., 2007. Two different Argonaute complexes are required for siRNA generation and heterochromatin assembly in fission yeast. *Nature structural & molecular biology*, 14(3), pp.200–7. Available at: <http://www.ncbi.nlm.nih.gov/pubmed/17310250> [Accessed February 9, 2015].
- Burkhart, K.B. et al., 2011. A pre-mRNA-associating factor links endogenous siRNAs to chromatin regulation. *PLoS genetics*, 7(8), p.e1002249. Available at: <http://www.pubmedcentral.nih.gov/articlerender.fcgi?artid=3161925&tool=pmcentrez&rendertype=abstract> [Accessed March 2, 2015].
- Buscaino, A. et al., 2013. Distinct roles for Sir2 and RNAi in centromeric heterochromatin nucleation, spreading and maintenance. *The EMBO journal*, 32(9), pp.1250–64. Available at: <http://www.pubmedcentral.nih.gov/articlerender.fcgi?artid=3642681&tool=pmcentrez&rendertype=abstract> [Accessed December 29, 2014].
- Cam, H.P. et al., 2005. Comprehensive analysis of heterochromatin- and RNAi-mediated epigenetic control of the fission yeast genome. *Nature genetics*, 37(8), pp.809–19. Available at: <http://www.ncbi.nlm.nih.gov/pubmed/15976807> [Accessed February 18, 2015].
- Carmell, M.A. et al., 2007. MIWI2 Is Essential for Spermatogenesis and Repression of Transposons in the Mouse Male Germline. *Developmental Cell*, 12(4), pp.503–514. Available at: <http://www.sciencedirect.com/science/article/pii/S1534580707001001> [Accessed March 2, 2015].

- Cheloufi, S. et al., 2010. A dicer-independent miRNA biogenesis pathway that requires Ago catalysis. *Nature*, 465(7298), pp.584–9. Available at: <http://www.pubmedcentral.nih.gov/articlerender.fcgi?artid=2995450&tool=pmcentrez&rendertype=abstract> [Accessed February 12, 2015].
- Cifuentes, D. et al., 2010. A novel miRNA processing pathway independent of Dicer requires Argonaute2 catalytic activity. *Science (New York, N.Y.)*, 328(5986), pp.1694–8. Available at: <http://www.pubmedcentral.nih.gov/articlerender.fcgi?artid=3093307&tool=pmcentrez&rendertype=abstract> [Accessed February 12, 2015].
- Colmenares, S.U. et al., 2007. Coupling of double-stranded RNA synthesis and siRNA generation in fission yeast RNAi. *Molecular cell*, 27(3), pp.449–61. Available at: <http://www.cell.com/article/S1097276507004546/fulltext> [Accessed January 14, 2015].
- Djupeadal, I. et al., 2005. RNA Pol II subunit Rpb7 promotes centromeric transcription and RNAi-directed chromatin silencing. *Genes & development*, 19(19), pp.2301–6. Available at: <http://www.pubmedcentral.nih.gov/articlerender.fcgi?artid=1240039&tool=pmcentrez&rendertype=abstract> [Accessed February 18, 2015].
- Dutrow, N. et al., 2008. Dynamic transcriptome of *Schizosaccharomyces pombe* shown by RNA-DNA hybrid mapping. *Nature genetics*, 40(8), pp.977–86. Available at: <http://www.pubmedcentral.nih.gov/articlerender.fcgi?artid=2538488&tool=pmcentrez&rendertype=abstract> [Accessed February 12, 2015].
- Egan, E.D. et al., 2014. Post-transcriptional regulation of meiotic genes by a nuclear RNA silencing complex. *RNA (New York, N.Y.)*, 20(6), pp.867–81. Available at: <http://www.pubmedcentral.nih.gov/articlerender.fcgi?artid=4024641&tool=pmcentrez&rendertype=abstract> [Accessed March 12, 2015].
- Eissenberg, J.C. & Elgin, S.C., 2000. The HP1 protein family: getting a grip on chromatin. *Current opinion in genetics & development*, 10(2), pp.204–10. Available at: <http://www.ncbi.nlm.nih.gov/pubmed/10753776> [Accessed March 22, 2015].
- Ekwall, K. et al., 1997. Transient inhibition of histone deacetylation alters the structural and functional imprint at fission yeast centromeres. *Cell*, 91(7), pp.1021–32. Available at: <http://www.ncbi.nlm.nih.gov/pubmed/9428524> [Accessed February 13, 2015].
- Fire, A. et al., 1998. Potent and specific genetic interference by double-stranded RNA in *Caenorhabditis elegans*. *Nature*, 391(6669), pp.806–11. Available at: <http://www.ncbi.nlm.nih.gov/pubmed/9486653> [Accessed July 17, 2014].
- Folco, H.D. et al., 2008. Heterochromatin and RNAi are required to establish CENP-A chromatin at centromeres. *Science (New York, N.Y.)*, 319(5859), pp.94–7. Available at: <http://www.sciencemag.org/content/319/5859/94.full> [Accessed December 23, 2014].

- Frohn, A. et al., 2012. Dicer-dependent and -independent Argonaute2 protein interaction networks in mammalian cells. *Molecular & cellular proteomics : MCP*, 11(11), pp.1442–56. Available at: <http://www.pubmedcentral.nih.gov/articlerender.fcgi?artid=3494177&tool=pmcentrez&rendertype=abstract> [Accessed January 20, 2015].
- Ghildiyal, M. & Zamore, P.D., 2009. Small silencing RNAs: an expanding universe. *Nature reviews. Genetics*, 10(2), pp.94–108. Available at: <http://www.pubmedcentral.nih.gov/articlerender.fcgi?artid=2724769&tool=pmcentrez&rendertype=abstract> [Accessed July 13, 2014].
- Gibbins, D. et al., 2012. Selective autophagy degrades DICER and AGO2 and regulates miRNA activity. *Nature cell biology*, 14(12), pp.1314–21. Available at: <http://www.pubmedcentral.nih.gov/articlerender.fcgi?artid=3771578&tool=pmcentrez&rendertype=abstract> [Accessed January 9, 2015].
- Gu, S.G. et al., 2012. Amplification of siRNA in *Caenorhabditis elegans* generates a transgenerational sequence-targeted histone H3 lysine 9 methylation footprint. *Nature genetics*, 44(2), pp.157–64. Available at: <http://www.pubmedcentral.nih.gov/articlerender.fcgi?artid=3848608&tool=pmcentrez&rendertype=abstract> [Accessed February 5, 2015].
- Guang, S. et al., 2008. An Argonaute transports siRNAs from the cytoplasm to the nucleus. *Science (New York, N.Y.)*, 321(5888), pp.537–41. Available at: <http://www.pubmedcentral.nih.gov/articlerender.fcgi?artid=2771369&tool=pmcentrez&rendertype=abstract> [Accessed March 2, 2015].
- Gudipati, R.K. et al., 2012. Extensive degradation of RNA precursors by the exosome in wild-type cells. *Molecular cell*, 48(3), pp.409–21. Available at: <http://www.pubmedcentral.nih.gov/articlerender.fcgi?artid=3496076&tool=pmcentrez&rendertype=abstract> [Accessed February 24, 2015].
- Gunawardane, L.S. et al., 2007. A slicer-mediated mechanism for repeat-associated siRNA 5' end formation in *Drosophila*. *Science (New York, N.Y.)*, 315(5818), pp.1587–90. Available at: <http://www.ncbi.nlm.nih.gov/pubmed/17322028> [Accessed January 20, 2015].
- Halic, M. & Moazed, D., 2010. Dicer-independent primal RNAs trigger RNAi and heterochromatin formation. *Cell*, 140(4), pp.504–16. Available at: <http://www.pubmedcentral.nih.gov/articlerender.fcgi?artid=3020400&tool=pmcentrez&rendertype=abstract> [Accessed January 23, 2015].
- Hall, I.M. et al., 2002. Establishment and maintenance of a heterochromatin domain. *Science (New York, N.Y.)*, 297(5590), pp.2232–7. Available at: <http://www.ncbi.nlm.nih.gov/pubmed/12215653> [Accessed February 13, 2015].

- Halverson, D., Gutkin, G. & Clarke, L., 2000. A novel member of the Swi6p family of fission yeast chromo domain-containing proteins associates with the centromere in vivo and affects chromosome segregation. *Molecular & general genetics: MGG*, 264(4), pp.492–505. Available at: <http://www.ncbi.nlm.nih.gov/pubmed/11129054> [Accessed March 22, 2015].
- Han, B.W. et al., 2011. The 3'-to-5' exoribonuclease Nibbler shapes the 3' ends of microRNAs bound to Drosophila Argonaute1. *Current biology: CB*, 21(22), pp.1878–87. Available at: <http://www.pubmedcentral.nih.gov/articlerender.fcgi?artid=3236499&tool=pmcentrez&rendertype=abstract> [Accessed February 12, 2015].
- Hannon, G.J., 2002. RNA interference. *Nature*, 418(6894), pp.244–51. Available at: <http://www.ncbi.nlm.nih.gov/pubmed/12110901> [Accessed December 12, 2014].
- Hiriart, E. et al., 2012. Mmi1 RNA surveillance machinery directs RNAi complex RITS to specific meiotic genes in fission yeast. *The EMBO journal*, 31(10), pp.2296–308. Available at: <http://www.pubmedcentral.nih.gov/articlerender.fcgi?artid=3364741&tool=pmcentrez&rendertype=abstract> [Accessed February 13, 2015].
- Holm, L.R. & Thon, G., 2012. New romance between RNA degradation pathways: Mmi1 and RNAi meet on heterochromatic islands. *The EMBO journal*, 31(10), pp.2242–3. Available at: <http://emboj.embopress.org/content/31/10/2242.abstract> [Accessed March 22, 2015].
- Holoch, D. & Moazed, D., 2015. RNA-mediated epigenetic regulation of gene expression. *Nature reviews. Genetics*, advance on. Available at: <http://dx.doi.org/10.1038/nrg3863> [Accessed January 3, 2015].
- Hong, E.-J.E. et al., A cullin E3 ubiquitin ligase complex associates with Rik1 and the Ctr4 histone H3-K9 methyltransferase and is required for RNAi-mediated heterochromatin formation. *RNA biology*, 2(3), pp.106–11. Available at: <http://www.ncbi.nlm.nih.gov/pubmed/17114925> [Accessed October 8, 2015].
- Houseley, J., LaCava, J. & Tollervey, D., 2006. RNA-quality control by the exosome. *Nature reviews. Molecular cell biology*, 7(7), pp.529–39. Available at: <http://www.ncbi.nlm.nih.gov/pubmed/16829983> [Accessed February 17, 2015].
- Huang, J. & Moazed, D., 2003. Association of the RENT complex with nontranscribed and coding regions of rDNA and a regional requirement for the replication fork block protein Fob1 in rDNA silencing. *Genes & development*, 17(17), pp.2162–76. Available at: <http://www.pubmedcentral.nih.gov/articlerender.fcgi?artid=196457&tool=pmcentrez&rendertype=abstract> [Accessed February 11, 2015].
- Jia, S., Noma, K. & Grewal, S.I.S., 2004. RNAi-independent heterochromatin nucleation by the stress-activated ATF/CREB family proteins. *Science (New York, N.Y.)*, 304(5679), pp.1971–6. Available at: <http://www.sciencemag.org/content/304/5679/1971.long#F1> [Accessed March 18, 2015].

- Kanoh, J. et al., 2005. Telomere binding protein Taz1 establishes Swi6 heterochromatin independently of RNAi at telomeres. *Current biology: CB*, 15(20), pp.1808–19. Available at: <http://www.ncbi.nlm.nih.gov/pubmed/16243027> [Accessed March 20, 2015].
- Kato, H. et al., 2005. RNA polymerase II is required for RNAi-dependent heterochromatin assembly. *Science (New York, N.Y.)*, 309(5733), pp.467–9. Available at: http://www.sciencemag.org/content/309/5733/467.abstract?ijkey=ecddece0f236ea4ca75c32cb6bd7428f9b153374&keytype=tf_ipsecsha [Accessed January 11, 2015].
- Kawaoka, S. et al., 2011. 3' end formation of PIWI-interacting RNAs in vitro. *Molecular cell*, 43(6), pp.1015–22. Available at: <http://www.ncbi.nlm.nih.gov/pubmed/21925389> [Accessed December 29, 2014].
- Khair, L. et al., 2010. Roles of heterochromatin and telomere proteins in regulation of fission yeast telomere recombination and telomerase recruitment. *The Journal of biological chemistry*, 285(8), pp.5327–37. Available at: <http://www.jbc.org/content/285/8/5327.long> [Accessed March 14, 2015].
- Kim, H.S. et al., 2004. Regulation of Swi6/HP1-dependent heterochromatin assembly by cooperation of components of the mitogen-activated protein kinase pathway and a histone deacetylase Clr6. *The Journal of biological chemistry*, 279(41), pp.42850–9. Available at: <http://www.jbc.org/content/279/41/42850.full> [Accessed March 21, 2015].
- Knight, S.W. & Bass, B.L., 2001. A role for the RNase III enzyme DCR-1 in RNA interference and germ line development in *Caenorhabditis elegans*. *Science (New York, N.Y.)*, 293(5538), pp.2269–71. Available at: <http://www.pubmedcentral.nih.gov/articlerender.fcgi?artid=1855227&tool=pmcentrez&rendertype=abstract> [Accessed February 15, 2015].
- Lachner, M. et al., 2001. Methylation of histone H3 lysine 9 creates a binding site for HP1 proteins. *Nature*, 410(6824), pp.116–20. Available at: <http://www.ncbi.nlm.nih.gov/pubmed/11242053> [Accessed March 3, 2015].
- Lee, H.-C. et al., 2012. *C. elegans* piRNAs mediate the genome-wide surveillance of germline transcripts. *Cell*, 150(1), pp.78–87. Available at: <http://www.pubmedcentral.nih.gov/articlerender.fcgi?artid=3410639&tool=pmcentrez&rendertype=abstract> [Accessed February 25, 2015].
- Lee, H.-C. et al., 2010. Diverse pathways generate microRNA-like RNAs and Dicer-independent small interfering RNAs in fungi. *Molecular cell*, 38(6), pp.803–14. Available at: <http://www.pubmedcentral.nih.gov/articlerender.fcgi?artid=2902691&tool=pmcentrez&rendertype=abstract> [Accessed February 12, 2015].
- Lee, N.N. et al., 2013. Mtr4-like protein coordinates nuclear RNA processing for heterochromatin assembly and for telomere maintenance. *Cell*, 155(5), pp.1061–74. Available at:

- <http://www.pubmedcentral.nih.gov/articlerender.fcgi?artid=3974623&tool=pmcentrez&rendertype=abstract> [Accessed March 9, 2015].
- Liu, N. et al., 2011. The exoribonuclease Nibbler controls 3' end processing of microRNAs in *Drosophila*. *Current biology: CB*, 21(22), pp.1888–93. Available at: <http://www.pubmedcentral.nih.gov/articlerender.fcgi?artid=3255556&tool=pmcentrez&rendertype=abstract> [Accessed February 12, 2015].
- Marasovic, M., Zocco, M. & Halic, M., 2013. Argonaute and Triman generate dicer-independent priRNAs and mature siRNAs to initiate heterochromatin formation. *Molecular cell*, 52(2), pp.173–83. Available at: <http://www.ncbi.nlm.nih.gov/pubmed/24095277> [Accessed December 2, 2014].
- Maroney, P.A. et al., 2008. Direct detection of small RNAs using splinted ligation. *Nature protocols*, 3(2), pp.279–87. Available at: <http://www.ncbi.nlm.nih.gov/pubmed/18274530> [Accessed February 4, 2015].
- Mata, J. et al., 2002. The transcriptional program of meiosis and sporulation in fission yeast. *Nature genetics*, 32(1), pp.143–7. Available at: <http://www.ncbi.nlm.nih.gov/pubmed/12161753> [Accessed March 22, 2015].
- Moazed, D., 2011. Mechanisms for the inheritance of chromatin states. *Cell*, 146(4), pp.510–8. Available at: <http://www.pubmedcentral.nih.gov/articlerender.fcgi?artid=3244757&tool=pmcentrez&rendertype=abstract> [Accessed November 10, 2014].
- Mochizuki, K., DNA rearrangements directed by non-coding RNAs in ciliates. *Wiley interdisciplinary reviews. RNA*, 1(3), pp.376–87. Available at: <http://www.pubmedcentral.nih.gov/articlerender.fcgi?artid=3746294&tool=pmcentrez&rendertype=abstract> [Accessed February 28, 2015].
- Motamedi, M.R. et al., 2008. HP1 Proteins Form Distinct Complexes and Mediate Heterochromatic Gene Silencing by Nonoverlapping Mechanisms. *Molecular Cell*, 32(6), pp.778–790. Available at: <http://www.pubmedcentral.nih.gov/articlerender.fcgi?artid=2735125&tool=pmcentrez&rendertype=abstract> [Accessed March 17, 2015].
- Motamedi, M.R. et al., 2004. Two RNAi complexes, RITS and RDRC, physically interact and localize to noncoding centromeric RNAs. *Cell*, 119(6), pp.789–802. Available at: <http://www.ncbi.nlm.nih.gov/pubmed/15607976> [Accessed January 11, 2015].
- Murakami, H. et al., 2007. Ribonuclease activity of Dis3 is required for mitotic progression and provides a possible link between heterochromatin and kinetochore function. *PLoS one*, 2(3), p.e317. Available at: <http://www.pubmedcentral.nih.gov/articlerender.fcgi?artid=1820850&tool=pmcentrez&rendertype=abstract> [Accessed February 25, 2015].

- Nakayama, J. et al., 2001. Role of histone H3 lysine 9 methylation in epigenetic control of heterochromatin assembly. *Science (New York, N.Y.)*, 292(5514), pp.110–3. Available at: <http://www.ncbi.nlm.nih.gov/pubmed/11283354> [Accessed January 26, 2015].
- Nicolas, E. et al., 2007. Distinct roles of HDAC complexes in promoter silencing, antisense suppression and DNA damage protection. *Nature structural & molecular biology*, 14(5), pp.372–80. Available at: <http://www.ncbi.nlm.nih.gov/pubmed/17450151> [Accessed March 22, 2015].
- Noma, K. et al., 2004. RITS acts in cis to promote RNA interference-mediated transcriptional and post-transcriptional silencing. *Nature genetics*, 36(11), pp.1174–80. Available at: <http://www.ncbi.nlm.nih.gov/pubmed/15475954> [Accessed February 2, 2015].
- Partridge, J.F. et al., 2002. cis-Acting DNA from Fission Yeast Centromeres Mediates Histone H3 Methylation and Recruitment of Silencing Factors and Cohesin to an Ectopic Site. *Current Biology*, 12(19), pp.1652–1660. Available at: <http://www.sciencedirect.com/science/article/pii/S0960982202011776> [Accessed March 22, 2015].
- Provost, P. et al., 2002. Ribonuclease activity and RNA binding of recombinant human Dicer. *The EMBO journal*, 21(21), pp.5864–74. Available at: <http://www.pubmedcentral.nih.gov/articlerender.fcgi?artid=131075&tool=pmcentrez&rendertype=abstract> [Accessed January 11, 2015].
- Ragunathan, K., Jih, G. & Moazed, D., 2014. Epigenetic inheritance uncoupled from sequence-specific recruitment. *Science*, p.science.1258699–. Available at: <http://www.sciencemag.org/content/early/2014/11/19/science.1258699.abstract> [Accessed November 24, 2014].
- Rea, S. et al., 2000. Regulation of chromatin structure by site-specific histone H3 methyltransferases. *Nature*, 406(6796), pp.593–9. Available at: <http://www.ncbi.nlm.nih.gov/pubmed/10949293> [Accessed January 2, 2015].
- Reinhart, B.J. & Bartel, D.P., 2002. Small RNAs correspond to centromere heterochromatic repeats. *Science (New York, N.Y.)*, 297(5588), p.1831. Available at: <http://www.ncbi.nlm.nih.gov/pubmed/12193644> [Accessed January 4, 2015].
- Reyes-Turcu, F.E. et al., 2011. Defects in RNA quality control factors reveal RNAi-independent nucleation of heterochromatin. *Nature structural & molecular biology*, 18(10), pp.1132–8. Available at: <http://www.pubmedcentral.nih.gov/articlerender.fcgi?artid=3190054&tool=pmcentrez&rendertype=abstract> [Accessed February 25, 2015].
- Sadaie, M. et al., 2004. A chromodomain protein, Chp1, is required for the establishment of heterochromatin in fission yeast. *The EMBO journal*, 23(19), pp.3825–35. Available at:

- <http://www.pubmedcentral.nih.gov/articlerender.fcgi?artid=522800&tool=pmcentrez&rendertype=abstract> [Accessed December 23, 2014].
- Shirayama, M. et al., 2012. piRNAs initiate an epigenetic memory of nonself RNA in the *C. elegans* germline. *Cell*, 150(1), pp.65–77. Available at: <http://www.pubmedcentral.nih.gov/articlerender.fcgi?artid=3597741&tool=pmcentrez&rendertype=abstract> [Accessed February 25, 2015].
- Sienski, G., Dönertas, D. & Brennecke, J., 2012. Transcriptional silencing of transposons by Piwi and maelstrom and its impact on chromatin state and gene expression. *Cell*, 151(5), pp.964–80. Available at: <http://www.pubmedcentral.nih.gov/articlerender.fcgi?artid=3504300&tool=pmcentrez&rendertype=abstract> [Accessed February 20, 2015].
- Van Steensel, B., 2011. Chromatin: constructing the big picture. *The EMBO journal*, 30(10), pp.1885–95. Available at: <http://www.pubmedcentral.nih.gov/articlerender.fcgi?artid=3098493&tool=pmcentrez&rendertype=abstract> [Accessed March 3, 2015].
- Sugiyama, T. et al., 2005. RNA-dependent RNA polymerase is an essential component of a self-enforcing loop coupling heterochromatin assembly to siRNA production. *Proceedings of the National Academy of Sciences of the United States of America*, 102(1), pp.152–7. Available at: <http://www.pubmedcentral.nih.gov/articlerender.fcgi?artid=544066&tool=pmcentrez&rendertype=abstract> [Accessed February 22, 2015].
- Sugiyama, T. et al., 2007. SHREC, an effector complex for heterochromatic transcriptional silencing. *Cell*, 128(3), pp.491–504. Available at: <http://www.sciencedirect.com/science/article/pii/S0092867407000591> [Accessed March 9, 2015].
- Sugiyama, T. & Sugioka-Sugiyama, R., 2011. Red1 promotes the elimination of meiosis-specific mRNAs in vegetatively growing fission yeast. *The EMBO journal*, 30(6), pp.1027–39. Available at: <http://emboj.embopress.org/content/30/6/1027.abstract> [Accessed March 3, 2015].
- Tashiro, S. et al., 2013. Transcription-induced chromatin association of RNA surveillance factors mediates facultative heterochromatin formation in fission yeast. *Genes to cells : devoted to molecular & cellular mechanisms*, 18(4), pp.327–39. Available at: <http://www.ncbi.nlm.nih.gov/pubmed/23388053> [Accessed February 23, 2015].
- Thon, G. & Verhein-Hansen, J., 2000. Four chromo-domain proteins of *Schizosaccharomyces pombe* differentially repress transcription at various chromosomal locations. *Genetics*, 155(2), pp.551–68. Available at: <http://www.pubmedcentral.nih.gov/articlerender.fcgi?artid=1461114&tool=pmcentrez&rendertype=abstract> [Accessed March 22, 2015].

- Verdel, A. et al., 2004. RNAi-mediated targeting of heterochromatin by the RITS complex. *Science (New York, N.Y.)*, 303(5658), pp.672–6. Available at: <http://www.pubmedcentral.nih.gov/articlerender.fcgi?artid=3244756&tool=pmcentrez&rendertype=abstract> [Accessed November 27, 2014].
- Volpe, T.A. et al., 2002. Regulation of heterochromatic silencing and histone H3 lysine-9 methylation by RNAi. *Science (New York, N.Y.)*, 297(5588), pp.1833–7. Available at: <http://www.ncbi.nlm.nih.gov/pubmed/12193640> [Accessed August 21, 2014].
- Wang, S.H. & Elgin, S.C.R., 2011. Drosophila Piwi functions downstream of piRNA production mediating a chromatin-based transposon silencing mechanism in female germ line. *Proceedings of the National Academy of Sciences of the United States of America*, 108(52), pp.21164–9. Available at: <http://www.pubmedcentral.nih.gov/articlerender.fcgi?artid=3248523&tool=pmcentrez&rendertype=abstract> [Accessed February 20, 2015].
- Wang, W. et al., 2014. The initial uridine of primary piRNAs does not create the tenth adenine that is the hallmark of secondary piRNAs. *Molecular cell*, 56(5), pp.708–16. Available at: <http://www.ncbi.nlm.nih.gov/pubmed/25453759> [Accessed October 8, 2015].
- Watanabe, Y. & Yamamoto, M., 1994. *S. pombe* mei2⁺ encodes an RNA-binding protein essential for premeiotic DNA synthesis and meiosis I, which cooperates with a novel RNA species meiRNA. *Cell*, 78(3), pp.487–498. Available at: <http://www.sciencedirect.com/science/article/pii/009286749490426X> [Accessed March 22, 2015].
- Wirén, M. et al., 2005. Genomewide analysis of nucleosome density histone acetylation and HDAC function in fission yeast. *The EMBO journal*, 24(16), pp.2906–18. Available at: <http://emboj.embopress.org/content/24/16/2906.abstract> [Accessed March 22, 2015].
- Xue, Z. et al., 2012. Reconstitution of an Argonaute-dependent small RNA biogenesis pathway reveals a handover mechanism involving the RNA exosome and the exonuclease QIP. *Molecular cell*, 46(3), pp.299–310. Available at: <http://www.pubmedcentral.nih.gov/articlerender.fcgi?artid=3351553&tool=pmcentrez&rendertype=abstract> [Accessed February 12, 2015].
- Yamanaka, S. et al., 2013. RNAi triggered by specialized machinery silences developmental genes and retrotransposons. *Nature*, 493(7433), pp.557–60. Available at: <http://www.nature.com/nature/journal/v493/n7433/full/nature11716.html#ref10> [Accessed February 23, 2015].
- Yamane, K. et al., 2011. Asf1/HIRA facilitate global histone deacetylation and associate with HP1 to promote nucleosome occupancy at heterochromatic loci. *Molecular cell*, 41(1), pp.56–66. Available at: <http://www.sciencedirect.com/science/article/pii/S1097276510009652> [Accessed March 17, 2015].

- Yang, J.-S. et al., 2010. Conserved vertebrate mir-451 provides a platform for Dicer-independent, Ago2-mediated microRNA biogenesis. *Proceedings of the National Academy of Sciences of the United States of America*, 107(34), pp.15163–8. Available at: <http://www.pubmedcentral.nih.gov/articlerender.fcgi?artid=2930549&tool=pmcentrez&rendertype=abstract> [Accessed February 12, 2015].
- Yoda, M. et al., 2013. Poly(A)-specific ribonuclease mediates 3'-end trimming of Argonaute2-cleaved precursor microRNAs. *Cell reports*, 5(3), pp.715–26. Available at: <http://www.pubmedcentral.nih.gov/articlerender.fcgi?artid=3856240&tool=pmcentrez&rendertype=abstract> [Accessed January 9, 2015].
- Yu, R. et al., 2014. Determinants of heterochromatic siRNA biogenesis and function. *Molecular cell*, 53(2), pp.262–76. Available at: <http://www.ncbi.nlm.nih.gov/pubmed/24374313> [Accessed October 23, 2014].
- Zhang, K. et al., 2011. Ctr4/Suv39 and RNA quality control factors cooperate to trigger RNAi and suppress antisense RNA. *Science (New York, N.Y.)*, 331(6024), pp.1624–7. Available at: <http://www.ncbi.nlm.nih.gov/pubmed/21436456> [Accessed February 24, 2015].
- Zhang, K. et al., 2008. Roles of the Ctr4 methyltransferase complex in nucleation, spreading and maintenance of heterochromatin. *Nature structural & molecular biology*, 15(4), pp.381–8. Available at: <http://dx.doi.org/10.1038/nsmb.1406> [Accessed January 11, 2015].
- Zofall, M. et al., 2012. RNA elimination machinery targeting meiotic mRNAs promotes facultative heterochromatin formation. *Science (New York, N.Y.)*, 335(6064), pp.96–100. Available at: <http://www.ncbi.nlm.nih.gov/pubmed/22144463> [Accessed February 13, 2015].

7 CURRICULUM VITAE

Mirela Marasovic

Place of Birth: Zagreb, Croatia

Nationality: Croatian

Contact: mirela.marasovic@gmail.com

Education

2011 - 2015	Ludwig Maximilian University (LMU), Faculty of Chemistry and Pharmacy, Munich, Germany Dr. rer. nat. (equiv. to Ph.D.) degree in Biochemistry
2004 - 2011	University of Zagreb, Faculty of Science, Zagreb, Croatia Diplom (equiv. to M.Sc.), biology - molecular biology
2000 - 2004	Grammar school 'XV. Gimnazija', Zagreb, Croatia High school degree

Professional Experience

2011 - 2015	Ph.D. Student, Ludwig Maximilian University, Gene Center, Munich, Germany 'Toward unraveling biogenesis of Dicer-independent priRNAs and siRNAs in <i>Schizosaccharomyces pombe</i> '
2010 - 2011	Diploma research work, University of Zagreb, Faculty of Science, Department of Chemistry, Zagreb, Croatia Diploma thesis in Prof. Dr. Ivana Weygand-Durasevic's group 'Archeal RNA Polymerase subunit H: from cloning to investigation of interaction with atypical seryl-tRNA synthetase'
2009	Internship at Virginia Polytechnic Institute and State University (Virginia Tech), Blacksburg, Virginia, USA
2008	Internship at University of Zagreb, Faculty of Science, Zagreb, Croatia

Publication

Marasovic M, Zocco M, Halic M: Argonaute and Triman generate Dicer-independent priRNAs and siRNAs to induce heterochromatin formation. **Molecular Cell.** 2013 Oct

Research skills

Molecular Biology: molecular cloning in bacteria and yeast, PCR, real-time PCR

Working with proteins: recombinant protein expression, protein purification, protein activity assays, Western blotting, ChIP assays, co- immunoprecipitation

Working with RNA and DNA: DNA/RNA purification, working with radioactivity, Northern blotting, splinted ligation assays, preparing RNA libraries, analysis of deep sequencing data

Participation at Conferences and Workshops

- | | |
|----------------|--|
| 07-10/10/2014 | Selected talk at the European Molecular Biology Organization (EMBO) workshop ‘Non-coding RNAs in genome expression, maintenance and stability’, Cargèse, France |
| 21-23/05/2014 | Poster presentation at the conference ‘9 th Microsymposium on Small RNAs’, Vienna, Austria |
| 31/03-02/04/14 | Poster presentation at the conference ‘BioSysNet Symposium: From Functional Genomics to System Biology’, Munich, Germany |
| 24-29/06/14 | Participant at the EMBO conference ‘Pombe 2013: 7 th international Fission Yeast Meeting’, London, UK |
| 27-29/05/13 | Oral presentation at the conference ‘8 th Mycosymposium on Small RNAs’, Vienna, Austria |
| 07/03/2013 | Oral presentation at the ‘BioSysNet Symposium’, Munich, Germany |

Fellowships and awards

- | | |
|-----------|---|
| 12/2014 | PhD award for excellent research given by Dr. Klaus Römer foundation |
| 05/2013 | Poster award at the Gene Center get-together |
| 2006-2009 | Republic of Croatia, Ministry of Science, Education and Sports scholarship for outstanding academic achievements |

8 ACKNOWLEDGEMENTS

First of all, I would like to thank my parents. In the end, they are the ones that had put up with me for the longest period of time. ☺ I really appreciate the unconditional love and support to follow my interests. Big thanks go to my brother for being there during my whole education to help out with my numerous questions. Special thanks go to Filip. I feel really lucky that I have such a supportive person in my life.

Next, I would like to thank all people who contributed to this work. First and foremost, I thank Prof. Dr. Mario Halic for giving me the opportunity to do a PhD in his group. Being the first student and his open-door policy enabled me to learn a lot. Thank you Mario! Big thanks to Manu, who also contributed to this work. With his sense of humor he is really indispensable in the lab. Also big thanks to the other lab members – Sigrun, Nives, Silvija, Conny, Paola, Elias, Ilaria, Luca... You have set up a high criteria and it will be very hard to find such great colleagues in the future. Hvala, grazie und ein großes Dankeschön! Big thanks to Silvija; her persistence and passion for doing science are a great motivation.

Special thanks go to Nives for being such an amazing person and a friend. Since we had never met in Zagreb, where we had lived 10 min from each other, we both had to come here to meet in the lab. Also special thanks to Marko, who has always been such a supportive friend.

My appreciation also goes to all colleagues at the Gene Center for their help and friendly support. I would like to express my gratitude to the second evaluator Prof. Dr. Klaus Förstemann for providing us with protocols and material during the stressful period of revisions. I thank the remaining members of my committee Dr. Dietmar Martin, Dr. Franz Herzog, Prof. Dr. Karl-Peter Hopfner and Prof. Dr. Ulrike Gaul.

Finally, I would like to thank all my amazing friends for their big support that always means a lot!